Molecular Control of Pollen Tube Reception by the *FERONIA* Receptor-Like Kinase in *Arabidopsis thaliana*

Dissertation

zur

Erlangung der naturwissenschaftlichen Doktorwürde

(Dr. sc. nat.)

vorgelegt der

Mathematisch-naturwissenschaftlichen Fakultät

der

Universität Zürich

von

Juan Miguel Escobar Restrepo

aus

Kolumbien

Promotionskomitee

Prof. Dr.Ueli Grossniklaus (Leitung der Dissertation)

University of Zürich, Zürich, Switzerland

Prof. Dr. Beat Keller

University of Zürich, Zürich, Switzerland

Prof. Dr. Enrico Martinoia

University of Zürich, Zürich, Switzerland

Prof. Dr. Robert Pruitt

Purdue University, West Lafayette, Indiana, USA

Zürich, 2007

Acknowledgments

I am grateful to Ueli Grossniklaus for allowing me to continue the research on the *FERONIA* gene. His supervision and advice was crucial for this PhD work. I thank him as well for his support during difficulties and the confidence he laid on me.

My external committee member, Robert Pruitt, discussed with me in several opportunities my project and gave me excellent comments. I am very thankful for that and for him reviewing my thesis.

Sharon Kessler read my thesis and her comments substantially increased the quality of this work. I am grateful to her for discussions regarding the **FERONIA** research and for her constructive criticism. I thank Heike Wöhrmann for the translation to German of the summary of this thesis.

Valeria Gagliardini was always an important support to my research, scientifically as she did part of this work and personally as well. Thanks to her comments, I avoided many pitfalls.

I am very thankful to Jacqueline Gheyselinck as she did the laborious work for the *in situ* hybridization experiments. I thank her as well for the time I spent as her guest, and her support and advice during the difficult times of my PhD.

Margaret (Maggy) Collinge and Stephen (Skip) Schauer comments on previous manuscripts gave me the basis for learning scientific writing. I am grateful to Skip as well for his friendship and scientific discussions. Maggy's friendship, support, criticisms and capacity to motivate were of great help during my PhD work as well as for the rest of the Grossniklaus group.

Mark Curtis gave me excellent support in cloning, his comments and friendship were invaluable. To Amal Johnston, Petr Mozerov, Lukas Brand, Umut Akinci, Samuel Wüst, Stephane Pien and Brigitte Marazzi, I have nothing but gratefulness. Their company and discussions were important for my PhD.

I thank Philippa Barrell and Celia Baroux for teaching me the usage of Confocal Laser Scanning Microscopy as well for their friendship and scientific and non-scientific discussions.

Norbert Huck initiated the **FERONIA** project during his PhD. His comments and thesis work were indispensable for my own research. I thank him as well for his friendship and support.

Peter Kopf's work in the Grossniklaus' group was of invaluable help as he made most of the media and autoclave work for the lab. Arturo Bolaños helped me with an EMS screen and his job in ordering materials was of great help. I like to thank as well Alessio Grossi, Hiroko Asano-Shimosato, Olga Kirioukhova, Michael Federer, Miloslawa Jaciubek and Michael Raissig for their company and discussions.

Special thanks to the former members of the Grossniklaus' group: Claudia Köhler, Ramarmurthy Baskar, Vladimir Brukhin, José Costa Nunes, Damian Page, Andrea Steimer, James Moore, Felipe Aquea and Luiz Mors Cabral. Rita Gross-Hardt helped me with an EMS mutagenesis and Christina Kägi brought me plant material from Germany.

I am in debt to Charles Spillane. Thanks to him I came to Zurich, and through his supervision, I learned the basis for molecular biology research. I thank him as well for trusting in me and teaching me independence.

I thank Detlef Weigel and Ya-Long-Guo for providing seeds and Ulrike Schmidt for her help with the protoplast transformation.

Specially, I would like to thank Jasmin Gattlen for her company and support during the last stage of my PhD.

I thank Lucia Atehortua for her support and supervision during my Bachelor of Science studies as it set the path for my research in plant molecular biology.

Finally, I am grateful to my father Carlos, for encouraging my curiosity and for his guidance and to my mother Nelly, for teaching me the perseverance required for science and her positive attitude. To my sisters Juliana and Claudia and to my brother Carlos Santiago, I thank them for their company and friendship.

Summary

The focus of my research was the study of the interaction between sexes during plant reproduction, specifically in a process that requires direct communication between a male pollen tube and a female ovule that results in fertilization. Confirmation of this interaction comes from the analysis of the Arabidopsis female gametophytic mutant *feronia (fer)*, in which the communication between sexes does not occur. In *fer,* male pollen tubes correctly target the ovules but are unable to rupture and release their contents, the pollen tubes continue to grow inside the female tissues and fertilization is not achieved. This suggests that male behavior is affected by the absence of a female signal.

The *FER* open reading frame encodes a putative receptor-like serine/threonine kinase (RLK). RLKs are transmembrane proteins that receive signals in the form of ligands through an extracellular domain and subsequently activate signaling cascades via their intracellular kinase domain, a molecular function consistent with the role of *FER* in a signaling process between genders.

FER is expressed throughout the mature plant: specifically in leaves, roots, open flowers, floral buds, floral apices, young ovule primordia, and in young anthers with immature pollen, suggesting a role for *FER* in developing organs. In older anthers harboring mature pollen, *FER* was not detected, consistent with the role of *FER* in fertilization being female-specific. Moreover, promoter-reporter experiments demonstrated that *FER* is active in the synergid cells, where the interaction between the male pollen tube and the female ovule takes place.

A transcriptional fusion to a fluorescent protein (GFP) showed that FER is ultimately localized at the plasma membrane. Unfertilized ovules accumulated high levels of GFP signal in the plasma membrane–cell wall invaginations of the lower part of both synergid cells, a structure know as the filiform apparatus, which is the site for pollen tube entrance. Taken together, the data is consistent with a model where FER, localized in the filiform apparatus, binds a putative ligand on the approaching male gametophyte, which then results in the rupture of the pollen tube, sperm release, and fertilization.

As a signal transduction cascade initiated by the interaction of FER with a putative pollen ligand is necessary for fertilization, it is possible that changes in the components of this interaction could produce the *fer* phenotype. Interestingly, inter-

specific crosses between *A. thaliana* ovules and pollen from *A. lyrata* and *C. flexuosa* are phenotypically similar to wild-type *A. thaliana* pollen attempting to fertilize a *fer* female gametophyte. Sequence divergence between different species in either *FER* or its ligand could be responsible for the failure of the pollen tube to arrest. Higher Ka/Ks (nonsynonymous substitutions / synonymous substitutions) values occur in the putative ligand-binding extracellular region of *FER*, indicating that most amino acid replacements occur in this domain while the intracellular domain is conserved.

The data suggest that FER acts in the filiform apparatus to control the behavior of the pollen tube to achieve fertilization. The interaction between the putative male ligand and the extracellular domain of the FER-RLK triggers a signal transduction cascade inside the synergid cell. A subsequent signal then feeds back from the synergid to the pollen tube, causing growth arrest and the release of the sperm cells.

Zusammenfassung

Die hier vorgelegte Dissertation beschäftigt sich hauptsächlich mit dem Zusammenspiel zwischen den Geschlechtern in der Reproduktion von Pflanzen. Der Fokus liegt dabei in der Untersuchung der Vorgänge während der Befruchtung, die eine direkte Kommunikation zwischen dem männlichen Pollenschlauch und der weiblichen Samenanlage erfordert. Hinweise für diese Interaktion stammen von der Analyse der weiblich-gametophytischen Arabidopsis-Mutante *feronia* (*fer*), in der die Kommunikation zwischen den Geschlechtern extrem beeinträchtigt ist. Zwar findet der Pollenschlauch in *feronia* Pflanzen seinen Weg zu den weiblichen Samenanlagen, allerdings ist er nicht in der Lage, seinen Inhalt wie üblich nach Explosion des Pollenschlauchs freizugeben. Stattdessen wächst der Pollenschlauch weiter ins weibliche Gewebe ein, und eine Befruchtung findet nicht statt.

Das Gen *FERONIA* (*FER*) kodiert vermutlich eine sog. receptor-like serine/threonine kinase (RLK). Bei dieser Art von Kinasen handelt es sich um Transmembranproteine, die mit ihrer extrazellulären Domäne durch Bindung von Liganden Signale detektieren können. Die intrazelluläre Domäne der Kinase leitet das Signal schliesslich durch eine Kaskade von Phosphorylierungen ins Zellinnere. Diese molekulare Funktion veranschaulicht die Bedeutung von *FERONIA* in der Kommunikation zwischen den Geschlechtern.

FER ist in allen Geweben der adulten Pflanze exprimiert vor allem in Blättern, Wurzeln, offenen Blüten, Blütenknospen, Blütenmeristemen, jungen Primordien von Samenanlagen und jungen Antheren mit unreifem Pollen, was für eine Rolle des Proteins in der Entwicklung von Organen spricht. In älteren Antheren mit reifem Pollen findet sich *FER* allerdings nicht, was der Annahme entspricht, dass das Protein spezifisch von der weiblichen Seite exprimiert wird. Promoter-Fusionen von *FER* an Reportergene haben ausserdem die Expression von *FER* in Synergiden gezeigt, wo die Interaktion zwischen männlichem Pollenschlauch und weiblicher Samenanlage stattfindet.

Die transkriptionelle Fusion von *FER* an das grün fluoreszierende Protein GFP zeigt seine Lokalisation in der Plasmamembran. Unbefruchtete Samenanlagen akkumulieren ein starkes GFP-Signal in Membran-/Zellwandeinstülpungen im unteren Bereich der beiden Synergiden, eine Struktur, die als Filiform-Apparat

bekannt ist und den Eintrtittspunkt für den Pollenschlauch darstellt. Insgesamt lassen sich diese Daten zum folgenden Modell zusammenfassen: *FER* ist im Filiform-Apparat lokalisiert, bindet dort einen möglichen Liganden freigegeben vom wachsenden männlichen Pollenschlauch, und verursacht dadurch das Bersten des Pollenschlauchs, was die Spermien zur Befruchtung entlässt.

Die Beteiligung einer Signaltransduktionskaskade ausgelöst durch die Interaktion zwischen *FER* und einem möglichen Pollen-Liganden, führt zur Annahme, dass Abweichungen von der normalen Interaktion den *fer* Phänotyp auslösen. Interessanterweise zeigen interspezifische Kreuzungen mit *A. thaliana* als Pollenakzeptor und *A. lyrata* und *C. flexuosa* als Pollendonor phänotypische Ähnlichkeiten zu einer Kreuzung von *A. thaliana* Wildtyppollen auf eine *A. thaliana fer* Mutante. Sequenzunterschiede zwischen verschiedenen Pflanzen-Spezies in *FER* selbst oder seinem Liganden könnten für den kontinuierlich weiter wachsenden Pollenschlauch verantwortlich sein. Die höheren Ka/Ks-Werte (nichtkonservierte/ konservierte Sequenzunterschiede) betreffen ausschliesslich die möglicherweise Liganden-bindende extrazelluläre Domäne des Proteins, was für viele Aminosäureaustäusche in dieser Domäne spricht, während die intrazelluläre Domäne stark konserviert ist.

All diese Daten zeigen eindeutig, wie *FER* im Filiform-Apparat das Verhalten des Pollenschlauchs kontrolliert, um eine erfolgreiche Befruchtung zu erreichen. Die Interaktion zwischen einem möglichen männlichen Liganden und der extrazellulären Domäne der *FER* Proteinkinase löst eine Signalkaskade in der Synergide aus. Diese antwortet ihrerseits mit einem Signal an den Pollenschlauch, der in der Folge sein Wachstum einstellt und die Spermien zur Befruchtung freigibt.

Curriculum Vitae

Surname	ESCOBAR RESTREPO
First name	Juan Miguel
Date of birth	March 3, 1977
Nationality	Colombian
Place of birth:	Medellin, Colombia

Education

1988 – 1993	Secondary studies - Bachillerato. Montessori School. Medellin, Colombia
1995 – 2000	Bachelor of Science (BSc) Biology – Genetics. University of Antioquia. Medellin, Colombia
2000 – 2001	BSc Thesis under the supervision of Dr. Lucia Atehortua. "Preliminary assays for the Induction of Somatic Embryogenesis in *Heliconia psittacorum*". University of Antioquia. Medellin, Colombia
2001 – 2002	Post-Diplomand Praktikant under the supervision of Dr. Charles Spillane in Ueli Grossniklaus group. "Transposons and tandem repeats are not involved in the control of genomic imprinting at the MEDEA locus in Arabidopsis". University of Zürich. Zürich, Switzerland
2002 – Today	Employed as PhD student under the supervision of Prof. Dr. Ueli Grossniklaus. "Molecular Control of Pollen Tube Reception by the FERONIA Female Receptor in the *Arabidopsis thaliana* Plant". University of Zürich. Zürich, Switzerland. Year of graduation 2007

Table of Contents

1. Introduction

1.1 Reproduction and the evolution of sex

Each living organism is the product of the reproduction of another. This enables the maintenance of a species over generations if the characteristics passed on are sufficient to withstand the pressures of the environment. Organisms can reproduce sexually or asexually. Sexual reproduction requires halving of the chromosome number during meiosis, followed by fusion of two gametes to restore the original number of chromosomes. Asexual reproduction does not involve meiosis, ploidy reduction, and fusion of gametes. Sexual reproduction is found throughout all branches of the tree of life, and is present in the earliest Eukaryotes (Dacks and Roger 1999). Evolutionary analysis suggests that all multi-cellular asexual organisms that exist today are the result of a loss of sexuality (Charlesworth 2006). This indicates that the evolution of sex was a major evolutionary milestone during eukaryotic diversification.

Several hypotheses explain the widespread evolution of sex as an advantageous mode of reproduction: sex increases the rate of adaptation (spread of advantageous traits) (Fisher 1930), increases resistance to parasites (Van Valen 1973), and helps reduce deleterious mutational load (e.g. deleterious retrotransposons) (Chao 1988). Therefore, obligate asexually reproducing organisms would be more likely to become extinct (Maynard Smith 1978).

1.1.1 Sexual behavior and behavioral control between sexes

Natural selection selects and shapes genetic combinations that are able to confront and survive a certain environment. For example, in sexually deceptive orchids, behaviorally active compounds in the flower are identical to the sex pheromone of the pollinator species, these mechanisms have evolved in the flowers to attract pollinators that carry the pollen towards the stigma of a different flower (Schiestl 2005). Additionally, the presence of bright colors in the flowers and the production of nectar in plants attract insects and other animals for pollen transfer. These traits have co-evolved with the animals that use the flowers as a food resource. Natural selection could not have shaped by itself those mechanisms; most likely, an

interaction between sexual and natural selection may have driven the evolution of such traits.

Ultimately, molecular factors must be associated with the interactions between males and females. A good example of this is seen *Drosophila melanogaster*, where the development of the neural circuitry supports courtship rituals. In *fruitless (fru)* mutant male flies, there is a reduction or absence of courtship rituals towards the females and *fru* males perform courtship rituals with other males. *fru* encodes a set of transcriptional regulators that determines the development of the neural circuitry (Billeter, Rideout et al. 2006). Other molecules can influence the behavior of not only their own sex but also the opposite one: male Sex Peptide (SP), also from *D. melanogaster*, is contained in the male seminal fluid. After ejaculation it induces in the female an increase in the egg-laying rate and reduces the readiness to accept other males (Liu and Kubli 2003). SP is a 36-aa protein bound to the male's sperm, after ejaculation SP is cleaved inside the female and targeted to the female's brain, probably inducing the abovementioned changes (Nakayama, Kaiser et al. 1997)

1.1.2 Reproductive proteins and evolution

Molecular mechanisms not only influence the sexual behavior of some species, but also control reproductive processes by the interaction of male and female molecules. The most studied mechanism is the fusion between the egg and sperm in animals. In the marine gastropod abalone, the viteline envelope (VE) forms the coat of the egg and is composed of cross-linked glycoproteins. During the contact of sperm and the envelope, the sperm releases a soluble protein called lysin (Lewis, Talbot et al. 1982) from its acrosomal secretory organelle. Lysin binds tightly to the female VERL molecule (the VE receptor for lysin) (Swanson and Vacquier 1997). The binding causes the VERL molecules to lose cohesion creating a hole in the envelope where the sperm passes through in a species-specific manner. Interestingly, a Lysin related protein, sp18, is thought to be responsible for male control of the fusion between the sperm and the egg (Swanson and Vacquier 1995). *lysin, VERL* and *sp18* are rapidly evolving genes (Lee, Ota et al. 1995), (Galindo, Vacquier et al. 2003), (Swanson and Vacquier 1995) most probably as a result of adaptive evolution (positive Darwinian selection) (Yang and Bielawski 2000). In other words, they evolve through amino-acid changes promoted by natural selection that results in an increased fitness, in this case beneficial for reproduction. More important, co-evolution between female and

male interacting molecules (as in the case for *lysine* and *VERL*) could have a role in reproductive barriers to fertilization for the establishment of species (Lyon and Vacquier 1999).

1.2 Reproduction in plants

Plants differ from animals in their life cycle by having an alternation of diploid sporophytic and haploid gametophytic generations. The sporophyte produces spores through meiosis and these develop into haploid male and female gametophytes, which in turn produce gametes by mitosis. The fusion of the gametes produces a zygote, which in turn develops into a new sporophyte (Figure 1).

In the dominant group of land plants, the Angiosperms (flowering plants), the sporophytic phase is the predominant stage of the life cycle and in nonvascular plants, liverworts and mosses, the dominant stage is the gametophyte phase. Desiccating environments will favor a sporophytic generation as the necessity of water is decreased since neither the production or dissemination of spores is dependent on water. Instead, sperm cells are carried by the pollen tube to egg cells embedded in the sporophyte.

1.2.1 Pollen: The male gametophyte

The pollen is composed of three cells and is contained in the anthers where pollen development takes place. Pollen comes from the meiotic product of the pollen mother cell, which in turn undergoes an asymmetric mitosis producing two cells: a larger vegetative cell and a smaller generative cell. The generative cell undergoes an additional mitosis to produce two non-motile sperm cells, the timing of this second mitosis varies between species. A special coat of exine encloses the cells and a dehydratation process starts. Pollen grains are released from the anthers and deposited on the female stigmatic surface of the flower by wind, insects, birds, bats or direct contact, in the case of self-fertile plants like *A. thaliana.* On the stigma, the pollen grains re-hydrate and a pollen tube protrudes out and grows into the stigmatic cells of the female (Figure 1). The pollen tube carries the vegetative and generative cells towards the female ovules, with the vegetative cell supporting the growth of the pollen tube (Esau 1977).

1.2.1.1 The embryo sac: the female gametophyte

The female gametophyte is derived from the meiotic divisions of a megaspore mother cell. Four megaspores form, three of which degenerate and only one undergoes mitotic divisions to produce eight nuclei (polygonum type) inside a structure known as the embryo sac. The haploid embryo sac cellularizes and the eight nuclei organize into seven cells: an egg cell and two synergids cells that comprises the egg apparatus at the micropylar pole, three antipodals at the chalazal pole, and a central cell with two nuclei, which later will fuse (Mansfield 1991). The egg cell and the fused nuclei of the central cell fuse with the sperm nuclei from the pollen tube and will give rise to a zygote and the triploid endosperm, respectivly. Diploid sporophytic integument tissues surround the embryo sac leaving an open gap in the integuments known as the micropyle, which allows the entrance of the pollen tube to the filiform apparatus, a structure formed by the invaginations of the cell wall of the synergid cells (Figure 1). An exception to this organization of integuments is present in *Torenia fourninei* (Scrophulariaceae), in this species, the egg apparatus is outside the integuments but fertilization takes place in the same way (Figure 3).

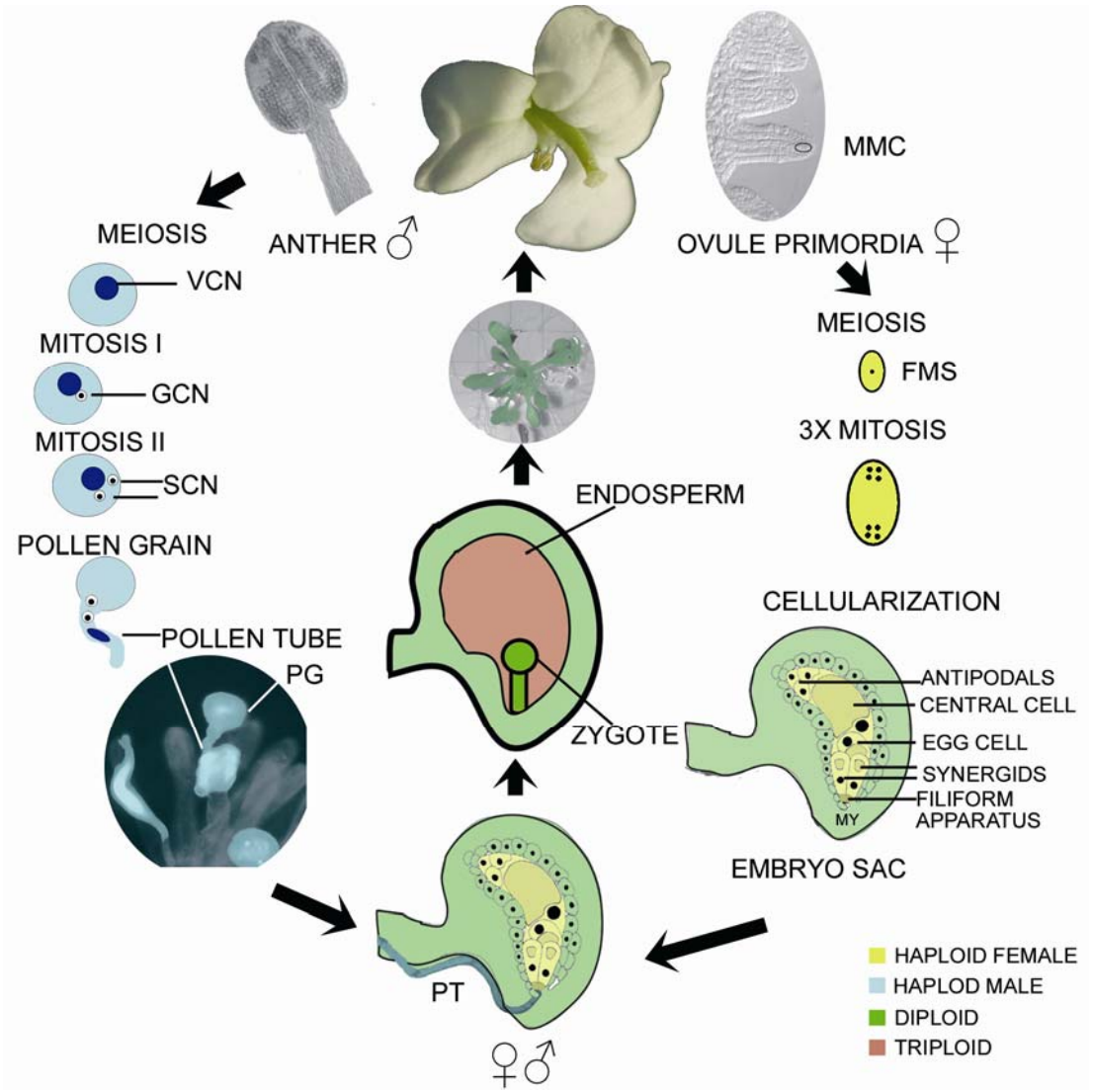

Figure 1. **The plant life cycle. Alternation of generations in an Angiosperm**. Meiosis in diploid sporophytic structures gives rise to haploid male and female gametophytes in the flower. The male gametophyte is a pollen grain carrying two sperm cells inside a vegetative cell. The female gametophyte is an embryo sac composed of seven cells. Fusion of one male sperm cell with the female egg cell forms a diploid zygote and fusion of the second sperm cell with a diploid female central cell forms a supporting triploid endosperm. The diploid central cell forms after the fusion of two haploid polar nuclei at maturity of the embryo sac. FMS, functional megaspore; MMC, megaspore mother cell; MY, micropyle opening; VCN, vegetative cell nucleus; GCN, generative cell nucleus; SCN, sperm cell nucleus; PT, pollen tube; PG, pollen grain.

1.2.2 Male – female communication in reproduction

Little information is known about the mechanisms in plants that are required for the interaction between sexes that leads to reproduction, which includes the following steps: 1) binding, hydration and germination of pollen grains on the stigma, 2) the

growth and guidance of pollen tubes in the style, 3) the guidance and reception of the pollen tube by the ovules and finally 4) the fusion of the sperm cells with the egg and central cell.

1.2.2.1 Pollination

After a pollen grain lands on the stigmatic surface of the female, hydration of the pollen grains commences (Figure 1). The control of this hydration depends on whether the stigma is wet or dry. In species with wet stigma surfaces, no barriers to hydration exist while in species with dry stigmas the complexity of the exine layer may determine species-specific discriminations (Zinkl, Zwiebel et al. 1999). Binding of molecules from the stigma and pollen allows cross-linking and hydration of the pollen through lipid conduits from both the pollen coat and stigmatic cells. This hydration provides nutrients for the development of the pollen tube that will grow through the stigma and style. The pollen tube penetrates the cuticle and cell wall of the stigmatic papillar cells and enters the transmitting tract at the base of the papilla. Once in the transmitting tract, the pollen tube grows down in the intercellular spaces between stylar cells (Dickinson, Doughty et al. 1998). Pollen tube growth through the style occurs very fast, maize pollen tubes can grow up to 1 cm/h, the metabolic rate for such a structure is therefore very high. Nutrients and other molecules from the stylar and transmiting tract must enter the pollen tube to maintain the growth rate. Molecules such as the floral transmitting tissue-specific glycoprotein from *Nicotiana tabacum* (Solanaceae) (Cheung, Wang et al. 1995) and gamma-aminobutyric acid (GABA) from *Arabidopsis* (Palanivelu, Brass et al. 2003) have been shown to have an effect on pollen tube growth.

The pollen tube cell wall consists of an inner callose wall and an outer coat containing pectin with cellulose and hemicellulose. At the tip of the pollen tube where polarized growth occurs, no callose or cellulose is found, instead there is only a single pectin layer (Ferguson, Teeri et al. 1998). Two major mechanisms act together to control pollen tube growth: calcium gradients at the pollen tube tip that orient the apical growth (Hepler 1985) and actin microfilaments that support vesicular transport (Geitmann, Snowman et al. 2000).

Plants with both male and female organs in the same individual or with male and female organs in the same flower are usually able to pollinate themselves. As noted above, inbreeding can be detrimental. Some plant species have evolved mechanisms

of self-incompatibility to allow the rejection of self-pollen and acceptance of foreign pollen. In sporophytic self incompatibility (SI), the rejection occurs at the level of the stigma, where self-pollen is unable to hydrate. In *Brassica*, the S locus controls this sporophytic SI mechanism and contains genes that encode the S-locus glycoprotein SLG (Nasrallah, Kao et al. 1985) and the S-locus receptor serine/threonine kinase SRK (Stein, Howlett et al. 1991). Expression of *SRK* occurs in the papillae cells of the stigma and localizes in the plasma membrane, while *SLG* encodes a soluble glycoprotein. SCR**,** a cystein rich protein from the pollen (Schopfer, Nasrallah et al. 1999), interacts with SRK (Kachroo, Schopfer et al. 2001) and triggers a kinase-mediated signaling cascade that ends in an incompatible pollination. *SLG* is not necessary for the induction of the self-incompatibility but enhances the response of self-rejection. The S locus is highly polymorphic and is haplotype dependant: different S haplotypes exist and the rejection occurs when pollen from a plant lands on the same plant or on a plant of the same haplotype (Boyes and Nasrallah 1993). In the self compatible *A. thaliana*, both SRK and SCR are pseudogenes (Kusaba, Dwyer et al. 2001).

Another example of self-rejection is the gametophytic self-incompatibility system of poppy (*Papaver rhoeas*) where the genotypes of the individual male gametophytes determine self-rejection, e.g pollen that do not share an S-haplotype with the pistil are compatible. The incompatibility response occurs at the level of the style where S-proteins interact with an unidentified pollen factor that results in inhibition of pollen-tube growth through a programmed-cell-death response that includes the release of mitochondrial cytochrome c, generation of a caspase-like enzyme activity and, DNA fragmentation. (Thomas and Franklin-Tong 2004). In *Petunia inflata* (Solanaceae), a similar system to allow self-rejection exists, the genetics are the same as in poppy but the molecular basis is different: pistil S-RNases interact with the male S-locus F-box PiSLF to inhibit the growth of self-pollen tubes in the style by degradation of RNA. S-RNases secreted along the path where the pollen tube grows through the pistil act as S-specific cytotoxins required for pollen rejection. The SLF protein contains an F-box motif, which mediates interactions with other proteins that make up the E3 ubiquitin ligase complex. Ubiquitination of cellular proteins acts as a signal for degradation or for targeting. The cytotoxic activity of S-RNase requires access to the cytoplasm. Therefore, SLF could provide resistance to S-RNase either by degradation of S-RNase or by preventing its access to

the cytoplasm (Sijacic, Wang et al. 2004). Antirrhinum (Plantaginaceae) AhSLF2 binds to S-RNase and interacts with components of the ubiquitination complex and experiments suggest degradation of S-RNase in compatible pollinations. The pistil secretes cytotoxic S-RNases to inhibit pollen and SLF provides resistance to that, except when the pollen and pistil have matching S-haplotypes (Qiao, Wang et al. 2004) (Qiao, Wang et al. 2004).

1.2.2.2 Guidance of pollen tubes

After germination of the pollen grains on the stigmatic cells, the developing pollen tubes grow intercellularly through the transmitting tract. When reaching the vicinity of a funiculus, the structure that attaches the ovule to the placenta, the pollen tube exits out of the intercellular space and grows along the funiculus reaching for the micropylar aperture of the ovule (Figure 2). The sporophytic female tissue provides nutrients and guidance cues to target the pollen tubes to the embryo sac in order to achieve fertilization. Sporophytic molecules proposed to mediate guidance of pollen tubes to the ovules are: glycoproteins (Cheung, Wang et al. 1995), GABA (Palanivelu, Brass et al. 2003), chemocyanins from lily (Liliaceae) (Kim, Mollet et al. 2003) and stigma-stylar Cys-rich adhesion protein (SCA) also from lily (Park and Lord 2003). Experiments in *T.fournieri* showed that none of the previous molecules are the sole attractants of pollen tubes (Higashiyama, Kuroiwa et al. 1998), (Higashiyama, Inatsugi et al. 2006).

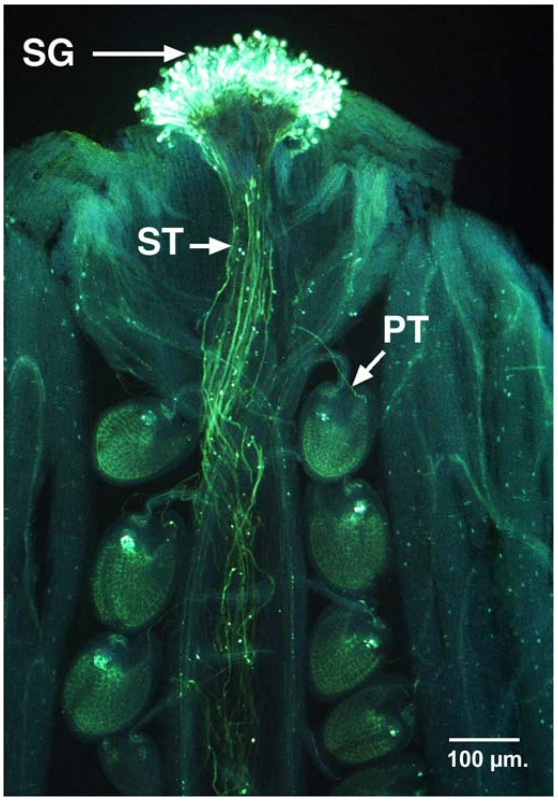

Figure 2. ***A. thaliana*** **pollination**. Aniline blue staining of callose observed under a fluorescence microscope. Pollen germinates on the stigma cells of the pistils and grows through the trasmitting tract. The pollen tube then emerges to a funiculs and grows towards the ovules. SG, stigma cells; ST, stylar tract; PT, pollen tube. Scale bar 100 µm.

Strong experimental evidence has shown that the embryo sac mediates the pollen tube guidance process. Examination of pollen tube behavior in different ovule defective mutants in Arabidopsis showed that only intact ovules are able to attract pollen tubes. For example, the 54D12 mutant has a variable phenotype in which some ovules arrest embryo sac development. In pistils of plants homozygous for the mutation, 92% of the ovules with the wild-type embryo sac phenotype received a pollen tube, whereas none of the ovules arrested during early embryo sac development received pollen tubes (Hülskamp, Schneitz et al. 1995). In an *in vitro* system in *T.fournieri*, the authors showed that dissected ovules laid down on a growth media attracted pollen tubes, showing that the ovule solely controls the guidance of germinated pollen grains. Interestingly, the pollen tubes only grew towards the ovules if they were germinated through a dissected style, suggesting an obligate capacitation of the pollen tubes through a stigma-pollen interaction (Higashiyama, Kuroiwa et al. 1998). In a later report, laser ablation of specific cells of the embryo sac of Torenia demonstrated that only the synergid cells of the female gametophyte are responsible for the attraction of the pollen tubes and that the secreted attractant has an effective distance of 100 – 200 um. One of the synergid cells is sufficient to attract pollen tubes, while two cells enhance this attraction. After

fertilization, the embryo sac no longer attracted pollen tubes despite the presence of one of the synergid cells, suggesting a termination of the production of the secreted attractant molecule, probably through down-regulation of gene expression (Huck, Moore et al. 2003). The block of the production of the attractant also indicates a role in blocking multiple pollen tubes reaching the micropyle (Higashiyama, Kuroiwa et al. 2003). The nature of this attractant is unknown. Research in the Arabidopsis *magatama* (*maa*) mutant, which displays a delayed development of the embryo sac causing the pollen tube to lose guidance just before entering into the mycropile, has unraveled that the embryo sac emits at least two types of attractants, one responsible for guidance to the funiculus and another for micropylar guidance. Inter-specific crosses between Arabidopsis and relative species supports this hypothesis. In these experiments, pollen tube arrest occurs at different stages and in some cases resembles the *maa* mutant. This also suggests that the attractant must be species-specific because ovules usually do not attract pollen tubes from other species (Shimizu and Okada 2000).

Once the pollen tube reaches the funiculus of the female gametophyte, the pollen tube continues to grow towards the micropylar aperture, which has a diameter that is about the same as that of the pollen tube. Reports from maize have shown that at least one molecule, ZmEA1, is involved in the short-range attraction responsible for micropylar guidance. ZmEA1 is a small protein produced by the egg apparatus and is cleaved and released out of the embryo sac through the filliform apparatus and into the surrounding nucellar cells. When the ZmEA1 gene is downregulated in RNAi and antisense lines, several ovules are unfertilized due to a failure in micropylar guidance. ZmEA1 shows similarity to two genes in rice and a ZmEA1 probe detects similar sequences in barley, wheat and in rice, but not in Arabidopsis and tobacco. This indicates that ZmEA1 may be a monocot-specific signal for micropylar guidance of the pollen tube (Marton, Cordts et al. 2005).

1.2.2.3 Role of synergids and filiform apparatus in pollen tube reception

Just before or during entrance of the pollen tube through the micropyle and to the filiform apparatus, one of the synergid cells degenerates. This degenerated synergid becomes the receptive synergid where the pollen tube explodes and releases its contents. The explosion of the pollen tube occurs as a fast potent burst that releases

the sperm cells and pollen tube contents. After a pollen tube bursts in the synergid, further attraction of other pollen tubes stops (Figure 3).

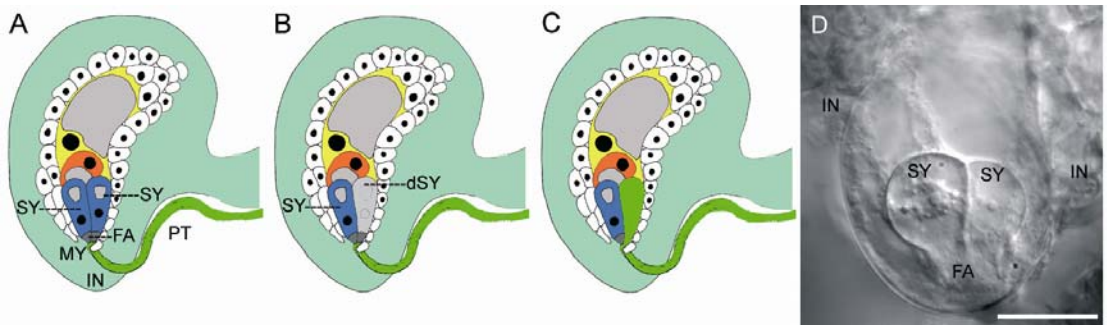

Figure 3. Pollen tube reception. (A) A pollen tube enters the ovules through the micropyle opening. (B) The receptive synergid degenerates shortly before or at the time of pollen tube entrance. (C) The pollen tube enters the gametophyte through the filiform apparatus, explodes and releases its contents in the degenerated synergid cell. (D) Partially naked female gametophyte in *Torenia fournieri*, notice the egg apparatus is not surrounded by the integuments as in *A. thaliana*. SY, synergid cell; dSY, degenerated synergid cell; FA filiform apparatus; MY, mycropile opening; IN, integuments; PT, pollen tube. Scale bar in (D) 40 μm.

The synergids produce and release the pollen tube attractant through the filiform apparatus (Higashiyama, Kuroiwa et al. 2003) (Marton, Cordts et al. 2005) and receive and control the pollen tube rupture. The synergid cells and the filiform apparatus are shared characters for most Angiosperms; the most basal and sister species to all Angiosperms, Amborella (Mathews and Donoghue 1999), possess synergids with a filiform apparatus (Friedman 2006). The conservation of such structures indicates they were important for the evolution of sexual reproduction in plants. Examples of species without a filiform apparatus are the obligate apomictic *Chondrilla juncea* (Koscinska-Pajak and Bednara 2006) and *Lilium longiflorum* cultivars (Gelria and White American), which reproduce vegetatively rather than through fertilization (Janson and Willemse 1995), suggesting that the lack of a filiform apparatus might be correlated with asexual reproduction.

Ultrastructural analyses of the synergid cells have shown that these cells are highly polarized with a chalazal vacuole and a micropylar nucleus. The cytoplasm of both synergid cells has a considerable amount of rough endoplasmic reticulum, dictyosomes, and large numbers of mitochondria adjacent to the filiform apparatus. Several plasmodesmata connect the synergid cells and both synergid cells seems to

be identical at the ultrastructural level (Mansfield 1991). As mentioned above, invaginations of the cell wall and plasma membrane of both synergids compose the filiform apparatus and resemble the walls of transfer cells (Jensen 1965). Transfer cells have secondary cell wall-plasma membrane ingrowths that are thought to enhance plasma membrane transport capacity. Transfer cells are located within nutrient transport pathways to facilitate apo/symplasmic exchange of solutes (Gunning and Pate 1969).

A characteristic feature of the synergids in Arabidopsis is the degeneration of one of the synergid cells 5 hours after pollination. The timing of synergid degeneration and pollen tube release correlate (Faure, Rotman et al. 2002). Synergid degeneration occurs in one of the synergid cells and is necessary for the reception of the pollen tube contents. In the *gfa2* mutant of Arabidopsis, pollen tube rupture does not occur due to the failure of the synergids to degenerate (Christensen, Gorsich et al. 2002).

The mechanisms of neither the molecular trigger to induce synergid degeneration nor the selection for the receptive synergid are known.

1.2.2.4 The process of double fertilization in plants

After pollen tube rupture, the non-motile sperm cells travel toward the egg and central cells and fuse in a process known as double fertilization (Nawaschin 1898). Observations in tobacco uncovered the existence of a large amount of actin in the degenerated synergid and the occurrence of aggregates termed “actin coronas”. One of the actin coronas forms at the chalazal end of the degenerating synergid and extends toward the egg. The second aggregate is at the interface between the egg and the central cell and extends to the region of the polar nuclei. These actin coronas could serve as a pathway for targeting the non-motile sperm cells to the egg and central cell (Huang and Russell 1994). Once targeting of sperm cells occurs, membranes of the sperm and female gametes fuse. This fusion probably involves cell surface receptors. Differential display analysis in *Lilium longiflorum* pollen identified a generative cell specific protein GCS1, which accumulates during late gametogenesis and localizes to the plasma membrane of generative cells. The protein possesses a carboxy-terminal trans-membrane domain and homologues are present in various species. In the *A. thaliana gcs1* mutant the gametes fail to fuse suggesting

that GCS1 is a critical for fertilization (Mori, Kuroiwa et al. 2006) and may be a candidate for a cell surface receptor.

There is variability in the ability of the sperm cells to fertilize either the egg cell or the central cell. In the orchid *Phaius tankervilliae*, the sperm nearest to the tip of the pollen tube fuses with the central cell and the other fuses with the egg cell (Ye, Yeung et al. 2002). Interestingly, the *A. thaliana cdc2a* mutant produces only one sperm cell that fertilizes the egg cell (Nowack, Grini et al. 2006), suggesting a preference for the egg over the central cell.

Sperm cell fusion to the egg cell generates a zygote, and fusion of the other sperm to the diploid central cell of a diploid plant generates an endosperm that nurtures the developing zygote (Figure 1). The process of double fertilization is widespread in both monocots and eudicots and suggests this is a characteristic of the common ancestor of these two angiosperm clades.

1.2.3 Evolution of plant sex related molecules

Knowledge is limited about the evolution of sex-related genes in plants. As in animals, plant proteins involved in reproduction may tend to evolve faster than non-reproductive proteins. For proteins involved in male-female interactions (e.g. receptor-ligand pairs) co-evolution mechanisms must exist in the same species to maintain the interaction between the molecules. The best example comes from the study of SLG, SRK, and SCR that contribute to the self-incompatibility system in Brassicaceae. As described above, self-alleles of the pollen coat Cys-rich SCR interacts with stigmatic the transmembrane Ser/Thr receptor kinase SRK to block pollen hydratation and germination. These three molecules are highly polymorphic and it has been shown that positive selection drives the adaptive diversification of the three genes (Sato, Nishio et al. 2002). It was demonstrated through likelihood ratio tests that positively selected SRK proteins are under physiochemical selective pressures to alter volume, polarity and charge (Sainudiin, Wong et al. 2005). In the case of SCR pseudogenes in the selfing *A. thaliana,* the low level of nucleotide variation in of SCR1 pseudogene suggests that it may have been the target of positive directional selection associated with the transition to selfing in *A. thaliana* (Shimizu, Cork et al. 2004).

As expected, in gametophytic self incompatibility systems, both female S-RNAse and male SLF show high levels of polymorphism and positive selection

acting among the functional domains necessary for the recognition of the binding partner (Ishimizu, Endo et al. 1998) (Takebayashi, Brewer et al. 2003) (Ikeda, Igic et al. 2004).

Pollen-specific oleosin-like proteins (or oleopollenins) may be involved in species recognition (Mayfield, Fiebig et al. 2001). Comparisons among pollen-specific oleosin-like proteins in *A. thaliana* and two closely related species showed that oleosins are among the most rapidly evolving proteins currently known from Arabidopsis, and may evolve under positive Darwinian selection, which is consistent with a putative function in species recognition (Schein, Yang et al. 2004).

1.3 The study of sexual reproduction in plants

Microscopic examination was the first approach to the analysis of the reproductive mechanism and led to the discovery of several important processes such as the double fertilization in plants. The development of model species such as *A. thaliana,* allowed for a genetic approach to be taken such as the screen of mutagenized populations of plants that show a reduced fertility.

The mutagenesis methods mostly used to identify genes involved in reproduction in *A. thaliana* are: chemical mutagenesis (EMS) and insertional mutagenesis (*Ac/Ds* transposon, T-DNA).

Ethyl Methane Sulfonate (EMS) mutagenesis on Arabidopsis seeds has been widely used for the production of mutants. EMS generally induces G to A transitions and has a range of effects on gene function such as reduced function, altered function, complete loss of function and constitutive function. Mutagenesis is performed in the mature seed (M0 generation) and only mutations in the cells that will produce the inflorescence will be transmitted to the next generation. Mutant sectors are formed, therefore several fruits must be scored in the first generation (M1). A problem arises when screening in the M1 generation because EMS produces lethality and sterility, making it difficult to identify gametophytic mutants. After identifying a candidate line, cleaning by repeated backcrossing is necessary to segregate away unwanted mutations. Afterwards the gene can be mapped by recombination or cloned by positional methods.

Insertional mutagenesis consists of the disruption of a gene through the introduction of transfer T-DNA from genetically engineered *Agrobacterium tumefacience* or genetically engineered *Ac/Ds* transposon elements to the plant

genome. Introduction of antibiotic resistance genes to either the T-DNA or transposon allows the tagging of mutants. This type of mutagenesis provides loss of function phentoypes. An advantage of insertional mutagenesis over EMS mutagenesis is that is relatively easier to identify the position of the inserted element trough PCR based amplification of its flanking sequences and subsequent sequencing of the products.

A difference between T-DNA and transposon mediated mutagenesis is the timing of insertion to the genome. The target of the Agrobacterium T-DNA is the female gametophyte (Desfeux, Clough et al. 2000), representing a drawback for the search for gametophytically active genes since the disruption of a gene required for female gametogenesis after the timepoint of insertion would not allow the recovery of mutant seeds. The *Ac/Ds* system allows the formation of chimeras in the F1 generation. The system is composed of a *Ds* transposon and an *Ac* transposase, if both transposon and the enzyme are in the same plant the *Ds* element moves from its original site of insertion to another location of the genome (Sundaresan, Springer et al. 1995). Recovery of gametophytic mutants is possible since the mobilization occurs only after the formation of gametes.

1.3.1 The study of *fer* unravels a new aspect of plant reproduction

Huck (Huck, Moore et al. 2003) reported the isolation of the *Arabidopsis* heterozygous mutant *feronia (fer)* from a segregation distortion *Ds* transposon mutagenesis screen (Moore, Calzada et al. 1997; Howden, Park et al. 1998) for reproductive defects in *A. thaliana.* In 50% of *fer* ovules, the pollen tube arrived at the micropyle and entered a degenerated synergid through the filiform apparatus, but instead of stopping and releasing its contents, it kept growing inside the female gametophyte. Therefore, fertilization of the mutant ovules was not achieved (Figure 4).

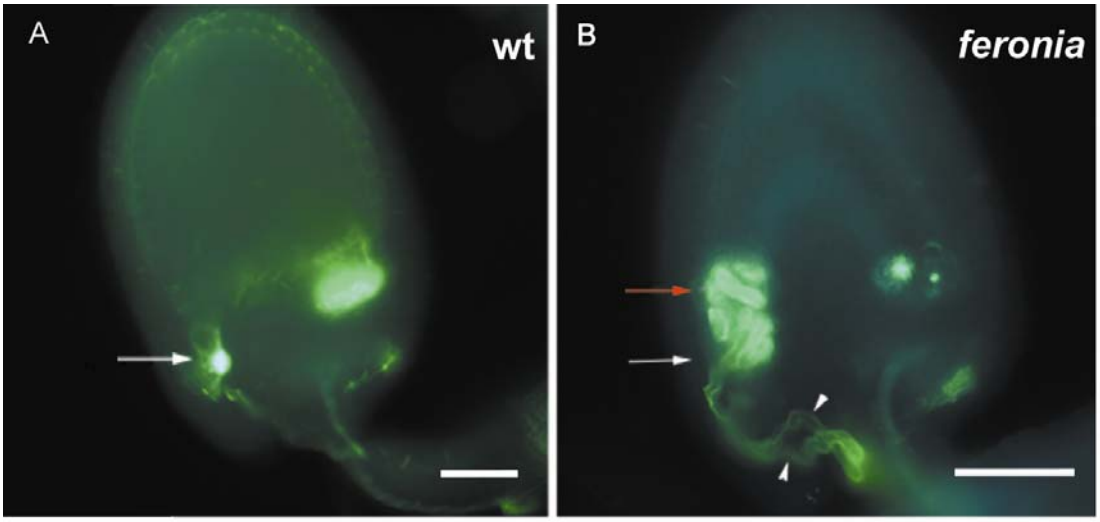

Figure 4. **Pollen tube overgrowth in the *fer* mutant**. Fluorescence micrograph of aniline blue stained callose in wild-type and mutant *A. thaliana* ovules. A. Normal pollen tube reception in a wild-type ovule. White arrow indicates site of pollen tube arrest. B. Aberrant pollen tube in *fer*. White arrow indicates site of pollen tube arrest in wild-type ovules. Red arrow indicates pollen tube overgrowth inside the embryo sac. Scale bars 30μm.

The authors showed correct specification of the synergids by analysis of synergid cell GUS markers and correct synergid degeneration in the mutant. Additionally, down-regulation of several synergid-specific markers occurs after arrival and burst of the pollen tube in wild-type ovules, whereas in *fer* mutant ovules, the synergid markers persisted after pollen tube entrance. Therefore, the gene responsible for the phenotype in *fer* not only controls the reception of the pollen tube, but also the mechanism involved in triggering down-regulation of synergid gene expression, which in turn could down-regulate or block the production of the unknown attractant. Support for this hypothesis comes from the observation that in several *fer* ovules more than one pollen tube enters the synergid cell. As the mutant propagates through the male and not through the female, the authors showed that *fer* is a female mutant that affects male behavior. In a very few cases, transmission of the mutation was observed through the female. An explanation is that a pollen tube that has already grown into a mutant ovule through the filiform apparatus ruptures in rare cases, releasing the sperm cells required for fertilization. Interestingly, it is not possible to recover homozygous mutants, suggesting that the gene might also be necessary for further development after fertilization. Another Arabidopsis mutant,

sirene (*srn*), shows the same features as *fer* but the gene responsible for the mutation was not identified (Rotman, Rozier et al. 2003).

In *fer* the *Ds* element is tightly linked to the mutant phenotype. The genomic location of the insertion was located to a protein phosphatase 2C (*PP2C)* gene (At3g51470) but complementation of the mutant with this gene was unsuccessful, indicating that the mutation in *PP2C* is not responsible for the phenotype in *fer*. Huck produced a mapping population and after identifying the last recombination event between the mapping markers and the phenotype, PCR amplification of 600-800 bp overlapping fragments of the coding regions of the genes contained in the region were used for a screen of polymorphisms through WAVE dHPLC mutation detection. Huck identified a polymorphism in a fragment from the coding region of At3g51550. Sequencing of the products showed a 4 bp insertion in the mutant which causes a premature stop codon in At3g51550 (Huck 2003).

The further characterization of *FER* in its role on pollen tube reception is the objective of this thesis work.

2. Material and methods

2.1 Plant material and growth conditions

A. thaliana plants were grown on ED73 soil (Universal Erde, Germany) in a growth chamber with 70% relative humidity, day-night cycle of 16 hours light at 21°C, and 8 hours darkness at 18°C. The same conditions were applied to *Arabidopsis lyrata* (JE-254 a gift from Detlef Weigel, University of Tubingen Max Planck Institute), *Brassica oleracea* (JE-211) (used for DNA extraction) and *Cardamine flexuosa* (JE-214) plants (collected at the Botanical Garden of the University of Zürich). For interspecific crosses, opened flowers from different Brassica species from the Botanical Garden of the University of Zürich were collected and the cut stem was put in MS media. Pollen was used to perform crosses onto emasculated *A. thaliana* plants of theLandsberg *erecta* (L*er)* accession.

2.2 Fluorescence staining of pollen tubes

The aniline blue staining protocol was adapted from (Hülskamp, Schneitz et al. 1995). Pollinated pistils were fixed with 9:1 EtOH-Acetic acid o/n at 4 C, the re-hydrated through an EtOH series: 70% EtOH 5 min, 50% EtOH 5 min, 30% EtOH 5 min. After removal of EtOH, tissues were incubated in 10% chloral hydrate for 5 min in a 60 to 65 C water bath. Chloral hydrate was removed and tissues were washed with sodium phosphate buffer pH 8.0 (Sambrook 1989). 5N NaOH was added and incubated at 60 C to 65 C for 10 min and subsequently washed with sodium phosphate buffer. Siliques were laid down in a microscopy slide and cover slide and the tissue was stained with 0.1% Methyl Blue (aniline blue; Sigma, St. Louis, U.S.A) prepared in sodium phosphate buffer pH 8.0. Pressing with forceps on the sides of the siliques opened the carpel valves and staining was repeated. Stained samples were observed using a Zeiss Axioplan microscope (Carl Zeiss, Oberkochen, Germany) with an epifluorescence lamp and UV-filter set (excitation filter at 365nm, dichronic mirror at 395 nm, barrier filter LP at 420 nm).

Pollen tubes were also stained with 0.2% Congo Red (Allied Chemical, Rochester,N.Y, U.S.A) for 15 min, washed with water and mounted in a microscopy slide for examination under a TCS SP2 confocal laser-scanning microscope (Leica,

Bensheim, Germany). Congo Red was exited with a HeNe laser at a wavelength 543nm and emission at 585 to 650 nm.

2.3 Microscopic observation of fluorescent proteins

GFP-tagged proteins were analyzed with a TCS SP2 confocal laser-scanning microscope (Leica, Bensheim, Germany) using excitation at 488 nm and recording the emission from 495 to 525 nm. DsRed tagged proteins were examined using excitation at 543 nm and recording the emission from 558 to 582. Single-focusing-plane images of 1024x1024 pixels were recorded with a scan speed of 400 Hz. 3D stacks were recorded as images of 1024x1024, using 20X and 40X glycerol-immersion objectives. GFP-tagged specimens were also analyzed using a Zeiss Axioplan microscope (Carl Zeiss, Oberkochen, Germany) with an epifluorescence lamp and UV-filter set (excitation filter at 365nm, dichronic mirror at 395 nm, barrier filter LP at 420 nm).

2.4 EMS mutagenesis of *A. thaliana* seeds

0.37g of *A. thaliana* seeds (aprox. 13000 seeds) of the Columbia (Col-0) accession carrying a *Lat52::EGFP* construct that stains the pollen tube with GFP (provided by Alice Cheung, University of Massachusetts, Amherst) were imbibed at 4 C for 3 days in the dark. Seeds were air dried for 24 hours and afterwards incubated in 0.15 % (v/v) of EMS (methanesulfonic acid ethyl ester, Sigma-Aldrich, St. Louis, U.S.A) for 10 hours under a fume hood. After incubation, EMS solution was removed from the seeds and seeds were washed at least 10 times with tap water. EMS treated seeds (M0) were grown in soil in small pots. After germination several plantlets were removed from the pots to leave only 3 plants per pot. After flowering, 3 consecutive siliques of the main stem (M1) of each plant of the pot were collected in a 24 well mictotiter plate (12 siliques per well), stained with aniline blue and observed as previously described. The screen was based on aberrant pollen tube behavior after contact with the female gametophyte. After identifying a putative mutant, the pot was re-screened for each separate plant and seeds were collected (M2). In total 1500 plants were screened in the M1 generation and 16 plants for each identified putative M1 mutant were grown and phenotyped in the next generation.

2.5 GUS assays

GUS assays were performed as described in (Vielle-Calzada, Baskar et al. 2000). The carpel walls of pistils were removed using insulin injection needles (Becton Dickinson, Franklin Lakes, U.S.A). Tissues were vacuum infiltrated for 15 minutes with GUS-staining buffer (50 mM Na-phosphate pH 7.0, 10 mM EDTA, 0.1% Triton X-100, 2 mM potassium ferrocyanide, 2 mM potassium ferricyanide, 100 μg/mL chloramphenicol and 1.5 mg/mL (5-bromo-4-chloro-3-indolyl)-β-D-glucuronide cyclohexamine) salt (X-gluc, Biosynth AG, Staad, Switzerland). After infiltration, tissues were incubated at 37°C in the dark for 12 hours to 3 days. Tissues were cleared in phosphate buffer saline (PBS, 50 mM sodium phosphate, pH 7.0) containing 20% lactic acid and 20% glycerol for examination with a Leica DMR microscope with Nomarski optics.

2.6 Molecular biology procedures

Standard molecular biology procedures were performed according to the suppliers' instructions or as described in (Sambrook 1989). Plant DNA was isolated with the phenol:chloroform method and ethanol precipitated (Sambrook 1989) and through the Nucleon PhytoPure kit (TEPNEL Life Sciences PLC, U.S.A). Bacterial DNA was isolated through Alkaline Lysis with SDS (Sambrook 1989). The PCR reactions were performed in a PTC-200 thermocycler (MJ Research,Waltham, U.S.A). PCR enzymes were from the following manufactures: Taq-DNA polymerase Sigma (St. Louis, U.S.A), "Home-made" Taq polymerase (produced by Valeria Gagliardini), Expand High Fidelity PCR (Roche Diagnostics, Penzberg, Germany), Expand Long Template PCR System (Roche Diagnostics, Penzberg, Germany), TripleMaster PCR system (Eppendorf, New York, U.S.A), TaKaRa Ex Taq (TAKARA Bio Inc. Otsu, Japan). RNA was isolated with the TRIZOL method (Invitrogen-Life technologies, Paisley, UK), SuperScript-First-Strand Synthesis System for RT-PCR Kit (Life technologies, Paisley, UK), DNA Walking Kit (Seegene, Inc. Seoul, Korea). Restriction endonucleases, reaction buffers and DNA modifying enzymes (New England Biolabs, Beverly, U.S.A). Gateway LR and BP clonase (Invitrogen, Carlsbad, U.S.A)

Chemicals were purchased from Sigma-Aldrich (St. Louis, U.S.A), unless otherwise indicated. The following kits were used: GFX PCR DNA and Gel Band Purification Kit (Amersham, Freiburg, Germany), QIAGEN PCR and Gel Band Purification Kit (Qiagen, Basel, Switzerland), JETSTAR Plasmid Purification Kit (Genomed, Bad Oeynhausen, Germany), PCR pTOPO® cloning Kit (Invitrogen-Life technologies, Paisley, UK), Qiagen PCR cloning kit (Qiagen, Basel, Switzerland).

2.7 Plant transformation

2.7.1 Transformation of *Agrobacterium tumefaciens*

Plants were transformed using the protocol described in (Clough and Bent 1998). Competent *Agrobacterium tumefaciens* GV 3101 cells were made by growing overnight at 28°C in 50 mL LB medium containing 40 µg/mL gentamicin and 100 µg/mL rifampicin in a 250 ml flask with shacking at 250 rpm until the culture reached an OD600= 0.5 to 1.0. The culture was chilled on ice for 5 min and centrifuged (5 minutes at 3000g) at 4 C. The supernatant was discarded and cells were resuspended in 1 mL ice-cold 20 mM CaCl2. 100 µL aliquots were frozen in liquid nitrogen and stored at -80 C. 30 ng of purified plasmid DNA were added to the frozen cells and incubated for 5 minutes at 37°C. The cells were allowed to recover in 1 mL LB medium without antibiotics at 28°C for 2-4 hours and then spread on LB plates containing 40 µg/mL gentamicin and 100 µg/mL rifampicin and the antibiotic for the selectable marker carried on the binary vector. After two days of incubation at 28°C, single colonies were picked and grown in liquid medium with antibiotics. DNA was isolated through alkaline-lysis and used for confirmatory restriction analysis and transformation of *E.c*oli DH5α cells. Cells were grown over night on LB agar plates containing the selective antibiotic. Plasmid DNA was isolated from *E.coli* and sequenced before proceeding with plant transformation.

2.7.2 Stable plant transformation by the *A.tumefaciens* floral dip method

Twenty plants of the L-*er* accession were planted in 4 pots and grown under standard conditions. Upon the transition to flowering, the main inflorescences were removed to promote lateral shoot formation. 8 days later, siliques and open flowers were removed from the plants. A 5 mL starter culture of *A. tumefaciens* from single

colonies was incubated o/n at 28 C. Afterwards, 100 µl of the starter culture was used to inoculate 200 ml LB liquid media containing 40 µg gentamicin, 100 µg rifampicin and the selective antibiotic for the binary vector. Bacteria were grown for 24-48 hours at 28°C. Bacteria were centrifuged and resuspended in a 5 % sucrose solution (infiltration media). Optical density of the suspension was measured at 600nm and adjusted to an OD600 of 0.8 with sucrose solution and Silwet-77 was added to 0.2 ul/ml (Lehle Seeds, Round Rock, U.S.A). Plants were dipped into the infiltration medium for 10-15 seconds, wrapped in transparent plastic bags and pots were laid on their sides for 24 hours before being returned to the upright position. The same procedure was repeated for each pot once more after five days. T1 transformants were selected on MS plates (Murashige and Skoog, 1962) containing 25 mg/L hygromycin, for pCambia1391Z or pMDC derived plasmids. For the construct derived from pCambia3300, plants were grown on soil and sprayed with 50 mg/L BASTA® (Oyma, Oftringen, Switzerland).

2.7.3 Transient transformation of plant tissues

Transient biolistic bombardment was performed using the protocol described by (Varagona, Schmidt et al. 1992). 5 to 10 µg of plasmid DNA of constructs *pFER::FER-GFP, 35S::FER-GFP, 35S::FER-GUS, 35S::GFP-FER and 35S::GFP,* were precipitated in 1.8 mg of 1.0 micron gold beads (Bioloistic® Bio-Rad, California U.S.A) with 125 µl CaCl2 (2M) and 40 µl 0.1M spermidine free base (Sigma-Aldrich, St. Louis, U.S.A). After 3 washes with 100% EtOH, the gold particles were resuspended in 40µl of 100% EtOH and 10µl were used for each bombardment giving a total of 4 bombardments for each construct. Gold particles coated with plasmid DNA were delivered to onion skins and *A. thaliana* leaves placed on MS media through a Biolistic PDS-1000/He unit (Bioloistic® Bio-Rad, California U.S.A). After plasmid delivery the samples were incubated in the dark o/n at 20 C. GFP observation and GUS assays were performed as described above.

Ulrike Schmidt (University of Zurich, Institute of Plant Biology, Switzerland) provided *A. thaliana* protoplasts from leafs that were isolated trough enzymatic digestion of the cell wall. 20 to 50 µg of plasmid DNA were used to transform the protoplasts with Polyethylene Glycol mediated transformation as by (Lee, Kim et al. 2001).

2.8 Caspase inhibition

Onion cells were transiently transformed through biolistic bombardment with construct *35S::GFP-FER,* but instead of resuspending the coated gold particles in 100% EtOH they were resuspended in 40µl of 200µM of N-Ac-Asp-Glu-Val-Asp-CHO (Ac-DEVD-CHO) (Cayman Chemical, Michigan, U.S.A) dissolved in 100% EtOH. After bombardment, 50 to 100µl of 100µM of Ac-DEVD-CHO were added directly on top the media below the onion skin sample and incubated o/n at 20 C in dark conditions. GFP fluorescence was investigated as previously described.

2.9 Cellular transport inhibition

Roots from *A. thaliana* plants transformed with the *pFER::FER-GFP* construct were incubated for 65 min at room temperature in 25µM BFA (Brefeldine A fungal toxin provided by Aurélien Bailly, Universty of Zurich, Switzerland) and observed under a CLSM.

2.10 Mapping of *sirene*

DNA extracted from leaves of s*rn/SRN* plants was used for PCR amplification and sequencing of the genomic region that comprises the *FER* gene in overlapping fragments of 600 to 800 bp. Analysis of sequence chromatograms from heterozygous plants revealed a 1 bp deletion in a 640 bp PCR fragment amplified with primers 5'-GTG AAA CCA GAG TCA ATG CTG-3' and 5'-CCC TGT AGC ATC AGG TCG-3'. This PCR product was subsequently cloned into pDRIVE vector (Qiagen, Basel, Switzerland), and several clones were sequenced. The deletion was confirmed in almost half of the sequenced clones while the rest showed the wt sequence

2.11 Complementation

To confirm that the insertion in the At3g51550 gene is responsible for the *fer* phenotype, a 6.4 kb fragment spanning 2.5 kb upstream of the initiation codon to 1.2 kb downstream of the stop codon of At3g51550 was PCR amplified from L*er* with Expand High Fidelity PCR (Roche Diagnostics, Mannheim, Germany) using primers 5'-CTT CAA CAT CTT CCA ATG GAG-3' and 5'-TGT TGC GGA TCC AAC TAG GCC AGG-3' (with an introduced BamHI site). The product was cloned into

pTOPO vector (Invitrogen). Positive clones were digested with BamHI and cloned into pCAMBIA-3300 linearized with BamHI. Plasmids containing the gene were sequenced and introduced into *Agrobacterium tumefaciens* strain GV3101 by the freeze-thaw method, and used for transformation of *Arabidopsis fer/FER* plants using the floral dip method (Clough and Bent 1998). The progeny were collected, grown, and sprayed with BASTA® (Oyma, Oftringen, Switzerland) to select transformants. To identify homozygous plants for the *Ds* element in complemented lines DNA was extracted from BASTA® (Oyma, Oftringen, Switzerland) resistant plants to genotype with primers G1 5'-AAG CAC TCC TTG TTG CCT TC-3' and G2 5'-CAC ATT GGA AGT CGC AGA TG-3' specific for the *PP2C* gene and primer Ds3-3 5'-GTT ACC GAC CGT TTT CAT CC-3' specific for 3' end of *Ds* element (Fig. 6B).

2.12 Quantitative Real-time RT-PCR

Quantitative Real-time RT-PCR was performed as described previously (Baroux, Gagliardini et al. 2006). Quantitative analyses of transcript levels were carried out using Sybr Green or Taqman real-time PCR assays (Applied Biosystem). Three PCR replicates were performed for each cDNA sample. Transcript levels were normalized to the level of ACTIN11 with primers Act11F 5'-AAC TTT CAA CAC TCC TGC CAT G-3'and Act11R 5'-CTG CAA GGT CCA AAC GCA GA-3'. *FER* transcripts were amplified with the intron spanning primers RT1 5'-CTC TCT CCG ATT TCA TCG CTT AGG-3' and RT2 5'- GGA TCT TGT GTT AAC GCT GG-3' (Fig. 6B).

2.13 *In vitro* transcription of *in situ* probes

To generate a probe for *in situ* hybridization, a 1.7 kb fragment of *FER* was amplified from genomic DNA with primers 5'-CTA ATC TAG ACG ACA CAG ATA ACC G-3' (with an introduced XbaI site) and 5'-CAA TCA AGG ACA CAA GAT GAC G-3'. The fragment was cut with HindIII and XbaI and inserted into pBluescript KS. To eliminate a 680-bp region of homology to other *Arabidopsis* kinases, the plasmid was digested with HindIII and SpeI, the single stranded overhangs filled in with T4 DNA polymerase, gel purified and religated to obtain a plasmid containing a 941-bp *FER* specific sequence. The antisense probe was obtained by *in vitro* transcription of the XbaI linearized plasmid with T3 RNA polymerase in the presence of digoxigenin-labeled rUTP (Roche Diagnostics, Mannheim, Germany). The sense

probe was generated identically, except that SalI was used to linearize the vector and T7 RNA polymerase was used for *in vitro* transcription (Roche Diagnostics, Mannheim, Germany). These probes were hydrolyzed with alkaline carbonate buffer (60 mM Na_2CO_3, 40 mM $NaHCO_3$; pH 10.2) to a size of approximately 150-200 bp according to the manufacturer's instructions (Roche Diagnostics).

2.14 *In situ* hybridization

In situ hybridization was performed by Jacqueline Gheyselinck (University of Zurich, Switzerland) as described previously (Vielle-Calzada, Thomas et al. 1999)

2.15 β-glucuronidase (GUS) expression analysis

To generate a *FERpromoter::GUS* construct (provided by Norbert Huck), 1.3 kb of putative upstream regulatory sequence was amplified with Long Expand PCR (Roche Diagnostics, Mannheim, Germany) from genomic DNA using primers 5'-AGG CTT CAA CAT CTT CCA ATG GAG-3' and 5'-GAG ACG GAA TCG TCC CAT GGT GAT CTT CAT CGA TC-3' (with an introduced NcoI site). The PCR product was digested with NcoI and BamHI, ligated into pCAMBIA-1391z linearized with NcoI and BamHI, and transformed into *Escherichia coli* strain DH5α. Transgenic plant lines were created as described above. More than 20 primary transformants were isolated on 0.5X MS medium agar plates containing hygromycin (20μg/ml) and subsequently transferred to soil. After flowering, ovules were dissected and *GUS* assays were performed as described previously (Vielle-Calzada, Baskar et al. 2000).

2.16 Subcellular localization of FER-GFP

2.16.1 *pFER::FER-GFP*

A PCR product, spanning 1.3 kb upstream of the *FER* start codon until the end of the coding region, without the stop codon, was obtained using gene specific primers with attB recombination sites**:** 5'-**GGG GAC AAG TTT GTA CAA AAA AGC CT**G GTA AGC TTC GAT TTA AGC G-3**';** and 5**'-GGG GAC CAC TTT GTA CAA GAA AGC TGG GT**A CGT CCC TTT GGA TTC ATG-3**'** **(**with the attB sites in bold). The amplified product was cloned into pDONR207 by the BP recombination reaction via the GATEWAY system (Invitrogen, Carlsbad, U.S.A) according to the

manufacturer's instructions. This construct was used to transfer the promoter and coding region upstream of a GFP reporter gene (mGFP6) in the plant transformation vector pMDC111 (Curtis and Grossniklaus 2003) (a gift of Dr, Mark Curtis) by the LR recombination reaction (Invitrogen, Carlsbad, U.S.A), resulting in the *pFER::FER-GFP* construct. Subsequent sequencing confirmed the reading frame of the fusion. This vector was used both for transient expression assays (by biolistic bombardment of onion skin epidermal cells and *Arabidopsis* leaves, as described previously (Varagona, Schmidt et al. 1992)) and for generation of transgenic plant lines (as described above). To distinguish between the cell membrane and cell wall in the transient expression assays, plasmolysis was induced by incubation of the onion cells in 0.8M mannitol. Non-specific localization in the transient expression assays was demonstrated using the plasmid ppk100, in which the *GFP* is under the control of a double *Cauliflower mosaic virus* 35S RNA promoter (*35S::GFP*) (a gift of Drs. Robert Blanvillain and Patrick Gallois, University of Manchester, UK). Seeds of *A. thaliana* plants transformed with *pAtD123::EGFP-AtROP6C* were provided by Wei-Cai Yang (Institute of Genetics and Developmental Biology, Beijing China) and were used as a control for a plasma membrane localized protein in the female gametophyte (unpublished results).

2.16.2 *35S::FER-GFP*, *35S::FER-GUS* and *35S::GFP-FER*

A PCR product spanning the complete coding region of *FER* without the stop codon was generated using primers 5'-**GGG GAC AAG TTT GTA CAA AAA AGC AGG CT** ATG AAG ATC ACA GAG GG-3'and 5**'-GGG GAC CAC TTT GTA CAA GAA AGC TGG GT**A CGT CCC TTT GGA TTC ATG-3**' (**with the attB sites in bold) and introduced into pDONR207 as described above. This construct was used to transfer the *FER* coding region, without the stop codon, downstream of a *35S* promoter and upstream of a GFP reporter gene in the plant transformation vector pMDC84 resulting in *35S::FER-GFP* as well as downstream of a *35S* promoter and upstream of a GUS reporter gene in the plant transformation vector pMDC141 resulting in *35S::FER-GUS*. For construction of *35S::GFP-FER,* the introduced PCR product into pDONR207 was introduced into pMDC43. Note that in this construct the *GFP* is located upstream of the predicted signal peptide of *FER*. These vectors

were used for transient expression assays by biolistic bombardment of onion skin epidermal cells as described above. Specimens were analyzed as described above

2.17 Isolation of related sequences and phylogenetic relationships

DNA was extracted by the phenol chloroform method from *A. lyrata, A. thaliana* (L*er*)*, B. oleracea* and *C. flexuosa*. For *A. lyrata* and *A. thaliana*, primers that amplify the genomic region of *FER* were designed based on the deposited sequences in the *A. thaliana* public database (Rhee, Beavis et al. 2003). Nucleotide sequences from the putative extracellular domain of *Arabidopsis* were used for BLAST searches in the TIGR *B. oleracea* database (http://www.tigr.org/tdb/e2k1/bog1). Best matches were used to design primers to amplify the *FER* gene as two overlapping products: 5'-CCG AAA CTC ACC GAG TTC-3' and 5'-CCA CTG CTC CTC GAG TCT G-3' for fragment 1 and 5'-CGT GCG TCT CCA CTT CTA C-3' and 5'-GGA TGG AGC CGG TTA AGA C-3 for fragment 2. For isolation of divergent sequences from *C. flexuosa,* primers based on the 5' region of *FER* in *A. thaliana* were used with the DNA Walking Kit (Seegene, Inc. Seoul, Korea). After amplification, fragments were cloned and sequenced to design primers: 5'-GAG CTG CTC CGA TCG ATG-3' and 5'-CGG TCT CCT TTG GAT GGA GC-3' that amplify the complete coding region of *FER*. All PCR products were cloned into pDRIVE and several clones were sequenced. 4 different sequences were found for *C. flexuosa*, indicating the presence of several homologues in this species. The PROSITE motif search (Bairoch, Bucher et al. 1997) and CBS Prediction Servers (Sonnhammer, von Heijne et al. 1998; Bendtsen, Nielsen et al. 2004) were used to predict the protein domains.

To examine the phylogenetic relationships of *FER* homologs, related RLK sequences were compiled from four sources: the direct sequencing described above; the ARAMEMNON plant membrane protein database (Schwacke, Schneider et al. 2003) (http://aramemnon.botanik.uni-koeln.de/) with similarity coefficient ranging from 65 to 75; NCBI protein BLAST searches using a cut off E-values of 0.0; and previously identified members of the CrRLK1-l family of *A. thaliana* (Shiu and Bleecker 2003). The amino acid sequences were aligned using ClustalX (Higgins, Thompson et al. 1996). Pairwise parameters were set to protein weight matrix Gonnet 250 with gap opening penalty of 35.00 and gap extension penalty of 0.75 and for multiple alignments gap opening penalty of 15.00 and gap extension penalty of

0.30 (Hall 2001). The phylogeny of the aligned sequences was generated using the neighbor-joining method and bootstrap analysis was conducted with 1,000 replicates. The software Treeview (Page 1996) was used for the display of the unrooted tree. Pairwise alignments of nucleotide and amino acid sequences were processed with BioEdit Sequence Alignment Editor v 5.0.9 to improve the alignment quality (Hall 1999). To maintain the correct reading frame, triplet gaps were introduced in the pairwise nucleotide sequence alignments using the amino acid alignment as reference with the CodonAlign 2.0 nucleotide sequence alignment program (http://sinauer.com/hall). DNASP 4.0 (Rozas and Rozas 1995) program was used to calculate and Ka/Ks ratios in sliding windows of 10% of the total length (86 codons) and a step size of 50% of the window size of the aligned sequences (43 codons). The signal peptide sequence was excluded.

The signal peptide was predicted using the Signal-P 3.0 server (Bendtsen, Nielsen et al. 2004) (http://www.cbs.dtu.dk/services/SignalP/). UTR analysis was performed with UTR scan (Pesole and Liuni 1999) (http://www.ba.itb.cnr.it/BIG/UTRScan/). mRNA secondary structure prediction was perfomed with GeneBee (Brodskii, Ivanov et al. 1995) (http://www.genebee.msu.su/services/rna2_reduced.html).

2.18 Evolutionary analysis and tests of natural selection

The ratio $\omega = d_N/d_S$ with d_N as the number of nonsynonymous substitutions per nonsynonymous site, and d_S as the number of synonymous substitutions per synonymous site was used to test whether protein coding sequences evolve under positive selection (Yang and Bielawski 2000). Pairwise sequence alignments from *A. thaliana FER* orthologs were constructed and analyzed with the CODEML program of the PAML package (Yang and Nielsen 1998), which uses maximum likelihood (ML) estimation of parameters. An initial Maximum likelihood tree was constructed with the PROTML program of the MOLPHY package (Adachi and Hasegawa 1996) to input in the CODEML program. To test for positive or purifying selection, ω - ratios for different site classes of the coding sequence were estimated. The likelihood of this estimate was then compared with the likelihood of other models with different numbers of parameters. A likelihood ratio test (LRT) was applied by calculating the test statistic as the two-fold difference of the two likelihoods [$2\delta = 2 * (l_1 - l_2)$]; the

critical values were looked up in a χ^2 table with the degrees of freedom calculated as the difference of the parameters that were estimated by each model. Two types of models were analyzed. Branch models allow different ω ratios in different branches of the phylogeny and can be used to address whether selection pressures on proteins are variable among species or among paralogs of a gene family. For the tests we used branch models with one (Model M0), two, three, four or *n* (the total number of branches; free-ratio model) ω ratios (Yang and Nielsen 1998). The second type of models analyzed were branch-site models (Yang and Nielsen 2002). These models allow to test whether positive selection occurred in a subset of codons in a particular branch of the phylogeny (the foreground branch) by assuming two types of codons with $0<\omega<1$ and $\omega=1$ in the entire tree and an additional class of codons with $\omega>1$ in the foreground branch. After estimating ω ratios, a Bayesian Empirical Bayes algorithm was applied to identify amino acid residues with a high posterior probability of $\omega>1$.

2.19 Sequence analysis of divergent accessions of *A. thaliana*

Sequences of *FER* were amplified from 11 divergent accessions of *A. thaliana* (Col-0, L-er, UK-1, Le-0, RLD-1, Di-0, Sah-0, Cvi-0, Kas, Wei-0, Mt-0. DNA provided by Arco Brunner, University of Zurich, Switzerland) using overlapping PCR primers. PCR products were directly sequenced and sequence data were assembled and aligned with the BioEdit Sequence Alignment Editor v 5.0.9. All polymorphisms were inspected visually. Molecular population genetic analysis was carried out with the DnaSP program (Rozas and Rozas 1995). The methods used to test neutral evolution included Tajima's *D* (Tajima 1989), the McDonald-Kreitman test (McDonald and Kreitman 1991) and Fu and Li (Fu and Li 1993).

2.20 Image processing

Images were digitally captured with a Magnafire camera (Optronics, Goleta, U.S.A) and Image Pro Express software (Media Cybernetics, Silver Spring, U.S.A). Confocal images were acquired and processed using the Leica Confocal Software, Version 2.0 and IMARIS (BITPLANE AG, Aargau, Switzerland). All images were processed using Adobe Photoshop 5.5 (AdobeSystemsInc. San Jose, U.S.A).

3. Results

3.1 Complementation of the *fer* mutant

To confirm that the 4 bp insertion in the At3g51550 gene is responsible for the *fer* phenotype, a 6.4 kb fragment spanning 2.5 kb upstream of the initiation codon to 1.2 kb downstream of the stop codon of At3g51550 (Figure 5A) was PCR amplified from L*er* wild-type plants and used for transformation of *Arabidopsis fer/FER* plants using the *Agrobacterium tumefaciens* floral dip method. If the introduced copy of At3g51550 successfully complements the female gametophyte lethality, the *Ds* element linked to the mutant allele should be transmitted through the female and male gametophytes obtaining homozygous progeny for the *Ds* element, otherwise not possible because of the zygotic lethality of *fer* (Huck, Moore et al. 2003). Moreover, a reduction of unfertilized ovules is expected due to an active copy of the gene that allows pollen tube reception and fertilization to occur in the mutant ovules.

To identify homozygous plants for the *Ds* element in complemented lines, DNA was extracted from resistant plants to genotype with primers G1 and G2 specific for the *PP2C* gene (At3g51470) where the *Ds* is inserted and primer Ds3-3' specific for the 3' end of the *Ds* element (Figure 5B). A single 634-bp band for wild type is expected as well as bands of 634 and 460 bp for *pp2c-Ds/PP2C; fer/FER* heterozygous and a single 460-bp band for double homozygous *pp2c-Ds/pp2c-Ds; fer/fer* plants. Of the 39 BASTA® resistant primary transformants, 11 did not have a *Ds* element (wild type), 21 were heterozygous and 7 were homozygous for the *Ds* element (Figure 5C). The occurrence of plants homozygous for the *Ds* element shows that wild-type At3g51550 complements the *fer* phenotype, enabling transmission of the *Ds* element to the next generation through the female gametophyte.

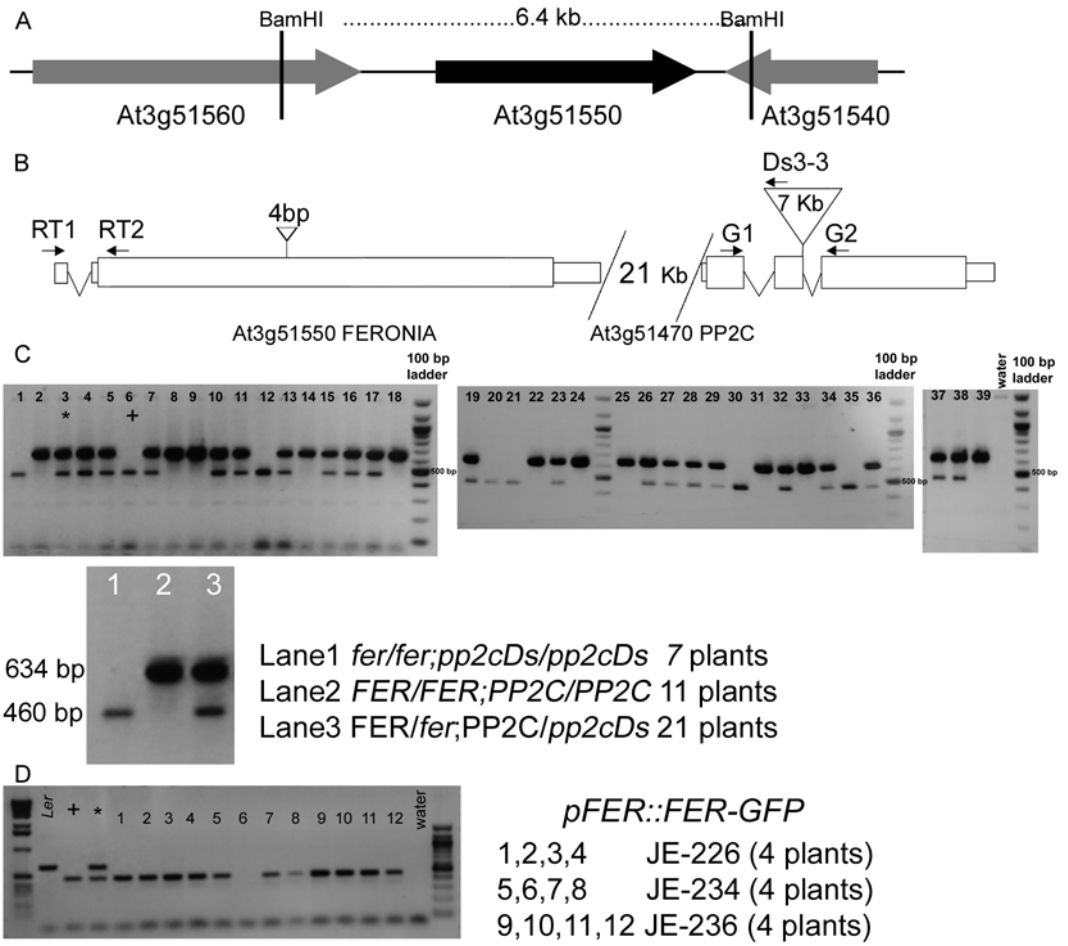

Figure 5. **Complementation and transposon insertion in *fer* mutant**. (A) Region used for the complementation construct. (B) Diagram of the *FER* and *PP2C* loci showing the position of the *Ds* element and the 4-bp insertion. The positions of primers G1, G2, and Ds3-3 (used in for genotyping *PP2C*) as well as the intron spanning primers RT1 and RT2 used in for *FER* QT-RTPCR. (C) Genotyping PCR of the *Ds* element for complementation. A single 634-bp fragment indicates a wild-type plant, a 634, 460-bp doublet indicates a heterozygous plant, and a single 460-bp band indicates a homozygous mutant. The presence of homozygous *pp2c-Ds/pp2c-Ds; fer/fer* plants containing a wild type At3g51550 transgene indicates complementation. (D) Genotyping PCR for complementation with construct *pFER::FER-GFP* (as above).

To confirm complementation, seed counts were performed on 7-14 siliques from different branches of nine transformants. Large, brown seeds were scored as normal; shrunken, dark seeds as aborted; and small, white structures as unfertilized ovules. As would be expected for hemizygous plants segregating the transgene, plants genotyped as heterozygous for the *Ds* element had approximately 75% normal seeds compared to the 50% normal seeds of the *fer* mutant, homozygous plants showed about 50% normal seeds (Table 1). Aniline blue staining of these lines demonstrated

a reduction in the number of ovules with a *fer* phenotype. Thus, the 4-bp insertion in the At3g51550 gene is responsible for the *fer* mutant phenotype.

Genotype	Fertilized (%)	Unfertilized (%)	N (Ovules)	P-Value
L*er* wild type	98	2	363	-
fer/*FER*	51	49	2004	0.92[a]
fer/*FER* ; T[*gFER*]/ -	74	26	738	0.47[b]
fer/*FER* ; T[*gFER*]/ -	77	23	367	0.35[b]
fer/*fer* ; T[*gFER*]/-	50	50	550	1.00[a]
fer/*FER* ; T[*pFER::FER-GFP*]/-	75	25	201	0.97[b]

[a] χ^2-Test based on the expectation that 50% of the gametophytes carry a wild-type *FER* allele (endogenous or transgenic).

[b] χ^2-Test based on the expectation that 50% of the *fer* gametophytes also carry an unlinked complementing *FER* allele (transgenic).

Table 1: ***At3g51550*** **complements the** ***feronia*** **mutant.** Representative data of 4 the 41 complementation lines are shown, either carrying a genomic (T[*gFER*]) or a FER-GFP fusion protein (T[*pFER::FER-GFP*]) complementation construct. Lines carrying a single, unlinked complementation construct were chosen. Homozygosity for *fer* was determined by PCR

Homozygous plants are expected to be null mutants for the *PP2C* gene as this fragment was not included in the complementation experiment. Homozygous plants looked stunted but no other striking phenotypes were observed.

3.2 FER encodes a Receptor-like Serine/Threonine kinase (RLK)

Plant RLK's belong to a monophyletic gene family with over 600 members (Shiu and Bleecker 2001). RLKs are transmembrane proteins that receive signals through an extracellular domain and subsequently activate signaling cascades via their intracellular kinase domain.

FER is a unique gene in *A. thaliana.* It belongs to the CrRLK1L-1 subfamily of kinases, no members of which have a known function (Figure 6A) (Shiu and Bleecker 2003). *FER* homologues are present in dicotyledonous species as well as monocotyledonous species such as *Zea mays* and *Oryza sativa.*

Protein prediction programs indicate several features in FER: a signal peptide, a transmembrane domain and an intracellular kinase domain. *FER* posses a membrane

transfer stop signal (RRRKR) next to the transmembrane domain (Schwacke, Schneider et al. 2003). This suggests that FER is processed through the secretory pathway and putatively localizes in the plasma membrane (Figure 6B and Appendix Figure1).

Phosphorylation sites experimentally verified are present in *FER* kinase domain (Nuhse, Stensballe et al. 2004). This indicates that FER is phosphorylated *in vivo* (Figure 6B and Appendix Figure1).

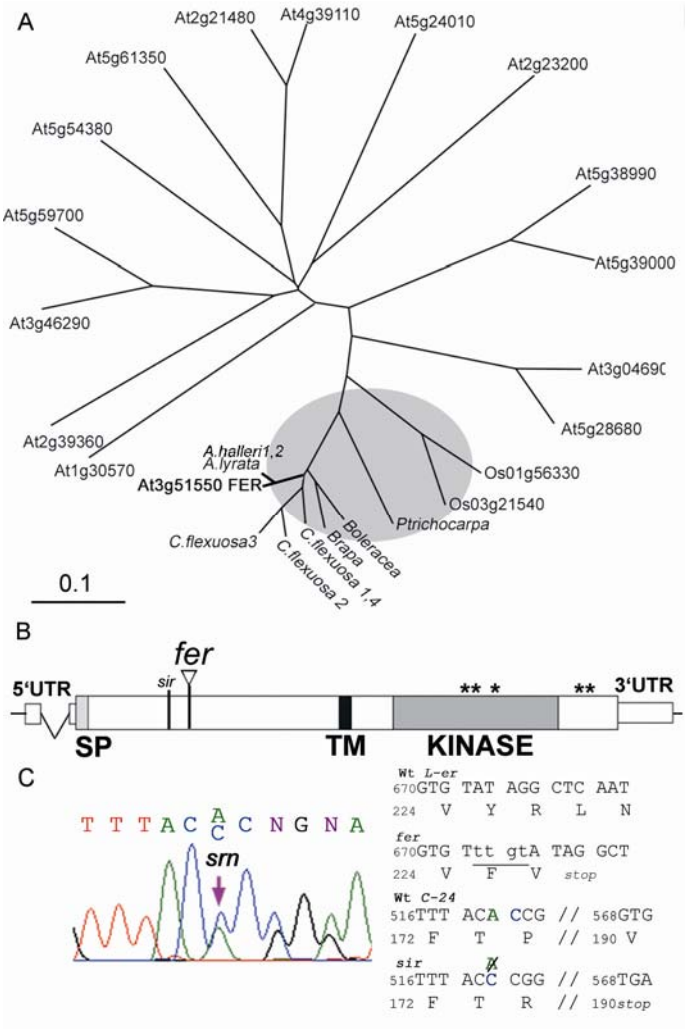

Figure 6. Phylogenetic relationships of *FER*, protein features, and mutations in *fer* and *srn*. (A) Unrooted tree showing *FER* and homologs from different species. The *FER* homologs, whose clade is supported by a 100% bootstrap value, are indicated in gray. The other plant species together with *A. thaliana* in this clade are: *Arabidopsis lyrata*, *Arabidopsis halleri*, *Brassica oleracea*, *Brassica rapa* and *Cardamine flexuosa* homologues 1, 2, 3 and 4 belonging to the Brassicaceae, *Oryza sativa* (Os., Poaceae), and *Populus trichocarpa* (Salicaceae). The rest of the tree contains the *A. thaliana* members of the CrRLK1L-1 subfamily of kinases. The branch length scale bar represents 0.1 substitutions per site. (B) Diagram of *FER's* predicted domains: SP, signal peptide; TM, transmembrane domain, and Kinase domain. Sites of *fer* and *srn* mutations are indicated with black vertical bars, asterisks indicate experimentally found phosphorylation sites. (C) Sequence difference between wild-type and *srn*. Left, sequence chromatogram of *srn/SRN* (in C24 accession), arrow shows a double peak indicating a sequence mismatch. Right, sequence and coordinates of the same chromatogram region indicating a 1 bp deletion and subsequent frame shift that leads to a premature stop codon in *srn*.

3.2.1 *FER* 5' and 3' UTR

FER does not contain any introns in its coding region. Only one intron is present in the 5'UTR between coordinates -216 and -40 (Figure 6B). Interestingly, a scan for UTR motifs in this area identified an Internal Ribosomal Entry Site (IRES) between -90 bp and the initiation codon. Internal mRNA ribosome binding is a mechanism of translation initiation alternative to the conventional 5'-cap dependent ribosome scanning mechanism (Le and Maizel 1997). The same analysis was performed in the 3'UTR of *FER* and an IRES motif was identified as well between coordinates +2892 and +2981bp. Additionally an AU-rich class-2 Element (ARE2) motif (Chen and Shyu 1995) was identified in the 3'UTR of *FER* between coordinates +2795 and 2836bp (Appendix figure 2).

3.3 *fer* alleles

3.3.1 *srn* is allelic to *fer*

As *sir* shows the same phenotype as *fer*, the coding region of At3g51550 was sequenced in the heterozygous mutant and a single base pair deletion was identified. Both mutations lead to frame-shifts that result in premature stop codons in the predicted extracellular domain in At3g51550 (Figure 6C), therefore *fer* and *srn* are allelic.

3.3.2 T-DNA GABI-KAT106A06.04 (JE-250)

To isolate additional alleles of *fer,* a search through mutant catalogues (http://www.gabi-kat.de/) identified a T-DNA insertion in At3g51550. The insertion is shown by the distributors to be located 880 bp from the ATG in Col-0 accession in the extracellular domain of *FER*. The selection marker is sulfadazine and they show that out of 50 seeds, 49 germinated and 33 were resistant to sulfadazine approximating a 2:1 ratio. Aniline blue observation of pollinated pistils revealed the presence of pollen tube overgrowth as in *fer*, surprisingly 72.5 % of the ovules were fertilized and 27.5% showed *fer*-like pollen tube overgrowth (n=883). Seed counts from one plant revealed that 63% of the ovules were fertilized, 36% unfertilized and 1% aborted (n=365 ovules). Neither the insertion location nor the sulfadazine resistant:sensitive ratio were confirmed in our laboratory.

3.4 Temporal and spatial expression pattern of *FER*

3.4.1 Quantitative real-time RT-PCR

To determine the expression pattern at the organ level, quantitative real-time RT-PCR of *FER* transcripts was performed. *FER* mRNA was detected throughout the mature plant: specifically in leaves, buds, flowers and siliques but it was not detected in mature pollen (Figure 7).

Figure 7. Quantification of *FER* transcripts in leaves, closed flower buds, open flowers, siliques collected 1 to 4 days after hand pollination (1-4 dap) and mature pollen grains. Transcript levels were normalized to ACTIN11; average and standard deviation of three quantification replicas are shown.

3.4.2 mRNA *in situ* hybridization

To investigate the spatio-temporal expression pattern of *FER* at the cellular level, *in situ* hybridization of *FER* mRNA was performed. *FER* transcripts were detected in floral apices, young ovule primordia, and in young anthers with immature pollen (Figure 8A,B,C). In older anthers harboring mature pollen, *FER* message was not detected (Figure 8D), consistent with the quantitative real-time RT-PCR experiments. In emasculated flowers, rarely a very weak *FER* signal was detected throughout mature unfertilized ovules, and a somewhat stronger signal could be detected in the synergid cells (Figure 8E). After fertilization *FER* transcripts were detected in globular embryos (Figure 8G) consistent with the finding that, in rare cases where fertilization of *fer* gametophytes is achieved, the resulting homozygous embryos abort (Huck, Moore et al. 2003). In the complementation experiments both the defect in pollen tube reception and embryo lethality were rescued by a wild-type copy, demonstrating that *FER* is also required after fertilization.

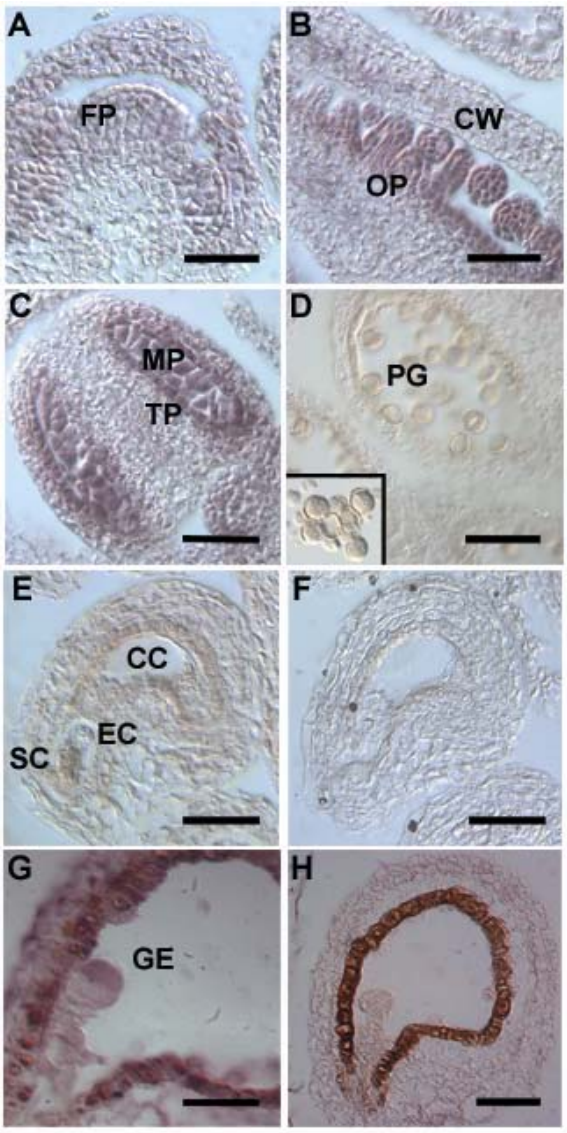

Figure 8. Temporal and spatial expression of *FERONIA*. (A-H) *in situ* hybridization. Panels (A-E) and (G), were hybridized with an antisense *FER* probe, while panels (F) and (H) were hybridized with a sense probe. (A) and (B) *FER* mRNA is present in the floral apex (A) and in ovule primordia (B). (C) *FER* mRNA is expressed in anthers and microspores during early pollen development but the transcript levels in mature pollen (D) are below the limit of detection (inset shows the sense control). (E) *FER* transcript can be detected in the synergid cells of the female gametophyte. (F) Sense control in the female gametophyte. (G) After fertilization, *FER* mRNA was detected in globular embryos. (H) Sense control in a fertilized ovule with a globular embryo.

3.4.3 GUS reporter analysis of *FER* promoter activity

To confirm the results of the *in situ* hybridization and the quantification of *FER* transcripts, a genomic fragment containing the putative *FER* promoter (1.3 kb upstream of the start codon) was fused to the bacterial *uidA* ORF encoding β-glucuronidase (GUS) (Provided by Norbert Huck) (*pFER::GUS*). Using a chromogenic substrate for GUS, in six independent lines it was found that the *FER* promoter is active in the leaves (Figure 9A), young anthers (Figure 9B), mature anther filament (Figure 9C) and roots (not shown). GUS activity was not found in mature pollen (Arrow in Figure 9B). In female tissues, GUS activity could not be detected in ovule primordia (Inset in Figure 9D) and it started to be detected in ovules with closed integuments containing an immature gametophyte (Figure 9D).

When mature unfertilized ovules from independent transformants were analyzed, GUS activity was present in the integument sporophytic tissues, and much stronger in the synergid cells of the female gametophyte (Figure 9 E,F).

The paternal copy of the *FER* transgene is silenced after fertilization (Figure 9G) while the maternal copy of the gene is active throughout in the endosperm and embryo (Figure 9H). The paternal copy of the transgene is activated after 6-7 days after pollination in the embryo and lesser activity was detected in the endosperm (Figure 9I).

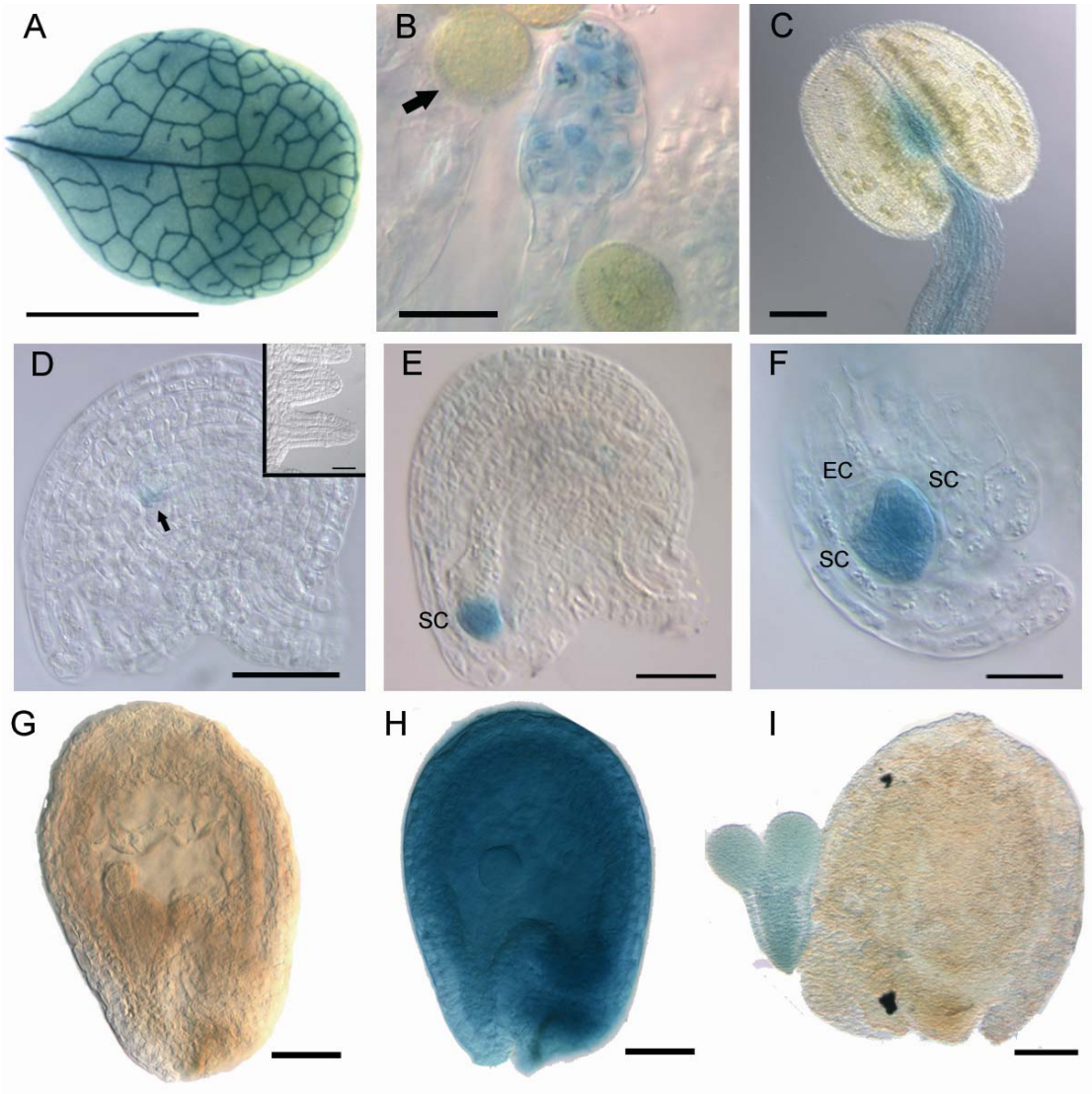

Figure 9. **Analysis of the *FER* upstream transcriptional regulatory region**. *pFER::GUS* (line JE-167) is active in: (A) leaves; (B) young developing anthers; (C) filament of the mature anther; (D) lower part of young embryo sac (arrow), inset shows an absence of signal in ovules primordia and (E) both synergid cells. (F) Higher magnification of the synergids from another ovule. (G) Paternal copy of the transgene is silenced (L-*er* x JE-167) while (H) maternal copy is active in the whole developing seed (JE-167 x L-*er*). (I) Paternal copy is active in the heart-shaped embryo (L-*er* x JE-167). EC, egg cell; SC, synergid cell. Scale bars: (A) 0.5 cm; (B,D) 20 µm; (C) 100 µm; (E,I) 30µm; (F) 15 µm; (G,H) 50 µm. Inset panel (D) 5 µm.

3.5 *FER* gene product localization

3.5.1 Transient expression of GFP tagged proteins under a constitutive promoter

To investigate the subcellular localization of FER, two types of plasmids were designed depending of the position of the *GFP* with respect to *FER*. Plasmids were sequenced and introduced into onion epidermal cells by biolistic bombardment:

Construct *35S::GFP-FER* has the *GFP* positioned upstream of *FER*. Epifluorescence microscopic examination of the fusion protein showed GFP localization in the cytoplasm, nucleus, and in patches surrounding the nucleus (Figure 10A,B).

Construct *35S::FER-GFP* has the *GFP* positioned downstream of *FER*. Epifluorescence microscopic examination detected three GFP positive cells out of 52 bombarded samples, while for the control plasmids, several cells were transformed (aprox. 9 cells per bombarded sample). The transformed cells with *35S::FER-GFP* appeared stressed, either very turgid or plasmolyzed and the nuclei were rough shaped. In one cell, GFP seemed to be both inside and outside the transformed cell in punctuate vesicle-like structures (Figure 10C). 26 hours after the initial observation, the GFP-positive cell could not be found. In the remaining two positive cells, GFP fluorescence was weak, just above the limit of detection and it was localized in small punctuate structures in the surrounding cytoplasmic area of the nucleus (data not shown). 26 hours after initial observation, the GFP positive cell could not be found. Transformed cells with the plasmid controls were observed up to 6 days and no similar signs of stress were found on these cells. Strikingly, a considerable amount of dead-shrunken onion cells were found in samples bombarded with *35S::FER-GFP* as compared to samples bombarded with the control plasmids.

Stressed cells autofluoresce under U.V excitation, and were therefore, not necessarily glowing by the presence of introduced GFP. A third plasmid was constructed to discriminate if the low amount of transformed cells was due to a non-functional plasmid. The same **att***FER***att** fragment used for the *35S::FER-GFP* plasmid, was used to construct the plasmid *35S::FER-GUS* (see Material and Methods) and introduced into onion cells. After incubation of samples in a chromogenic substrate for GUS, a similar amount of GUS positive cells as GFP positive cells from the control were recovered (Figure 10E). As the construct seemed

to be functional, the small amount of *35S::FER-GFP* cells compared to *35S::FER-GUS* cells (GFP can only be observed in live cells) and the big amount of dead-shrunken cells in *35S::FER-GFP* bombarded samples suggested that the construct itself is toxic to plant cells.

A new set of bombardments with construct *35S::FER-GFP* were performed. In this experiment, samples were incubated with an apoptosis inhibitor (Ac-DEVD-CHO). Several GFP-positive cells were recovered (aprox. 6 cells per bombarded sample). With epifluorescence microscopy, GFP was observed throughout in the onion cell and preferentially accumulated towards the periphery of the cell (Figure 10F,G). CSLM observation of the same samples showed a specific accumulation in the periphery of the cell towards the plasma membrane and less in the cytoplasm (Figure H,I). Additionally, several dead-shrunken cells were also found in the same GFP-positive samples. Bombarded onion samples transformed with control plasmids and incubated with the apoptosis inhibitor did not change the localization of the GFP (data not shown).

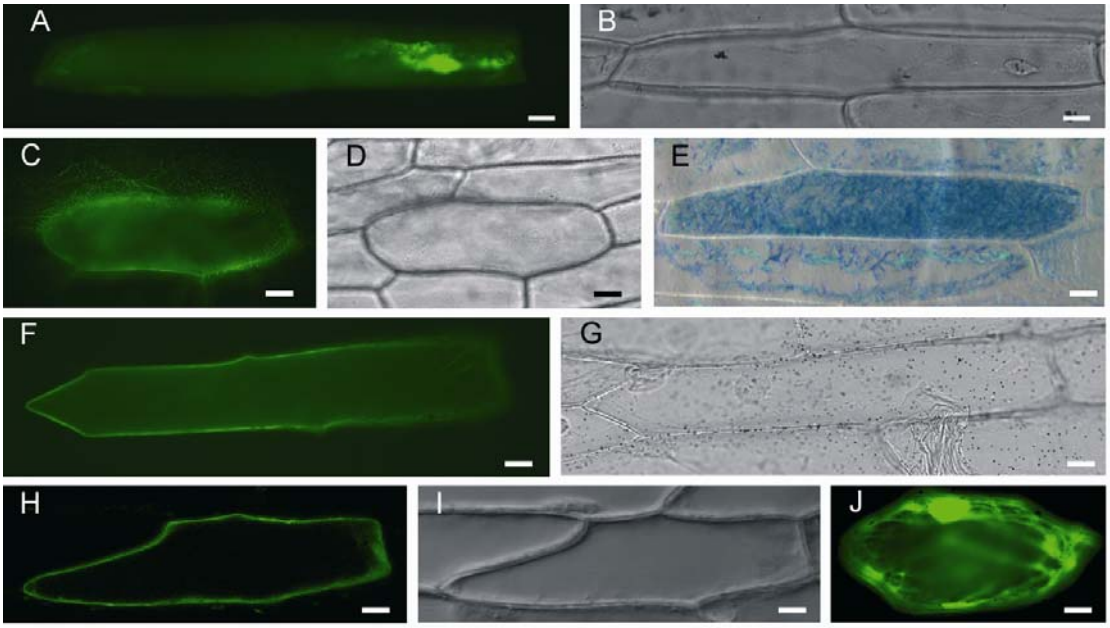

Figure 10. **Transient subcellular localization of FER in onion cells driven by a constitutive promoter**. (A) Epi-fluorescence micrograph of cell expressing *35S::GFP-FER;* GFP is located in patches around the nucleus, in the nucleus, and in the cytoplasm. (B) same cell as in (A) under Nomarski microscopy. (C) Epi-fluorescence micrograph of a cell expressing *35S::FER-GFP;* GFP is located in the cytoplasm, at the edge of the cell and in small punctuate structures inside and outside the cell. (D) The same cell as in (C) under Nomarski microscopy. (E) Cell expressing *35S::FER-GUS.* (F) Epi-fluorescence micrograph of a cell expressing *35S::FER-GFP* and treated with a Caspase3 inhibitor; GFP is seen in the cytoplasm and preferentially at the edge of the cell. (G) Same cell as in (F) under Nomarski microscopy. (H) CLSM optical section of a cell expressing *35S::FER-GFP* and treated with a Caspase3 inhibitor; GFP is preferentially located at the edge of the cell. (I) Same cell as in (H). (J) Epi-fluorescence micrograph of cell expressing *35S::GFP;* GFP has no specific localization to a cell compartment but it is preferentially accumulated in the nucleus and cytoplasm. All scale bars are 30 μm.

3.5.2 Transient expression of GFP-tagged proteins under the *FER* native promoter

Since the *35S::FER-GFP* construct seemed to be lethal to bombarded cells, a plasmid was constructed in which the *FER-GFP* fusion is driven by *FER*'s native promoter: *pFER::FER-GFP*. The construct was used to transiently transform onion epidermal cells, *A. thaliana* protoplasts and *A. thaliana* leaves.

CLSM analysis of bombarded onion epidermal cells showed that FER-GFP is localized in the plasma membrane as shown in Figure 11A,B, after induction of incipient plasmolysis, GFP remained in the plasma membrane and not in the cell wall. Additionally, GFP was observed at low levels in small vacuoles (data not shown).

CLSM analysis of transformed protoplast showed three distinct localizations: GFP was localized in one side of the plasma membrane of the protoplast (Figure 11C), in small vesicles (Figure 11D), and in vacuolar compartments as concluded from co-transfection with a KCO1-DsRED-tagged vacuolar protein (Figure 11 E,F) (provided by Krasimira Marinova, University of Zürich, Switzerland).

CLSM analysis of bombarded *A. thaliana* leaves showed GFP localization in the tonoplast (vacuolar membrane). Figure 11G shows an *A. thaliana* leaf cell were the GFP is located at the periphery of the cell and forms a nuclear pocket (Figure 11G inset), this structure is formed by the space between the nucleus and the tonoplast as the nucleus resides outside of the vacuole in the cytoplasm of the cell and it is characteristic of tonoplast markers.

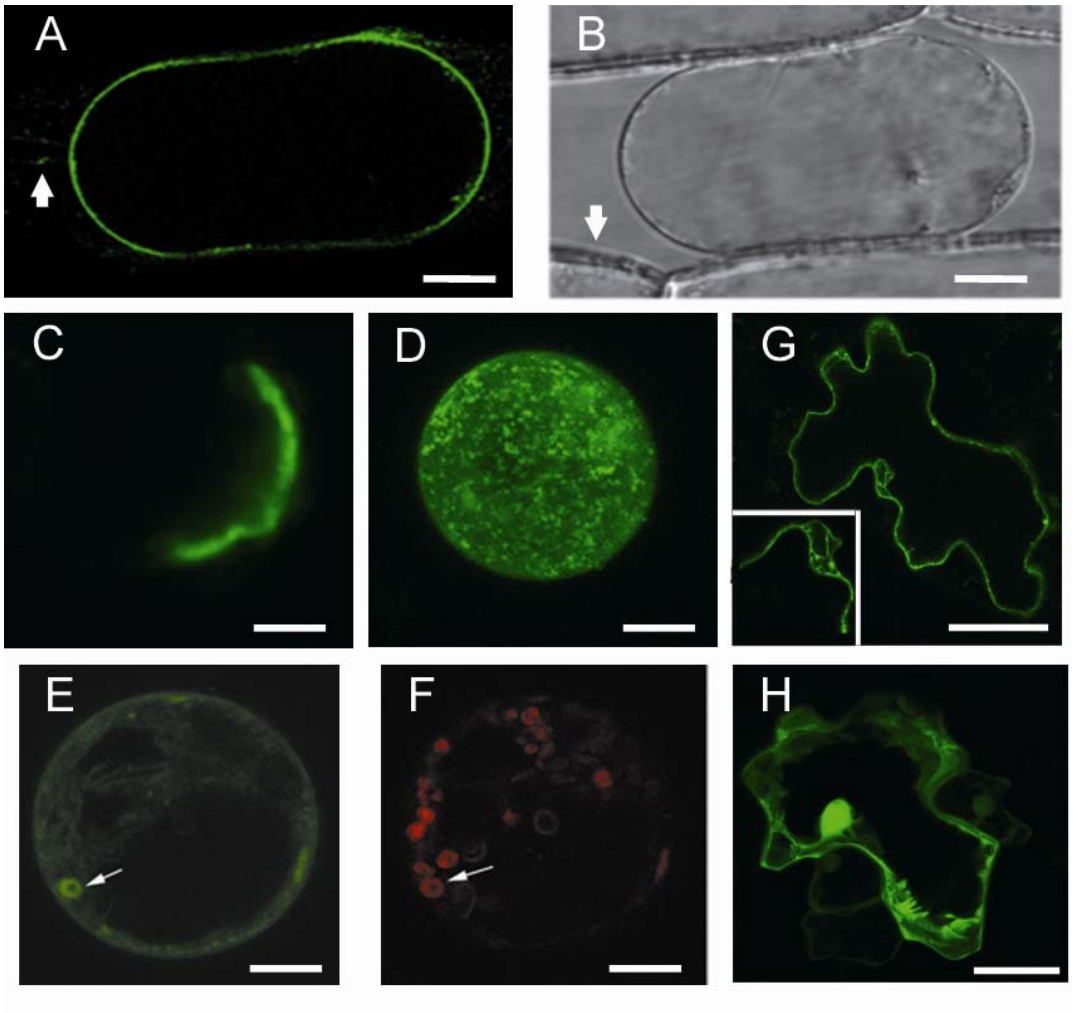

Figure 11. **Transient subcellular localization of FER-GFP driven by *FER* promoter in onion cells, *A. thaliana* protoplasts and *A. thaliana* leaves**. (A) CLSM single section of a plasmolysed onion cell expressing *pFER::FER-GFP;* GFP is located at the plasma membrane, white arrow shows Hechtian strands stained with GFP. (B) Same cell as in (A), white arrow shows the cell wall; retracted contents of the protoplast are due to incipient plasmolysis. (C) CLSM maximum projection of several sections of *A. thaliana* protoplast; GFP is located at the periphery of the cell at the plasma membrane at only one side of the cell. (D) CLSM maximum projection of several sections of *A. thaliana* protoplast; GFP is located in the cytoplasm and in small vesicles. (E) CLSM section of *A. thaliana* protoplast; GFP is located in tonoplast of small vacules, perifery of the cell and cytoplasm. (F) Same cell as in (E) co-stained with Ds-Red; Ds Red is observed in tonoplast of small vacuoles and co-localizes with one of the vacuoles observed in (E) (arrow). (G) CLSM single section of an *A. thaliana* leaf; GFP is located at the periphery of the cell in the tonoplast membrane of the vacuole. Inset shows a magnification of a nuclear pocket formed by the space between the nucleus and tonoplast. (H) CLSM single section of an *A. thaliana* leaf expressing *35S::GFP;* GFP has no specific localization to a cell compartment but it's preferentially accumulated in the nucleus and cytoplasm. Scale bars: (A,B) 30 µm; (C-F) 3 µm; (G,H) 50 µm.

3.5.3 Stable expression of GFP-tagged proteins under the *FER* native promoter

As the above mentioned trangene showed no lethal effect in transient experiments, the *pFER::FER-GFP* plasmid was used to stably transform *A. thaliana* wild-type and *fer* mutant plants,.with the objective to study the subcellular localization and dynamics of the introduced construct. The introduced transgene complemented the *fer* mutation (Table 1, Figure 5D). CLSM examination of transformants showed *pFER::FER-GFP* activity in roots (Figure 12A), leaves (Figure 12B), stamens but not in pollen grains (Figure 12C), stigmatic papillae cells (Figure 12F), ovules (Figure 13A,B,C,D,E,F), carpels and stems. Single optical sections on leaves (Figure 12B), roots (Figure 12D) and ovules (Figure 13B) demonstrated a plasma membrane localization of the fusion protein, in addition, GFP was occasionally observed in small vesicles (Figure 12F). Treatment of roots with a vesicle trafficking inhibitor, Brefeldine-A, confirmed the presence of GFP in vesicles (Figure12 E).

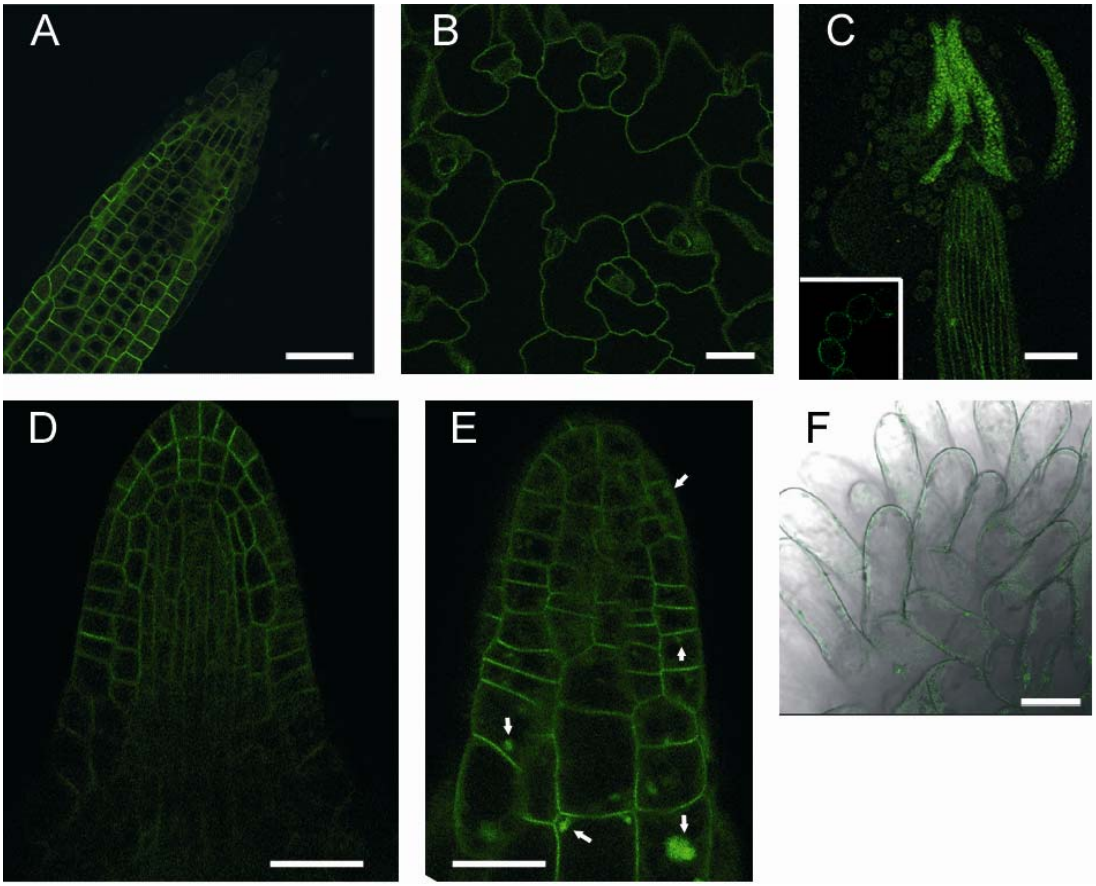

Figure 12. **Subcellular localization of stably transformed *A. thaliana* plants with *pFER::FER-GFP* observed under CLSM**. (A) Single optical section of a root (line JE-216) showing GFP at the plasma membrane and weaker in the cytoplasm. (B) Single section of leaf epidermal cells (line JE-216) showing GFP localization at the plasma membrane, note that no nuclear pocket is found (inset Fig. 11G). (C) Maximum projection of several sections an anther (line JE-236) showing GFP at the periphery of the cells of the filament, GFP is found as well in the cells surrounding the pollen sacks. Inset shows autofluorescence of pollen grains from a plant without the transgene. (D) Single section of a root (line JE-216) showing GFP at the plasma membrane and weaker at the cytoplasm. (E) Single section of the same root as (D) after treatment with Brefeldin-A; GFP is found at the plasma membrane and in Brefeldine compartment-vesicles (arrows). (F) Single section of the top region of the stigma (line JE-226); GFP is at the periphery of papillae cells and in vesicles as well. Scale bars: (A) 40 µm; (B) 10 µm; (C) 50 µm; (D,E) 30 µm; (F) 20 µm.

Closer observation of unfertilized ovules revealed the accumulation of high levels of GFP signal in the filiform apparatus of both synergids. Weaker GFP fluorescence was detected in the membranes of the synergid cells, the surrounding maternal sporophytic cells, as well as faintly in the egg cell (Figure 13D). Since the filiform apparatus is a structure rich in plasma membrane, it was tested if the asymmetric accumulation of FER in the synergid plasma membrane is an artifact by comparing with another plasma membrane localized GFP fusion in the female gametophyte, *pAtD123::EGFP-AtROP6C* (JE-238). Under the same growth conditions, FER-GFP levels were much higher in the filiform apparatus than in the rest of the synergid cells when compared to EGFP-AtROP6C (Figure 13D and inset). Analysis of the region of the filiform apparatus, revealed an uneven distribution and accumulation of FER-GFP in several vesicle like structures (Figure 13E).

Analysis of pollinated pistils revealed that the GFP localization in the lower part of the synergid cells co-localizes with the entrance of the pollen tube (Figure 13F). Probably due to toxicity of Congo Red staining, GFP localization in the sporophytic tissues was no longer at the plasma membrane, but cytoplasmic.

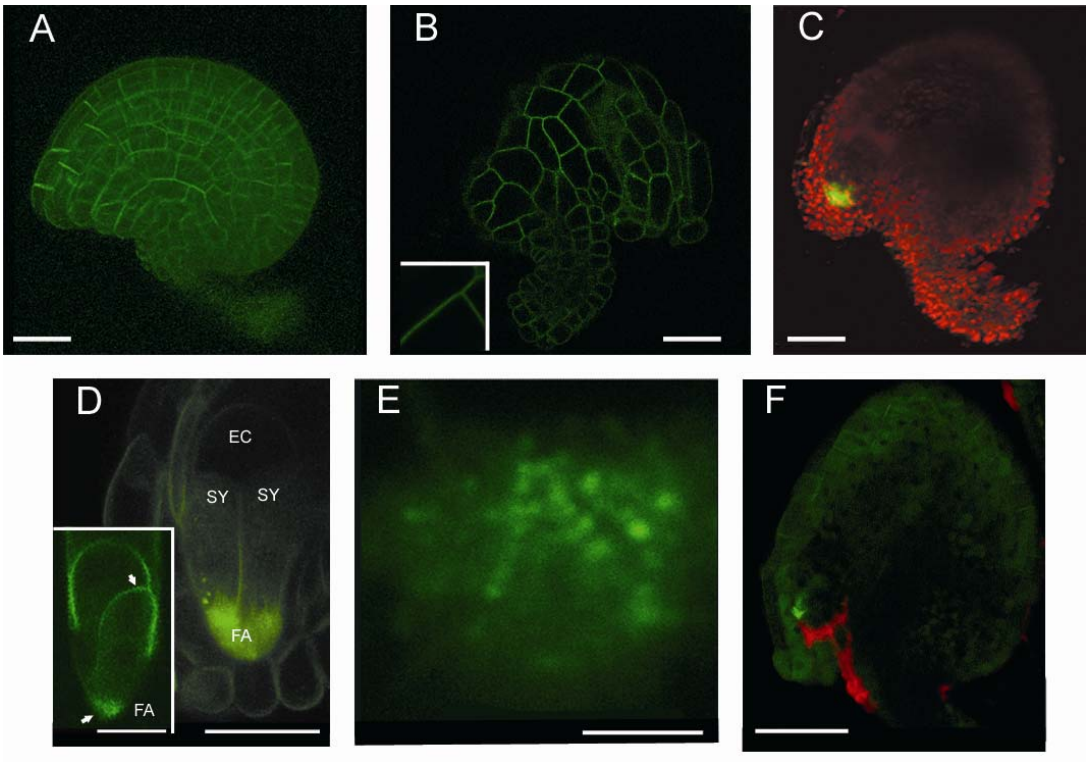

Figure 13. **CLSM analysis of *A. thaliana* ovules stably expressing *pFER::FER-GFP*.** (A) 3D reconstruction of several sections of an ovule (line JE-217). GFP is present in sporophytic cells. (B) Single section of surface region of an ovule (line JE-236); GFP is present at the plasma membrane, inset shows a magnification of the area comprising 3 cells were GFP is at the periphery. (C) Maximum projection of several sections of an ovule (JE-217); GFP is shown in green and chlorophyll autofluorescence is shown in red; levels of GFP are stronger in the lower part of the synergid cells. (D) Maximum projection of several sections of the micropyle area of an unfertilized ovule (line JE-217); GFP accumulates in the filiform apparatus of the synergids. Inset shows a maximum projection of several sections of another plasma membrane protein in the female gametophyte. Top arrow indicates upper part of synergids, lower arrow indicates region of filiform apparatus of synergids. (E) Magnification of the area of a filiform apparatus (line JE-236), GFP is located in a diffuse mass and in punctuate structures. (F) Maximum projection of several sections of a fertilized ovule 7 hours after pollination (line JE-235), GFP is shown in green and pollen tube stained with Congo Red is shown in red; GFP in the gametophyte is localized at the site of pollen tube entry, GFP signal in the sporophyte cells is at the cytoplasm and not a the plasma membrane. Scale bars: (A-C) 40 µm; (D) 20 µm; (E) 2.5 µm; (F) 50 µm.

3.6 Interspecific pollinations between *A. thaliana* and relative species

In incompatible inter-specific crosses of Rhododendron species pollen tube growth does not arrest. This results in pollen tube overgrowth in the female gametophyte similar to the phenotype observed in *fer* (Kaul, Rouse et al. 1986; Williams, Kaul et al. 1986). An inter-specific cross where wild-type *A. thaliana* is pollinated by a related Brassicaceae species might also produce a *fer* phenotype. Pollen from different species was used to pollinate emasculated *A. thaliana* plants of the L*er* accession and observed under an epifluorescence microscope after aniline blue staining of callose for scoring of *fer* like phenotypes.

A. thaliana x *Brassica oleracea:* pollen tubes germinate but do not leave the transmitting tract towards the funiculus.

A. thaliana x *Cardamine bulbifera:* no germination of pollen tubes.

A. thaliana x *Cardamine trifolia*: no germination of pollen tubes.

A. thaliana x *Cardamine flexuosa* (JE-214): only 7.7% of *A. thaliana* ovules attracted pollen tubes, 1.6% had pollen tubes that entered the micropyle and stopped as previously reported, 0.8 % had pollen tubes coiling outside their micropyles, and in 5.3% of the ovules the pollen tubes entered the micropyles but failed to arrest their growth (Figure14B) (n=363 ovules).

A. thaliana x *Cardamine hirsuta*: pollen germinated and grew towards the funiculus but did not find the ovules.

A. thaliana x *Erysimum linifolium*: pollen tubes found the ovules and caused severe pollen tube overgrowth (counts not performed).

A. thaliana x *Arabidopsis lyrata* (JE-254): In crosses with the close relative *Arabidopsis lyrata*, pollen tubes were correctly targeted to the female gametophytes but only 43.9% of the ovules received pollen tubes and were fertilized, 5.2 % of the ovules were fertilized with more than one pollen tube in the same micropyle and had pollen tube overgrowth inside the female gametophyte (Figure 14C) and 50.9 % of the ovules had pollen tubes that continued to grow inside the female tissues and unsuccessful fertilization is seen as in *fer* mutants (Figure 14A) (n= 813 ovules). (The reciprocal cross was performed but *A. thaliana* pollen tubes do not grow further than the stylar tract in *A. lyrata* pistils).

A. thaliana x *Arabidopsis halleri*: all ovules were targeted and successfully fertilized (the reciprocal cross was performed but *A. thaliana* pollen tubes do not grow further than the stylar tract as seen in *A. lyrata* x *A. thaliana* cross).

A. thaliana x *Capsella bursa pastoris – rubella?*: pollen tubes germinate but the majority do not find the ovules. Two pollen tubes had balloon-like tips.

A. thaliana x *Boechera holboellii*: 15.8% of ovules had pollen tubes that continued to grow inside the female tissues as seen in *fer*. The rest of the ovules had pollen tubes close to the micropyle but no fertilized ovules were observed (n=190 ovules). A few pollen tubes had balloon-like structures at the tip.

A. thaliana x *Cardaminopsis arenosa* (JE-245, 246): 77.4% of the ovules were fertilized, 18.5% were unfertilized and 4.1% had *fer* pollen tube overgrowth phenotypes (n=146 ovules).

A. thaliana x *Lobularia maritima*: pollen tubes germinate but stop to grow after leaving the style.

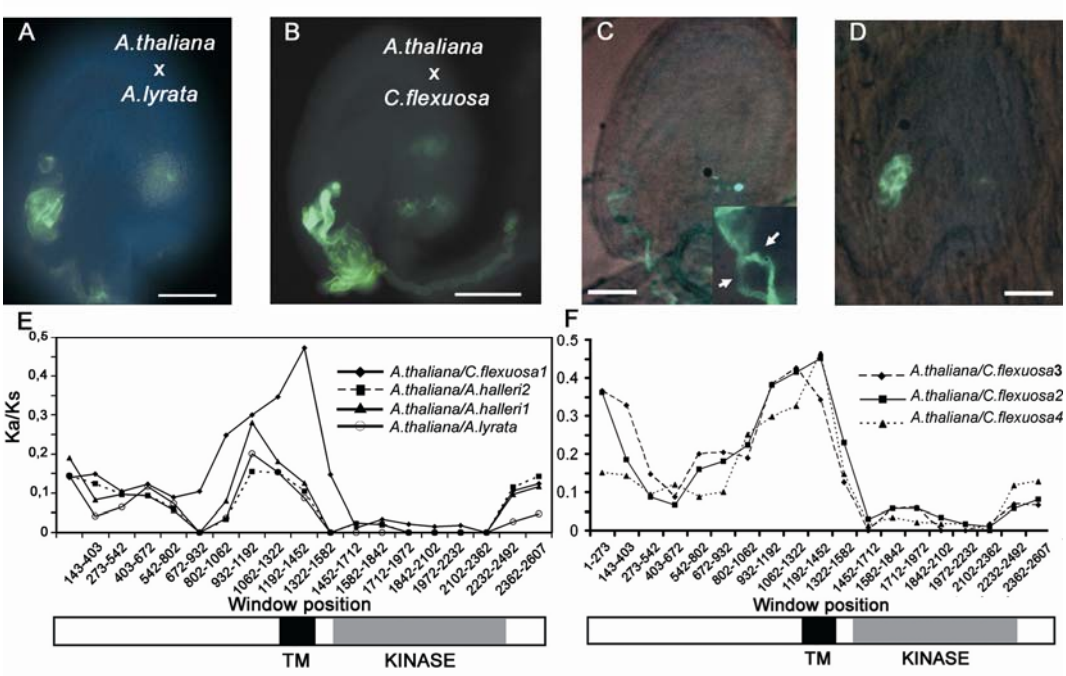

Figure 14. **Inter-specific crosses and Ka/Ks ratios of pairwise comparisons**. (A,B) Fluorescence micrograph of aniline blue stained callose of pollen tubes. Pollen tube overgrowth is seen in unfertilized ovules as in the *fer* mutant. (C) Interspecific cross between *A. thaliana x A. lyrata;* pollen tube overgrowth is observed and two pollen tubes (arrows) approach the same ovule. (D) Pollen tube overgrowth in a fertilized ovule of an *A. thaliana x A. lyrata* cross. (E,F) Sliding window analysis of pairwise comparisons. Higher Ka/Ks ratios are found in the extracellular portion of *FER* while the intracellular is more conserved. Signal peptide was excluded from the analysis. All scale bars represent 30 μm.

3.7 Evolutionary forces driving *FER* evolution

As genes involved in reproduction may evolve at different rates than other genes (Swanson and Vacquier 2002), four types of evolutionary analyses were performed on the *FER* coding region to unravel the evolutionary forces acting on *FER*.

3.7.1 Ka/Ks pairwise analysis of FER

This analysis measures the rate between Ka (the number of nonsynonymous substitutions per nonsynonymous site), and Ks (the number of synonymous substitutions per synonymous site) for pairs of aligned windows of sequences (Nei and Gojobori 1986). Ka/Ks can be used to determine if parts of a protein are under different selective pressures. Additionally, when Ka/Ks = 1 it suggest a neutral type of selection. In the case of purifying selection, Ka decreases and results in ratios of Ka/Ks < 1. Finally, cases where Ka/Ks > 1 are suggestive of positive Darwinian selection.

Ka/Ks ratios were high in the extracellular portion of *FER* (highest peak at 0.5) and lower in the intracellular part (lowest peak at 0) for *A. thaliana* x *C .flexuosa, A. thaliana* x *A. lyrata*, *A. thaliana* x *A. halleri* pairwise comparisons (Figure 14E,F). This indicates that different selective pressures acts in different parts of the protein and its suggestive of positive selection acting in the extracellular portion of *FER*.

3.7.2 Phylogenetic analysis by maximum likelihood

A phylogenetic tree of *FER* homologues from different species was constructed (Figure 15) and used in the CODEML program of the PAML package (Yang 1997) to estimate synonymous (dS*)* and nonsynonymous (dN) substitution rates, likelihood ratios tests of positive selection or relaxed selective constraints along lineages based on the dN/dS rate ratios (ω) and to identify amino acid sites or evolutionary lineages potentially under positive selection.

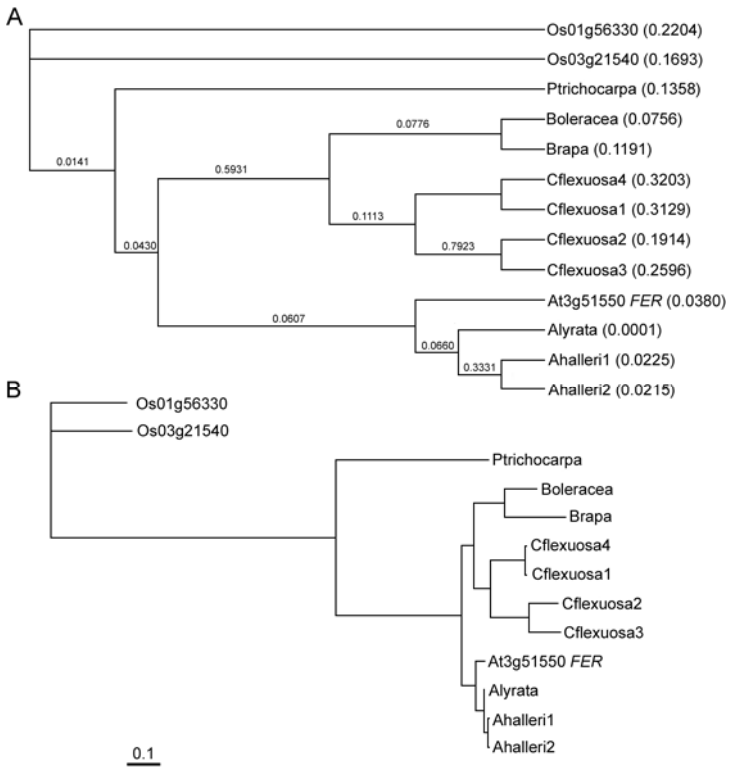

Figure 15. **Unrooted trees used for maximum likelihood analysis of positive selection.** (A) Maximum likelihood tree of *FER* and homologues from different species. **ω** ratios are depicted on top of each analyzed branch. (B) Same tree as (A) with branch lengths in parenthesis. The branch length scale bar represents 0.1 substitutions per site.

The ω ratio is a measure of natural selection acting on the protein. Values of ω >1, =1 and <1 suggest positive selection, neutral evolution, and negative purifying selection, respectively. The ratio averaged over all sites and all lineages is rarely >1, because positive selection most likely affects only some sites or some lineages. Several models were tested: Model 0 (M0) allows one ω for the whole phylogeny. Branch model M1 assumes an independent ω ratio for each branch. Site models M1a (nearly neutral), M2a (positive selection), M3 (discrete), M7 (beta) and M8 (beta and ω) allows the ω ratio to vary among sites. Finally, branch-site model A (with ω=1 and ω =estimated) attempts to detect positive selection that affects only a few sites along a few lineages.

Maximum likelihood evaluates the probability that the chosen evolutionary model will have generated the observed changes in the coding sequence. Therefore, likelihood ratio tests (LRT) between the models were performed for testing positive selection (see Material and methods).

The phylogeny shows the ω ratios obtained from model M1 (Figure 15A) and none of the ω's were higher than 1. Comparison between M0 and M1 revealed that certain branches in the phylogeny experience different selective pressures and therefore, have different dN/dS values, but none of the models tested showed signs of positive selection (Table 2).

Comparisons of different ω between branches did identify that in the following branches the ω ratio is significantly different from each other: *C. flexuosa / Arabidopsis*, *A .flexuosa / A. thaliana*, *A. halleri / A. thaliana*. The comparison between *A. lyrata / A. thaliana* was not significantly different.

MODEL	**ln L**	**P-value LRT**
M0	-13360.908668	M0/M1=0 *
M1	-13280.516366	
NSsites		
M1a	-14065.780791	M1=M2a
M2a	-14065.780791	
M7	-13973.987765	M7/M8=**0.1763**
M8	-13972.252374	
Branch-flexuosa		
ω fixed	-13099.278681	**1** (same lnL)
ω not fixed	-13099.278681	
Branch-site flexuosa		
Model A **ω** =1	-13099.278681	**1** (same lnL)
ModelA **ω** =estimated	-13099.278681	
ω different between branches		
C.flexu/Arabidopsis		*0.0203**
C.flexu/A.thaliana		*<0.0001**
A.halleri/A.thaliana		*0.0303**
A.lyrata/A.thaliana		*0.1575*

Table 2. **Summary of tests for positive selection under the CODEML program**. None of the test performed found signatures of positive selection. * statistical evidence that **ω** is different between the compared branches.

3.7.3 Neutral tests of selection

The neutral theory of evolution postulates that the majority of molecular changes in evolution are due to the random fixation of neutral or nearly neutral mutations (Kimura 1968). Deviations from the theory predict that the variability within species is caused either by positive selection or balancing selection.

3.7.3.1 Tajima's D and Fu – Li (D* and F*) tests

Tajima's D tests the hypothesis that all mutations are selectively neutral. The D test is based on the differences between the number of segregating sites and the average number of nucleotide differences (Tajima 1989). The statistical tests D* and F* (Fu and Li 1993), test the hypothesis that all mutations are selectively neutral.

Positive values of Tajima's D, D* and F* arise from an excess of intermediate frequency alleles and can result from population bottlenecks, population structure and/or balancing selection. Negative values of Tajima's D, D* and F* indicate an excess of low frequency alleles and can result from population expansions or positive selection.

Table 3 summarizes the results for *FER* and the *FER* extracellular domain compared with other published genes where the tests were performed (Olsen, Womack et al. 2002). Positive values for Tajima's D, D* and F* were found for *FER* and the *FER* extracellular domain, while negative values were found for *AP3* and *TFL1* suggesting that sampled alleles show an excess of rare polymorphisms over that expected in a population at mutation-drift equilibrium (Olsen, Womack et al. 2002).

Gene	Length (kb)	*n*	$\bar{\pi}$ (silent)	π(non-synonymous)	Tajima *D*	Fu and Li *D**
FER	2.6	11	0.0053	0.00087	0.25328 ($P > 0.10$)	0.21201 ($P > 0.10$)
FER(ECD)	1.2	11	0.0089	0.0018	0.863 ($P > 0.10$)	0.399 ($P > 0.10$)
AP3	1.7	19	0.0077	0.0040	-2.151 ($P<0.05$)*	-3.373 ($P<0.02$)*
TFL1	1.1	14	0.0007	0.0014	-2.032 ($P<0.05$)*	-2.600 ($P<0.02$)*

* Significant at the 0.05 level

Table 3. **Comparisons with published Tajima's D, Fu and Li's D* neutrality tests for different genes with *FER*.**

3.7.3.2 McDonald Kreitman test

The neutral theory predicts that the variation within populations and the differences between populations are due to neutral or nearly neutral mutations. For this test, a nucleotide site is polymorphic if it shows variation in both species, in this case for *FER* accessions in *A. thaliana* (intraspecific variation) compared to *FER* in *A. lyrata* (interspecific variation). If divergence and polymorphism are due solely to genetic drift acting on neutral mutations, then the ratio of nonsynonymous to synonymous fixed differences between species will be the same as the ratio for polymorphisms within species. A significant deviation from these ratios can be used to reject the neutral mutation hypothesis.

Table 4 summarizes the results for *FER* and the *FER* extracellular domain compared to published analysis of other plant genes that are involved in developmental processes (Olsen, Womack et al. 2002). Analysis on *FER* and *TFL1* shows that the ratios are not significantly different and, therefore, do not show a deviation from the neutral theory hypothesis. In contrast, for *AP3* the test was

significant, although the authors conclude that there is no positive selection on this gene based on additional data (Olsen, Womack et al. 2002).

	Polymorphisms		Fixed differences[a]		
Gene	**Replacement**	**Synonymous**	**Replacement**	**Synonymous**	**McDonald-Kreitman**
FER	4	10	22	106	P= 0.466
FER(ECD)	4	7	19	49	P =0.721
AP3	19	9	6	14	P = 0.018*
TFL1	3	1	3	13	P = 0.061

* Significant at the 0.05 level.

[a] Compared with *A. lyrata*.

Table 4. **Comparisons with published McDonald-Kreitman test for neutrality for different genes with *FER*[a]**

3.8 Components of the *FER* cascade

In an attempt to identify novel components of the *FER* signaling cascade, *A. thaliana* plants containing the LAT52::EGFP construct that stains the pollen grains and pollen tubes with GFP, were mutagenized with EMS. The screening strategy was to screen for aberrant pollen tube reception, based on GFP fluorescence of pollen tubes under an epifluorescence microscope. An initial test on the screening strategy proved it to be unrealistic. Carpels from pollinated pistils had to be dissected to observe the ovules under the epifluorescence microscope. As autofluorescence from chlorophyll is strong, and after dissecting away the carpel walls, the dead surrounding tissue autofluoresced, the GFP inside the synergids after pollen tube explosion was difficult to observe even under high magnification (Figure 16A). Another problem was the remaining pollen grains in the tissue to be analyzed, as the strong GFP fluorescence blocked the observation of pollen tubes and exploded pollen tubes. A wash step was necessary to remove the pollen grains and was not always successful.

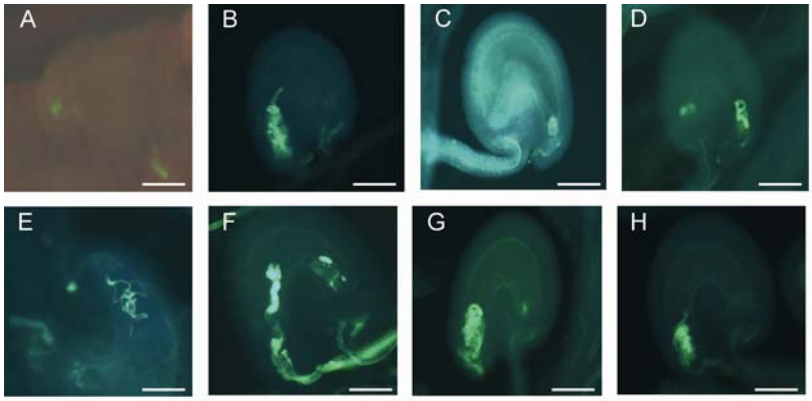

Figure 16. **M1 EMS mutagenesis screen**. Fluorescence micrograph of aniline blue stained callose of pollen tubes. (A) Observation of Lat52::EGFP under epi-fluorescence microscope. GFP signal in a pollen tube and in synergids is weakly present, red is chlorophyll autofluorescence. (B) Pollen tube overgrowth in an ovule from mutagenized tray 12. (C) Ovule from tray 5. (D) Ovule from tray 6. (E,F) Ovules from tray 13, pot 335. (G,H) Ovules from tray 14, pot 364. All scale bars represent 30 μm.

A second screening strategy was based on aniline blue staining of callose. This strategy, although laborious, proved to be better as the tissue could be kept for several days and observation of callose fluorescence of pollen tubes was evident under an epifluorescence microscope (see Material and Methods).

In total 1500 plants were screened in the M1 generation and six independent pools of material (See Material and Methods) showed a *fer*-like phenotype of pollen tube overgrowth (Figure 16B,C,D,E,G). None of the material showed more than two ovules with pollen tube overgrowth per analyzed silique (aprox. 40 - 50 ovules in one silique). None of the analyzed material showed 50% unfertilized ovules as in *fer*. Several other defects were observed in the majority of analyzed tissue, such as shrunken unfertilized ovules and aborted dark shrunken ovules. On the re-screen of the analyzed pools only two phenotypes were traced back to a single pot (which contained three plants). The phenotype could be recovered in the M2 generation (Figure 17A,C,D,F,G,H) but the amount of ovules with *fer* pollen tube overgrowth phenotype was too small, with a maximum two ovules in seven siliques of the same plant. No candidates from this screen were selected for mapping due to the low penetrance of the phenotype.

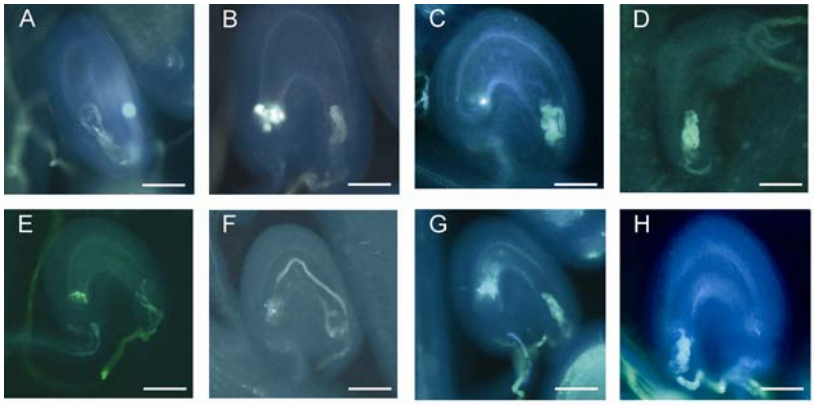

Figure 17. **M2 EMS mutagenesis screen**. Fluorescence micrograph of aniline blue stained callose of pollen tubes. (A) Pollen tube overgrowth from an ovule from line JE-4-8. (B) Ovule from line JE-4-12. (C) Ovule from line JE-6-5. (D,E) Ovules from line JE-13-5. (F) Ovule from line JE-21-14. (G) Ovule from line JE-22-4. (H) Ovule from line JE-24-6.

A second EMS mutagenesis was performed and an additional 500 plants were screened and not a single *fer*-like phenotype was observed.

4. Discussion

The interaction between the female embryo sac and the male pollen tube is necessary for the establishment of a new generation in *A. thaliana*. Most of the mechanisms underlying this event are currently unknown. *FER* is the first identified gene that is involved in one of the steps required for plant reproduction, the reception of the male pollen tube by the synergid cell of the female gametophyte. The results presented in this PhD thesis suggest that *FER* in *A. thaliana* is a female receptor that receives a male signal. The *FER* receptor – male ligand interaction triggers a signaling cascade that allows the explosion of the pollen tube inside the embryo sac, which in turn, leads to a block of the attraction of other pollen tubes and eventually fertilization (Figure 18).

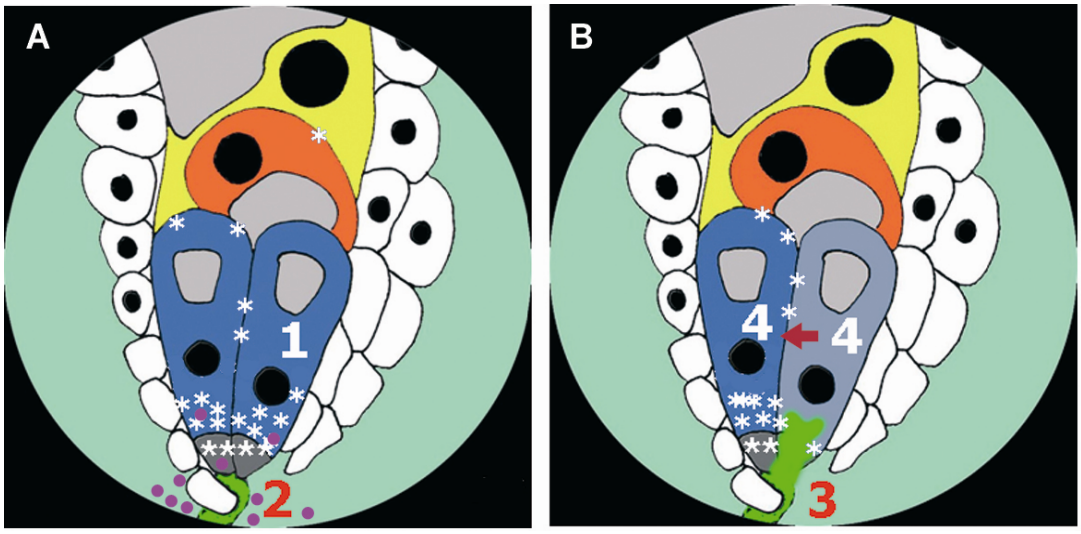

Figure 18. **Model for FER function in the synergids**. (A) FER (*) is produced in the synergids and is mobilized towards the filiform apparatus. Both synergids produce the attractant for the pollen tube (purple circles). **1**. A signaling cascade starts with the interaction between FER and a putative male ligand at the filiform apparatus of the synergids. **2.** Signaling from the synergid feeds back to the pollen tube (green). (B) **3.** Pollen tube explodes in a degenerated synergid. **4.** After pollen tube explosion signaling events cause downregulation of gene expression in the remaining synergid, preventing the production of the pollen tube attractant.

4.1 *FER* At3g51550 controls pollen tube reception in *A. thaliana*

The *fer* mutant was isolated from a collection of transposants containing enhancer detector *Ds* transposable elements. Isolation of flanking sequences indicated that the

Ds element is inserted in *PP2C*, a protein phosphatase gene (At3g51470) on BAC F26O13. However, excision of the *Ds* element failed to revert the *fer* allele to wild type and a genomic fragment containing *PP2C* failed to complement the mutation, indicating that *FER* is not disrupted by the *Ds* element (Huck 2003). From our analysis, we propose that at least two transposition events have occurred in the *fer* mutant line: an initial *Ds* insertion in At3g51550 and then a subsequent excision and re-insertion 21 kb away in the *PP2C.*

The introduction of a wild-type copy of At3g51550 into *fer* mutants complements the *fer* mutation and demonstrates that the insertion in the *PP2C* does not contribute to the mutant phenotype in *fer.* The *FER* gene is therefore responsible for the pollen tube reception event that allows the pollen tube to rupture inside the degenerated synergid cell in *A. thaliana.*

Moreover, complementation experiments with the *pFER::FER-GFP* fragment used for subcellular localization indicates that the 3'UTR of *FER* is interchangeable with the 3' elements included in the plasmid used for the fusion as *FER*'s native 3'UTR was not included in the construct.

4.1.1 Other mutants with pollen tube overgrowth are mutated in At3g51550

The *srn* mutant phenotype was isolated from a cytological screen for mutants in which seeds fail to develop in the absence of structural anomalies in the embryo sacs and pollen (Rotman, Rozier et al. 2003). *srn* displays the same features as *fer:* pollen tube overgrowth, attraction of multiple pollen tubes, and a reduced transmission through the female due to the absence of pollen tube rupture. Therefore, it was not surprising that in both *fer* and *srn,* mutations were found in the same gene causing premature stop codons in the region of the extra cellular domain of At3g51550 (Figure 6B,C).

The T-DNA insertion mutant in the GABI-KAT line (JE-250) raises the question of how the mutant was recovered and why it has differences in the percentage of unfertilized ovules and segregation of the marker compared to *fer*. The embryo sac is the target for T-DNA integration (Desfeux, Clough et al. 2000). If the integration occurs before maturity of the embryo sac, a mutation in *FER* that impairs its function would not be recovered as it is necessary for fertilization. Three alternatives can explain this observation: 1) the mutant copy is not completely dysfunctional or 2) the pollen tube explodes rarely without the need of a functional FER (as seen in *fer*

where transmission through the female is not completely abolished). 3) Enough FER protein was produced before the insertion event occurred. The insertion in JE-250 is yet to be re-confirmed by our laboratory, as well as confirmation of the percentage of sulfadazine resistant and unfertilized ovules in the mutant. First indications point to an allele that is less penetrant.

4.2 *FER* belongs to an uncharacterized family of receptor-like kinases

As observed in Figure 3A, *FER* clusters with sequences from other species (e.g rice, Populus, Brassica) and not with other members of RLK's from *A. thaliana.* This suggests that *FER* is unique in the *A. thaliana* genome and no other gene can substitute for the *FER* function, which is consistent with the severe phenotype of the mutant.

RLKs are transmembrane proteins that receive signals through an extracellular domain, and subsequently activate signaling cascades via their intracellular kinase domain. *FER* is the first gene of the CrRLK1L-1 subfamily of kinases to have an identified function. The phenotype of the mutant and the features of its protein suggest that the reception of the pollen tube is mediated by a signaling mechanism between genders, with *FER* responding to a putative male ligand from the pollen tube.

It is worthwhile to point out the presence of *FER* homologues in other species including monocots. Therefore, it would be interesting to determine if these genes control the reception of the pollen tube as well, as the mechanisms of pollen tube reception are similar among most angiosperms.

Interestingly, the two genes inside the CrRLK1L-1 family that shows the highest identities to *FER,* At3g04690 (53% identical to *FER*) and At5g28680 (52% identical to *FER*), (Apendix Figure 3) are exclusively expressed in pollen according to TAIR annotation (Rhee, Beavis et al. 2003). Both proteins have high protein sequence identities (82%) and are predicted to be localized at the plasma membrane (Schwacke, Schneider et al. 2003). Neither introns nor 5' or 3'UTR are annotated for both genes.

4.3 *FER* shows peculiar features

4.3.1 *FER* does not have any intron in its coding region

As shown by *in situ* hybridization experiments, *FER* mRNA was difficult to detect in the gametophyte. Additionally, laser capture dissection of synergid cells and microarrays performed by Samuel Wüst (University of Zurich, Switzerland, unpublished data) were not able to detect *FER* transcript signal above the cut off values. However, in *pFER::GUS* (Figure 9E,F) and the *pFER::FER-GFP* experiments signals in the synergids were easily detected. This indicates that *FER* mRNA could be very unstable, and it is supported by the notion that in Arabidopsis, genes with unstable mRNA have fewer introns (Wang, Feng et al. 2007), as is the case for *FER* which possesses only one intron localized in the 5'UTR.

Software-prediction analysis of this area revealed the presence of a putative Internal Ribosomal Entry Site (IRES) in the intron and part of the exon. Internal mRNA ribosome binding is a mechanism of translation initiation alternative to the conventional 5'-cap dependent ribosome scanning mechanism. Analysis of known IRES in some cellular mRNAs identified a common structural motif forming a Y-type stem-loop structure followed by the AUG triplet or followed by additional stem-loop structures and the AUG triplet (Le and Maizel 1997). During conditions where cap-dependent initiation is impaired such as during apoptosis (Holcik, Sonenberg et al. 2000), IRES's recruit ribosomes directly to the vicinity of the initiation codon without the requirement of the cap binding protein and the eukaryotic initiation factor-4E (eIF4E). Several eukaryotic IRES have been found, but only one example was reported for plants in the Maize Hsp101 gene (Dinkova, Zepeda et al. 2005).

In many plant species, the receptive synergid cell begins to degenerate before the arrival of the pollen tube (Higashiyama, Kuroiwa et al. 2000). This suggest that, if this putative IRES is functional, it might mediate translation of *FER* in the synergid cell that undergoes programmed cell death as FER needs to be present for the reception of the pollen tube. In species where synergid degeneration occurs just before or during pollen tube entrance, as in *A. thaliana,* the IRES may serve as a mechanism to allow the production of the FER protein in the degenerated synergid cell in a rare case where the timing between synergid degeneration and pollen tube entrance is not synchronized. Another hypothesis is that, if the interaction required for pollen tube reception is dependant on the amount of FER receptor in the synergid

cell, the IRES could translate *FER* in the synergid that starts to degenerate in order to provide enough FER receptors for the reception of the pollen tube. Another alternative is that this IRES is a remnant of an ancestor species of *A. thaliana*, where synergid degeneration and pollen tube entrance to the ovule was not synchronized.

However, the presence of this structure in the 3'UTR as well, suggests that even if this feature does not operate as an IRES, it indicates that both 5' and 3' UTR of *FER* share similarities in their secondary structures.

4.3.2 *FER* has a putative extracellular ligand binding domain

RLKs usually possess an extracellular domain that interacts with ligands causing homodimerization or heterodimerization that activates the receptor. This is the case for the flagellin receptor kinase (FLS2), which recognizes the bacterial flagellin ligand. Flagellin activates the receptor and triggers a signaling cascade that enables a defense response from the plant towards the pathogen (Chinchilla, Bauer et al. 2006). Another example is brassinolide, an active steroid hormone in *A. thaliana*. Brassinolide binds to a cell surface receptor with serine-threonine kinase activity called BRASSINOSTEROID INSENSTIVE 1 (BRI1). This interaction induces BRI1 phosphorylation and control processes such as stress resistance and stem elongation (Kinoshita, Cano-Delgado et al. 2005).

FER has a predicted extracellular domain followed by a transmembrane domain and an intracellular domain containing a kinase domain (Figure 6B). The *FER* extracellular domain is specific for plants and no function has been assigned to it. The only recognized feature of this domain is two conserved cysteins (Appendix Figure1). Many plant receptor-like proteins have conserved Cys residues that are proposed to be involved in forming intermolecular disulfide bridges; this allows stable homodimer formation or coupling to signaling partners in the receptor complex (van der Hoorn, Wulff et al. 2005).

4.3.3 *FER* has an active kinase domain

As mentioned above, RLK's receive signals through their extracellular domains. This ligand-receptor interaction causes homodimerization or heterodimerization of the receptors, which activates their intracellular kinase domain by auto- or trans-phosphorilation and starts a cytoplasmic signaling cascade by phosphorilation of other intracellular targets (Pawson and Scott 1997).

Serine 695 and Threonine 696 of the kinase domain (Col-0) of *FER* are phosphorilated *in vivo*. Additionally, either one or two residues located outside of the kinase domain of *FER*, Serine 861 or Serine 866 are phosphorylated *in vivo* as well (Figure 6B and Appendix Figure1) (Nuhse, Stensballe et al. 2004). Cytoplasmic non-catalytic residues could create docking sites for cytoplasmic targets (Pawson 2002), suggesting that these two residues could be involved in the interaction with downstream elements of the *FER* signaling cascade, possibly after ligand-mediated activation of *FER*.

Moreover, experiments performed by Sharon Kessler (University of Zurich, Switzerland, unpublished data) determined that the predicted intracellular kinase domain of *FER* autophosphorylates in an *in vitro* kinase assay.

4.4 *FER* is required for and after fertilization

Quantitative RT-PCR demonstrated that FER is expressed in female reproductive tissues (Figure 7). This result is supported by the *FER* promoter:GUS fusions where both synergid cells, the site of pollen tube reception, were stained with GUS (Figure 9E,F). In addition, the FER-GFP fusion protein driven by the native FER promoter was found in the synergid cells and faintly in the egg cell (Figure 13C,D,F). In i*n situ* mRNA hybridization experiments, *FER* mRNA was found rarely and weakly in the female gametophyte (Figure 8E). The results from the complementation experiment, mutant analyses, expression and protein localization, suggests that *FER* controls the reception of the pollen tube in the synergid cells of the female gametophyte. However, *FER* is found as well in diploid sporophytic organs such as leaves (Figure 7, 9A, 12B), roots (Figure 12A), anther filament (Figure 9C, 12C), floral and ovule primordia (Figure 8A,B), the developing embryo (Figure 8G, 9H,I) and ovule integuments (Figure 13A,B,F).

Some important hypotheses can be drawn of these results:

1) *FER* function is required for pollen tube reception and for development after fertilization. As shown by (Huck, Moore et al. 2003), *FER* is a female gametophytic as well as a zygotic lethal mutant, as even with 14% transmission through the female no homozygous mutants were recovered. This is supported by the *in situ* hybridization signal of the *FER* probe in the developing embryo (Figure 8G), which shows an early transcription of *FER* after fertilization. Furthermore, *FER* mRNA is abundant in developing

structures such as floral primordia (Figure 8A), young ovule primordia (Figure 8B), and young anthers (Figure 8C), supporting the hypothesis of an additional role of *FER* after fertilization in development as *FER* is also expressed in mature structures.

2) *FER* and the putative ligand required for pollen tube reception are located in different cells. *FER* is expressed in all organs except the mature pollen grains; the compartmentalization of *FER* and the mechanism of pollen tube rupture suggest that after contact of *FER* with its ligand, one of the cells, in this case the male cell, dies. Therefore, if *FER* is required for the development and differentiation of plant cells it is possible that *FER* is active in young anthers, but after maturity, other genes perform *FER* function in the pollen grain/pollen tube. The closest *FER* homologues, At3g04690 and At5g28680 (Apendix Figure 3) are good candidates for this function as they are exclusively expressed in pollen.

Until now, no research has been done to investigate *FER* function after fertilization as homozygous mutants were never recovered. An alternative is the use of inducible complementation for *fer* mutants during pollen tube reception and removal of the inducer after fertilization to score the phenotype of a plant without *FER*.

Some RLKs are also involved in the response to pathogens. This is the case for the Arabidopsis LRR-receptor kinase *FLS2*, which binds the flagellin peptide flg22 (Chinchilla, Bauer et al. 2006), and the bacterial elongation factor Tu (Ef-Tu), which is recognized by the Arabidopsis LRR-kinase *EFR,* restricting Agrobacterium-mediated transformation (Zipfel, Kunze et al. 2006). It is possible that *FER* is involved in similar pathogen-response mechanisms due to its wide expression pattern and membrane localization. Therefore, Gernot Kunze (ETHZ, Zurich, Switzerland) performed a microarray analysis of FER expression after treatment with bacterial / fungi elicitors and by living organisms. FER-RLK expression was not affected by these treatments (data not shown), suggesting that *FER* is not involved in the response to plant pathogens.

Additionally, in an analysis performed through the GENEVESTIGATOR platform (Zimmermann, Hirsch-Hoffmann et al. 2004) (https://www.genevestigator.ethz.ch/at/index.php?page=tair&option=stress&agi=AT3G51550) *FER* appears to be upregulated after the treatment with 6-benzyl adenine

(1.51), which is a synthetic cytokinin that elicits plant growth and development, indicating a possible link with hormones and development. *FER* was also upregulated after treatment with cycloheximide (1.47) which is an inhibitor of protein biosynthesis. It is possible that a silencer element is present in the *FER* promoter; therefore, after inhibition of the repressor, the synthesis of *FER* mRNA is upregulated.

4.5 FER is localized ultimately at the plasma membrane, but is also found in other compartments

Plasma membrane receptors mediate the interaction between signals of the extra cellular space and the cytoplasm of the cell. Correct processing, localization and anchoring of the receptors to the membrane is achieved, in some cases, by the recognition of signal sequences encoded in the amino acid sequence of the protein itself. Ultimately, transport through several cellular compartments is necessary to localize a protein in the plasma membrane.

To determine the subcellular localization of *FER,* several types of plasmids were constructed in which *GFP* was fused to *FER.* The results of the tests with each construct will be discussed separately.

4.5.1 N-terminal fusions to *FER* do not represent *FER's* localization (*35S::GFP-FER*)

FER has a predicted signal peptide in its N-terminus (Appendix Figure1). Signal peptides mark proteins for translocation across the endoplasmic reticulum (ER). This signal is a sequence of amino acids in the N-terminus of the nascent polypeptide chain and directs the ribosome to the ER membrane through binding to a signal recognition particle soon after the emergence of the N-terminal signal sequence from the ribosome. The signal sequence is then cleaved on the luminal side of the ER membrane (Stryer 1995). In transient expression of *35S::GFP-FER,* the GFP was localized in the cytoplasm, the nucleus, and in patches surrounding the nucleus (Figure 10A,B). This pattern is similar to that obtained with a *35S::GFP* construct (Figure 10J), where the GFP lacks localization signals and remains cytoplasmic, moving freely even into the nucleus due to its small size (238 amino acids). Is possible that in *35S::GFP-FER*, *FER*'s signal peptide is not recognized due to the

upstream addition of the GFP sequence (Szczesna-Skorupa, Mead et al. 1987), causing miss-localization of the protein fusion.

4.5.2 *FER* over-expression induces programmed cell death

In an attempt to localize FER, the *35S::FER-GFP* construct was delivered to onion epidermal cells by particle bombardment. This construct hypothetically maintains the correct targeting sequences and correct processing mechanisms compared to *35S::GFP-FER* (see above). As described in the Results section, only a few GFP positive cells were observed from *35S::FER-GFP* bombarded tissues, while normal numbers of transformed cells with the control plasmids were recovered. Higher numbers of dead cells were also found with *35S::FER-GFP* when compared to the controls. The few GFP positive cells showed signs of stress and could not be observed later during the day, probably due to death of the transformed cells. These results suggested that the construct itself is toxic to plant cells (and not to bacteria as plasmids were recovered). To determine if toxicity is through a Programmed Cell Death (PCD)-like pathway, an apoptosis inhibitor shown to work in plants and animals, Ac-DEVD-CHO, was used. The peptide DEVD is an inhibitor of caspase-3 and has been used to provide evidence for a caspase-like activity in apoptotic animal cells (Garcia-Calvo, Peterson et al. 1998) and in plant cells undergoing PCD (Danon, Rotari et al. 2004). In animal cells, Caspase-3 is involved in cleaving nuclear DNA during apopotosis (Wolf, Schuler et al. 1999). After co-bombardment of the construct with the caspase3 inhibitor, FER-GFP cells were easily recovered and studied. FER-GFP was localized mainly in the periphery of the cell, most likely at the plasma membrane and cytoplasm, as shown by epifluorescence microscopy (Figure 10F,G). This was confirmed by CLSM, where the GFP signal of a single section is at the periphery of the cell (Figure 10H,I). The results suggest that FER in high quantities is toxic and induces a PCD-like mechanism in plant cells. It is not possible to infer from these experiments a function of *FER* in PCD mechanisms, as over-expression of other kinases have been shown to be toxic (Toshiro Aigaki, Tokyo Metropolitan University – Japan, personal communication).

4.5.3 Transient expression of *pFER::FER-GFP* shows three distinct localizations of the FER protein

The usage of a strong constitutive promoter driving *FER* had deleterious effects for the cell; therefore, *FER's* native promoter was used to drive the chimeric fusion protein (*pFER::FER-GFP*). Leaves were transiently transformed as expression experiments demonstrated that the promoter is active in this tissue (Figure 7). Observations of transformed cells showed three distinct localizations: Plasma membrane (Figure 11A,B, Figure 11C), vesicles (Figure 11D) and vacuolar compartments including the Tonoplast (vacuolar membrane) (Figure 11E,F,G)

The presence of GFP stained vesicles suggested an early step of the transport of the protein towards the plasma membrane. Tonoplast localization and previous over-expression experiments suggest that high quantities of FER could be deleterious for the plant cell. In transient bombardments, several copies can be integrated in the same cell. Therefore, the amount of protein would be proportional and would mimic the effect of over-expression. One hypothesis is that FER is mobilized towards the vacuole either for degradation or to regulate the amount of protein. The vacuolar localization was found once in leaves and was found more frequently in protoplasts and onion cells. No other transformed *A. thaliana* leaf cell was recovered in the experiments, perhaps as a consequence of the *FER* promoter not being strong enough to detect GFP in leaves under transient expression conditions.

4.5.4 Stable expression of *pFER::FER-GFP* demonstrates that FER is mainly localized at the plasma membrane

pFER::FER-GFP was used to transform wild-type *A. thaliana* and *fer* plants. The construct complemented the mutation in *fer* as shown by an increase of fertilized ovules in the complemented *fer* plants (Table 1) and the presence of *Ds* homozygous plants (Figure 5D). This demonstrates that the fusion protein FER-GFP is functional and that the 3'UTR of *FER* is interchangeable with the plasmid's 3'sequences.

Analysis of stable transformants supports the expression patterns found by *pFER::GUS* fusions and quantitative real time RT-PCR experiments, where *FER* is expressed in roots (Figure 12A), leaves (Figure 12B), anther filaments (Figure 12C; note that the weak signal from the pollen grains is not GFP, as shown in the inset, wild type pollen has the same fluorescence when exited by the laser), and ovules (Figure 13A). CLSM analysis of leaves demonstrates that FER-GFP is localized at

the periphery of the cell at the plasma membrane (Figure 12B). Several sections were taken at the area of the nucleus and no nuclear pocket was observed. This indicates that the GFP signal is not at the tonoplast, which could be mistaken with the plasma membrane. CLSM single sections in roots revealed that FER-GFP is localized at the periphery of the root cell and weakly in the cytoplasm (Figure 12A). In some samples, FER-GFP was weakly observed in the root vascular tissue (data not shown). *FER* is also expressed in the stigma cells and its protein is localized at the periphery and in small vesicles (Figure 12F). In ovules, FER-GFP is observed at the periphery of the sporophytic integument cells (Figure 13B and inset showing magnification of cell borders).

These experiments and protein prediction programs (Schwacke, Schneider et al. 2003) show that *FER* is ultimately localized at the plasma membrane of plant cells. This result is corroborated by a recent publication in which a quantitative analysis of Arabidopsis plasma membrane using Trypsin-catalyzed ^{18}O labeling found peptides corresponding to *FER* (Nelson, Hegeman et al. 2006). The results also indicate a vesicular transport of FER, which is expected for membrane localized proteins and supported by an experiment in *pFER::FER-GFP* plants where membrane trafficking was inhibited with Brefeldin A. In treated roots, GFP was found in the plasma membrane and in vesicular compartments (brefeldin compartments) after treatment with the compound (Figure 12A,B).

4.6 FER protein is produced in the synergids cells and mobilizes to the filiform apparatus

The filiform apparatus is the structure in which the pollen tube enters the synergid cells. It is composed of cell wall invaginations of both synergid cells and it has been proposed to be involved in the transport of molecules in and out of the synergids; presumably, the pollen tube attractant is released through it.

Unfertilized *pFER::FER-GFP* ovules accumulated high levels of GFP in the filiform apparatus of both synergids. Weaker GFP fluorescence was detected in the membranes of the synergid cells, the surrounding maternal sporophytic cells, as well as faintly in the egg cell (Figure 13D). Since the filiform apparatus is a structure rich in plasma membrane, it was tested if the asymmetric accumulation of FER in the synergid plasma membrane is an artifact by comparing it to *pAtD123::EGFP-AtROP6C,* a plasma membrane localized GFP fusion expressed in the female

gametophyte (line provided by Wei Cai Yang, Institute of Genetics and Developmental Biology, Beijing - China). Under the same growth conditions, FER-GFP levels are much higher in the filiform apparatus than in the rest of the synergid cells when compared to EGFP-AtROP6C (Figure 13D inset). This suggests the existence of a polarized transport of FER to the filiform apparatus. Figure 13E is a CLSM stack of sections of the lower part of the synergid cell and it shows that the GFP is not evenly distributed throughout the filiform apparatus but in a punctuate pattern. It is difficult to determined if these foci are of a vesicular origin or if they are merely accumulations in the plasma membrane-cell wall invaginations of the filiform apparatus.

4.6.1 FER is present at the time of pollen tube entrance

The previous experiments demonstrated the presence of FER before fertilization. Figure 13F shows CLSM stacks from several sections from an *pFER::FER-GFP* ovule approached by a Congo Red stained pollen tube. The GFP at the base of the synergids is at the site of the red signal of the pollen tube. After treatment with the Congo Red solution, the membrane localization of GFP became cytoplasmic, this localization was observed in other tissues after long observation under the CLSM (data not shown) and is probably a stress response.

4.7 Interspecific crosses mimic the *fer* phenotype and correlates with divergence in the extracellular domain

As a signal transduction cascade initiated by the interaction of FER with a putative pollen ligand seems necessary for fertilization. It is possible that changes in the components of this interaction could act as reproductive isolation barriers. To some extent, the interaction between the pollen tube and the synergid is similar to sperm-egg interactions in animals (Primakoff and Myles 2002), but it occurs at the level of gametophytes rather than gametes. For example, divergence in the protein sequence of the putative ligand-binding extracellular domain of FER or changes in the pollen-specific ligand could prevent inter-specific fertilization events. Interestingly, in inter-specific crosses of Rhododendron species pollen tube growth does not arrest. This results in pollen tube overgrowth in the female gametophyte similar to the phenotype observed in *fer* (Kaul, Rouse et al. 1986; Williams, Kaul et al. 1986).

If the proposed model (Figure 18) is correct, an inter-specific cross where wild-type *A. thaliana* is pollinated by a related Brassicaceae species with a sufficiently divergent ligand might also produce a *fer*-like phenotype. Therefore, inter-specific crosses were performed between *A. thaliana* and different Brassicaceae species. In most crosses, the pollen germinated but failed to grow towards the ovules, as has been reported previously (Hiscock and Dickinson 1993; Kandasamy, Nasrallah et al. 1994; Hülskamp, Kopczak et al. 1995; Shimizu and Okada 2000). In crosses with the close relative *Arabidopsis lyrata*, pollen tubes were correctly targeted to the ovule but only 43.9% of the embryo sacs received pollen tubes and were fertilized, 5.2 % of the ovules were fertilized with more than one pollen tube in the same micropyle, showing pollen tube overgrowth inside the female gametophyte (Figure 14C,D), and 50.9 % of the ovules had pollen tubes that continued to grow inside the female gametophyte as was observed in *fer* mutants (Figure 14A) (n= 813 ovules). In crosses with a more distant relative, *Cardamine flexuosa*, only 7.7% of *A. thaliana* ovules attracted pollen tubes, 1.6% had pollen tubes that entered the micropyle and stopped as previously reported (Shimizu 2002), 0.8 % had pollen tubes coiling outside the micropyle, and in 5.3% of the ovules the pollen tubes entered the micropyles but reception failed, resulting in a *fer*-like phenotype (n=363 ovules) (Figure 14B).

These observations suggest that a *FER* signal transduction cascade may play a role in the failed pollen tube reception in these inter-specific crosses. It is possible that the sequence of the putative ligand has sufficiently diverged in *A. lyrata* and *C. flexuosa* such that it is not recognized or only poorly recognized by the *A. thaliana* FER. It is expected that divergence in the sequence of the putative ligand would also be reflected in sequence divergence in FER's extracellular domain, which is proposed to interact with this ligand. To test this hypothesis, I isolated *FER* homologues from these species and calculated the ratio between the number of non-synonymous substitutions per non-synonymous site (Ka) and the number of synonymous substitutions per synonymous site (Ks) (Nei and Gojobori 1986) in pair-wise comparisons between *A. thaliana* and *A. lyrata* (one *FER* homologue) or C. *flexuosa* (4 *FER* homologues) (Figure 14E,F). In all comparisons, higher Ka/Ks values occur in the putative ligand-binding extracellular region, indicating that this domain shows the greatest degree of amino acid diversification and evolves faster than the highly conserved intracellular kinase domain (Shiu, Karlowski et al. 2004). The high sequence divergence in the extracellular domain of FER may contribute to

reproductive isolation between two species, as has been proposed for other genes involved in recognition at fertilization (Swanson and Vacquier 2002).

The experiments fit a model where the incompatible interaction occurs through a *FER* signaling process. Nevertheless, pollen reception was normal in crosses between *A. thaliana* x *A. halleri* and same similar Ka/Ks ratios were found for this comparison (Figure 14E). This suggests that mechanisms other than simply FER sequence divergence mediate the failed interaction in this interspecific cross or that *A. halleri* has a set of ligands that have not acquired enough differences between the last common ancestor of *A. thaliana* and *A. halleri,* and they are therefore compatible.

4.8 The mechanisms that control *FER* evolution are unclear

Genes involved in reproduction are thought to evolve faster than other genes and positive selection (either directional or diversifying selection) is the mechanism which could drive the evolution of these genes. Receptor–ligand pairs are also thought to co-evolve as a faster evolution of one and not the other will lead to a failure of recognition.

The interaction of FER with a putative ligand and its role in reproduction, suggests that FER and its ligand could be evolving under positive diversifying selection. This is also suggested by the interspecific pollinations, as changes between species in the putative ligand – *FER* receptor pair probably cause the observed *fer*-like phenotype. Moreover, based on the pairwise sequence comparisons (Figure 14E,F), it is possible that positive selection only acts on particular sites of the extracellular part of the protein required for the interaction with the putative ligand.

Maximum likelihood tests on the cDNA sequence of *FER* and homologues from different species (excluding the signal peptide as it is not part of the mature protein) were performed under the CODEML program of the PAML package. Both, diversifying and directional positive selection hypotheses were tested using SITES models that allow the ω ratio to vary among sites (diversifying), BRANCH to detect positive selection in a specific branch and BRANCH-SITES models to detect positive selection that affects only a few sites along a few lineages (directional positive selection). The data did not fit any model of positive selection. Nevertheless certain branches in the phylogeny experience different selective pressures and, therefore, have different dN/dS values.

Furthermore, there is no evidence of positive selection between members of the CrRLK1-L subfamily of Arabidopsis RLK, for which FERONIA belongs (Strain and Muse 2005).

As the methods implemented in CODEMLl are known to be conservative and may fail to detect positive selection when it exists (personal communication, Ziheng Yang, University College London, London–England) several neutrality tests in population data were performed. These tests determine deviations from the neutrality mode of evolution

Positive Tajima's D values were found for *FER* and *FER(ECD)*. For an individual gene, a positive Tajima's D value is evidence for heterozygotes having a selective advantage, whereas a negative value is evidence for selection of one specific allele over alternate alleles (Stephens, Schneider et al. 2001). This, suggest an excess of intermediate frequency alleles and can result from population bottlenecks, population structure and/or balancing selection. Furthermore, the Tajima's D statistic was not zero or close to it, suggesting the data is not under neutral equilibrium.

McDonald Kreitman tests determined that the ratio of silent to replacements polymorphisms were not significantly different form the ratio of silent to replacement fixation, suggesting *FER* is not evolving under positive selection.

At present, there is not a simple hypothesis to explain which selective forces acts on *FER*. The analysis of haplotypes at the *FER* locus would provide a more informative test for positive selection.

4.9 FERONIA controls pollen tube reception at the plasma membrane of the synergids cells through a kinase mediated mechanism

The data indicate that FER acts in the filiform apparatus to control the behavior of the pollen tube to achieve fertilization. The interaction between the putative male ligand and the extracellular domain of the FER RLK triggers a signal transduction cascade inside the synergid cell. A subsequent signal feeds back from the synergid to the pollen tube, causing growth arrest and the release of the sperm cells (Figure 18). Conceptually, this process is similar to the signaling events occurring during the self-incompatibility reaction in *Brassica* spp (Kachroo, Nasrallah et al. 2002). In an incompatible pollination, a pollen ligand interacts with a stigma-expressed RLK

inducing a signaling cascade in female papillar cells, which then signal back to the pollen and inhibits its germination.

The nature of the rupture of the pollen tube is yet unclear. Pollen tube bursting is a potent and fast event in the degenerated synergid. Live imaging has demonstrated that in Arabidopsis the pollen tube bursts in the synergid 6 to 7 minutes after entrance of the pollen tube (Rotman, Rozier et al. 2003). This suggests that the signaling cascade activated through the *FER* receptor-ligand interaction must occur rapidly and that the other components, probably activated through FER phosphorylation, are already present in the degenerating synergid. Some hypothetical mechanisms of the FER signaling cascade are as follows:

1) The FER activation by the ligand interaction mediates the release of a female component that rapidly degrades the tip of the pollen tube (6 to 7 minutes). A release of pectinases by the receptive synergid is a possibility, as in *Brassica campestris L* and presumably in Arabidopsis, the pollen tube tip is composed of a single pectin layer, lacking callose or cellulose (Ferguson, Teeri et al. 1998). Another option is that FER signaling causes a rapid depletion of pectin methylesterase (PME) activity in the pollen tube tip. PMEs gradually de-esterify homogalacturonan, a polymer which is the major component of pectin (Catoire, Pierron et al. 1998). The *VANGUARD1 (VGD1)* gene, which encodes a PME-like protein, is expressed in the pollen tube and localizes to the plasma membrane and the cell wall. In the gametophytic *vgd1* mutant of Arabidopsis, pollen tubes invade the stigma but grow much slower than wild-type pollen tubes within the style and the transmitting tract. Furthermore, the *vgd1* pollen tubes are unstable and burst more frequently than wild-type pollen tubes when germinated and grown *in vitro*, suggesting that the mechanical properties of the cell wall is altered in *vgd1* mutants (Jiang, Yang et al. 2005).

2) FER activates a programmed cell death (PCD) mechanism in the penetrating pollen tube. PCD in plants occurs during development, environmental stress, and pathogen attack. Developmental PCD includes vacuolar swelling, cell wall modifications, collapse of the vacuole, and cell autolysis (reviewed in (van Doorn and Woltering 2005). Changes in mitochondrial permeability, *cytochrome c* release and caspase-like

proteolytic activity occurs in self incompatibility reactions in pollen tubes from *Papaver* (Thomas and Franklin-Tong 2004). It is possible that after FER-ligand interaction, a feedback signal from the synergid to the pollen tube triggers cell death in the penetrating pollen tube, allowing the rupture of the pollen tube membrane.

3) The mechanisms of synergid degeneration and pollen tube reception are connected through a plant-pathogen-like response event. Cell death mechanisms occur as well, during incompatible plant – pathogen interactions in the hypersensitive response that triggers localized host cell death (Greenberg and Ausubel 1993). As a pollen tube is reminiscent of invading fungal hyphae, it is possible that the reception of the pollen tube shares, to some degree, some of the mechanisms required for the response to a pathogen attack. For example, synergid degeneration occurs through a hyper-sensitive response, triggered by an elicitor-like molecule released by the pollen tube. In the challenged synergid, FER activates the release of patogenesis-related proteins such as hydrolytic enzymes with β-1,3-glucanase activity. This enzyme is usually stored in the vacuole of the cell and is released upon pathogen attack to degrade the cell walls of the pathogen (Kombrink, Schroder et al. 1988) or, in this case, the pollen tube.

4) Finally, it is possible that the factors required for the downregulation of synergid expression are contained in the exploding pollen tube, as transfer of signals between these two cells is possible since both synergids are connected by plasmodesmata (Mansfield 1991). Alternatively, *FER* itself sends a direct signal to the other synergid after recognition of the pollen tube through the FER-ligand interaction.

5. Conclusions and suggestions for further work

For double fertilization to occur, the pollen tube that carries the sperm cells must travel towards the female ovules and interact with the cells of the embryo sac. Proper female reception of the male pollen tube is mediated by the *FER* receptor like-kinase. In *A. thaliana,* the female FER-RLK localizes at the plasma membrane of the synergid cells in the region of the filiform apparatus. FER interacts with a putative male ligand and mediates the release of the sperm cells from the pollen tube required for double fertilization.

This important discovery opens new questions about the reception of the pollen tube in plants:

1) What are the male and female interacting partners of *FER* required for the reception of the pollen tube? Finding the ligand would also allow to test if both *FER* receptor and ligand cause cell death when expressed in the same cell. If this is true, this finding could also be applied as a new system to ablate cells by induced expression of the receptor and/or ligand in the same cell.
2) Which mechanisms are required to regulate the tight coordination of the process of synergid degeneration and *FER*-mediated pollen tube reception?
3) How does communication occur between these three cells, the two synergids and the pollen tube?
4) How is gene expression of the remaining synergid down-regulated after pollen tube rupture? In *fer* mutant ovules, a block to prevent multiple pollen tubes from entering the micropyle is lacking, possibly because a prolonged production of the pollen tube attractant.

Pull-down experiments with a GFP antibody in a complemented *fer/fer* plant with the pFER::FER-GFP construct could be used to find interacting partners of *FER.* Alternatively, an analysis of mutated populations of plants for defects in pollen tube reception could identify novel components. As mentioned before, some interspecific crosses mimic the *fer* phenotype. The manipulation of the *FER* pathway by swapping the extracellular domain of *A. lyrata* into *A. thaliana* will unravel if the extracellular domain of *FER* is responsible for mediating the recognition of the putative ligand in an *A. thaliana x A. lyrata* interspecific cross. Furthermore, domain swapping experiments between the extracellular domains of different species might

allow the formation of hybrids in otherwise incompatible species. The analysis of the evolutionary forces that act on *FER* as well as in its yet-to-be discovered ligand, will enrich the study of the evolution of sex-related proteins and may shed light on one of the most interesting questions in biology: how new species arise?

6. Appendix

6.1 Appendix Figure 1. Amino acid alignment and protein features of *FER* relatives

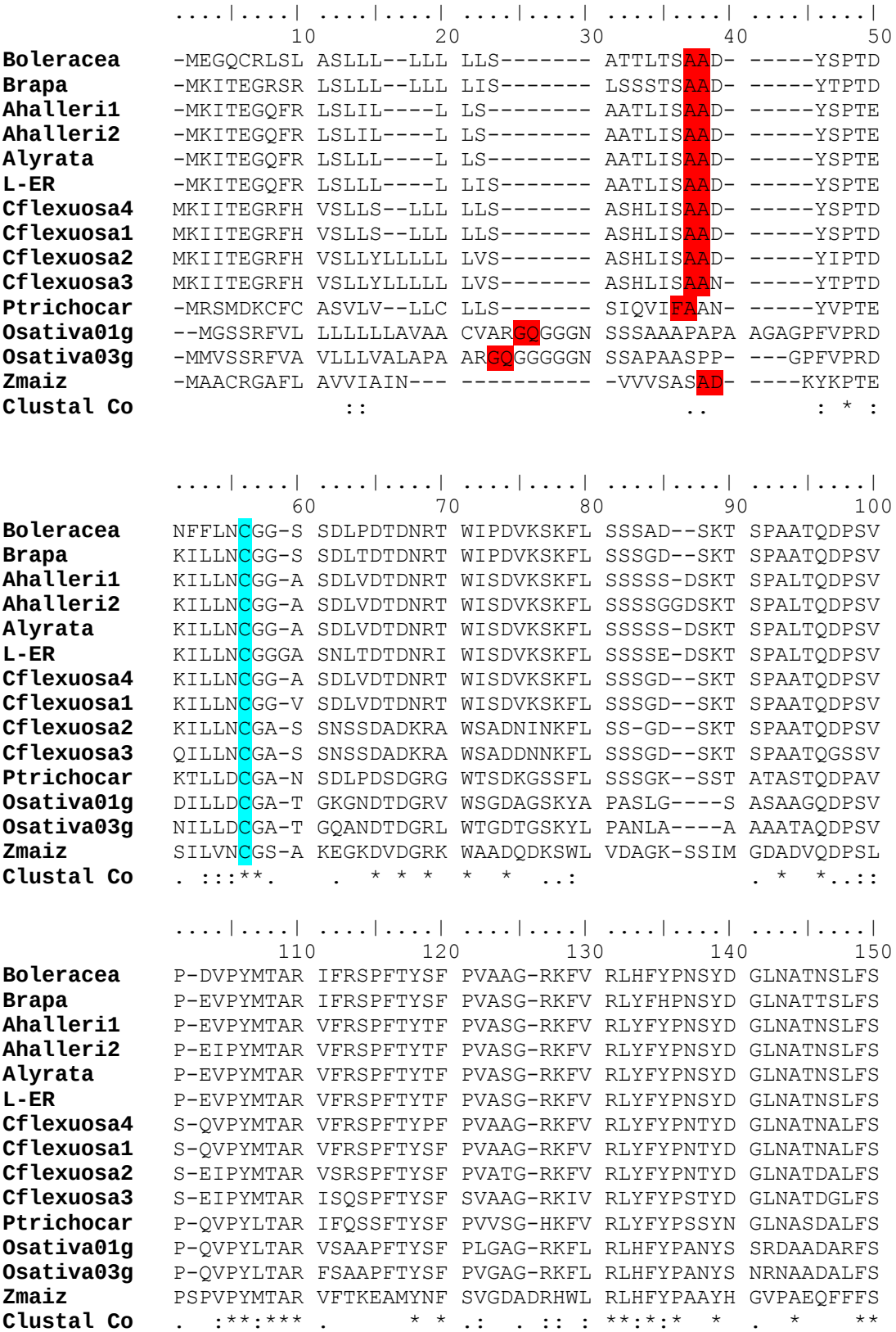

```
                 ....|....| ....|....| ....|....| ....|....| ....|....|
                         160        170        180        190        200
Boleracea        VSLG--SYTL LKNFSAAQTA QALTFSFIVK EFIVNVEGGA -LNVTFTPES
Brapa            VTLGS-SYTL LKNFSAAQTA QALSYSSIVK EFIVNVEGGA SLNITFTPES
Ahalleri1        VSFG--PYTL LKNFSAAQTA EALTYAFIVK EFVVNVEGGT -LNMTFTPES
Ahalleri2        VSFG--PYTL LKNFSAAQTA EALTYAFIVK EFVVNVEGGT -LNMTFTPES
Alyrata          VSFG--PYTL LKNFSAAQTA EALTYAFIIK EFVVNVEGGT -LNMTFTPES
L-ER             VSFG--PYTL LKNFSASQTA EALTYAFIIK EFVVNVEGGT -LNMTFTPES
Cflexuosa4       VSFG--PYTL LKNFSAAQTA EALTYAVIVK EFIVNVEGGS -LNMTFTPE-
Cflexuosa1       VSFG--PYTL LKNFSAAQTA EALTYAVIVK EFIVNVEGGS -LNMTFTPE-
Cflexuosa2       VSFG--PYTL LKNFSAAQTA EALTYAVIVK EFIVNVEGGS -LNMTFTPE-
Cflexuosa3       FSFG--PYTL LKNFSAAQTV EALPYAVIVK EFIVNVEGGS -LNMTFTPES
Ptrichocar       VTAG--SYTL LSNFSVAQTT DALNYVSIMK EYLINVNDDT -LNITFSPSS
Osativa01g       VSVPAANVTL LSNFSAYQTA TALNFAYIVR EFSVNVTTPT -MELTFTPEK
Osativa03g       VSIPDPNITL LSNFSAYQTA LALNFDYLVR EFSVNVTAST -LDLTFTPEK
Zmaiz            VSTS-TGITL LRNFSVYITA KALSQAYIIR EFTLPPMADG TLALTFKPTA
Clustal Co       .:      ** * ***.  *.  **    ::: *: :        : :**.*

                 ....|....| ....|....| ....|....| ....|....| ....|....|
                         210        220        230        240        250
Boleracea        APSNAYAYVN GIEVTSMPDL YS-STDGSLT VVGSSGGVTI DNSTALENVY
Brapa            TP-KAYAFVN GIEVTSMPDL YS-NTDGTLS IVGSSTAVDI DNSTALENVY
Ahalleri1        SPSNAYAFVN GIEVTSMPDI YS-STDGTLT MVGSSTSITI DNSTALENVY
Ahalleri2        TPSNAYAFVN GIEVTSMPDI YS-STDGTLT MVGSSTSITI DNSTALENVY
Alyrata          TPSNAYAFVN GIEVTSMPDI YS-STDGTLT MVGSSTSITI DNSTALENVY
L-ER             SPSNAYAFVN GIEVTSMPDM YS-STDGTLT MVGSSGSVTI DNSTALENVY
Cflexuosa4       --SNAYAFMN GIEVTSMPDI YS-STDGSLI MVGASSDFTI DNSTALENVF
Cflexuosa1       --SNAYAFMN GIEVTSMPDI YS-STDGSLI MVGASSDFTI DNSTALENVF
Cflexuosa2       --SNAYAFVN GIEVTSMPDI YS-STDGTLT MVGSSGAFTI DNSTALENVF
Cflexuosa3       TPSNAYAFVN GIEVTSMPDI YS-NTDGTLT MVGSSGAFTI DNSTALENVF
Ptrichocar       NPSSAYAFVN GIEIVSMPDI YS-NANG-VM IVGQGVPYVI DNTTALENVY
Osativa01g       GHPNAYAFVN GIEVVSSPDL FDISTPNLVT GDGNNQPFPI DAGTALQTMY
Osativa03g       GHPNAFAFVN GIEVVSSPDL FGSSNPMEVT GDGSGTPFPI DAGTAMQTMY
Zmaiz            MNNASYAFVN GIEIISMPDI FA----DPAT MVGLADQTVD TATSSLQTMY
Clustal Co           ::*::* ***: * **: :           *          ::::.::

                 ....|....| ....|....| ....|....| ....|....| ....|....|
                         260        270        280        290        300
Boleracea        RLNVGGNDIS PSDDTGLYRS WYDDQPYIFG AGLGITETAD PNMTIEYPSG
Brapa            RLNVGGNDIS PSEDTGLYRS WYDDSPYIFT AGIGVVETVD PNMTIKYPTD
Ahalleri1        RLNVGGNDIS PSADTGLYRS WYDDQPYIFG AGLGIPETAD PNMTIKYPTG
Ahalleri2        RLNVGGNDIS PSADTGLYRS WYDDQPYIFG AGLGIPETAD PNMTIKYPTG
Alyrata          RLNVGGNDIS PSADTGLYRS WYDDQPYIFG AGLGIPETAD PNMTIKYPTG
L-ER             RLNVGGNDIS PSADTGLYRS WYDDQPYIFG AGLGIPETAD PNMTIKYPTG
Cflexuosa4       RLNVGGNDIS PSADTGLYRS WYDDQPYIFA AGLGIPETAD PNMTIQYPTG
Cflexuosa1       RLNVGGNDIS PSADTGLYRS WYDDQPYIFA AGLGIPETAD PNMTIQYPTG
Cflexuosa2       RLNVGGNDIS PSADTGLYRS WYDDEPYVFG AAIGIPYTAD ANMTIKYPAD
Cflexuosa3       RLNVGGSDIS PSADTGLYRS WYDDQPYLFG AAIGIPYPAD PTMNITYPTG
Ptrichocar       RLNVGGNSIT PSGDTGLFRS WSDDQIYLYG SAFGVPESAD PNVKIRYPPG
Osativa01g       RLNVGGQAIS PSKDTGGYRS WDDDSPYVFG AAFGVSYPKD DNVTIAYPSN
Osativa03g       RLNVGGNAIS PSKDTGGYRS WEDDTPYIPF ASFGVSYAND TNVPINYPDS
Zmaiz            RLNVGGSYIA PTNDSGLSRD WYDDTPYLYG AAVGVTYKPD DNAQIKFPSP
Clustal Co       ******. *: *: *:*  *. * **  *:   :..*:    *  .  * :*
```

```
                 ....|....| ....|....| ....|....| ....|....| ....|....|
                         310        320        330        340        350
Boleracea        TPTYVAPVDV YSTARSMGPT PQINLNYNLT WIFSIDSGFS YLVRLHFCEV
Brapa            TPTYIAPVDV YSTARSMTPT AQINLNFNLT WVFSIDSGFT YLVRLHFCEV
Ahalleri1        TPTYVAPVDV YSTARSMGPT AQINLNYNLT WIFSIDSGFT YLVRLHFCEV
Ahalleri2        TPTYVAPVDV YSTARSMGPT AQINLNYNLT WIFSIDSGFT YLVRLHFCEV
Alyrata          TPTYVAPVDV YSTARSMGPT AQINLNYNLT WIFSIDSGFT YLVRLHFCEV
L-ER             TPTYVAPVDV YSTARSMGPT AQINLNYNLT WIFSIDSGFT YLVRLHFCEV
Cflexuosa4       TPTYVAPVDV YSTARSMGPT ASININYNLT WVFSIDSGFS YLVRLHFCEV
Cflexuosa1       TPTYVAPVDV YSTARSMGPT ASININYNLT WVFSIDSGFS YLVRLHFCEV
Cflexuosa2       TPTYVAPEDV YSTARTMGPN ATININYNLT WVFSIDSGFS YLVRLHFCEV
Cflexuosa3       TPTYVAPKDV YSTARTMGPN ARININYNLT WVFSIDSGFS YLVRLHFCEV
Ptrichocar       MPSYVAPDNV YLTARSMGPA PNVNLNYNLT WIFSVDSGFN YLVRLHFCEI
Osativa01g       VPEYVAPVDV YATARSMGPD KNVNLAYNLT WIMQVDAGFT YLVRLHFCEI
Osativa03g       IPQYVAPADV YSTARSMGPD NNVNLQYNLT WAMQVDAGYQ YLVRLHFCEI
Zmaiz            EAEYAAPASL YLSSRSMGPN PKVNQNYNLT WVFEVDSNFT YVVRLHFCEL
Clustal Co        . * ** .: * ::*:* *    :*  :*** * :.:*:.:  *:*******:

                 ....|....| ....|....| ....|....| ....|....| ....|....|
                         360        370        380        390        400
Boleracea        APNMTKINQR VFTVYLNNQT AEPEADVAGW TG---GHGIP LHKDYVVNPP
Brapa            LPDITKINQR VFTIYLNNQT AESEADVAGW TG---GNGIP IYKDYVVNPP
Ahalleri1        SSNITKINQR VFTIYLNNQT AEPEADIIAW TS---SNGVP FHKDYVVNPP
Ahalleri2        SSNITKINQR VFTIYLNNQT AEPEADIIAW TS---SNGVP FHKDYVVNPP
Alyrata          SSNITKINQR VFTIYLNNQT AEPEADIIAW TS---SNGVP FHKDYVVNPP
L-ER             SSNITKINQR VFTIYLNNQT AEPEADVIAW TS---SNGVP FHKDYVVNPP
Cflexuosa4       SPRITKINQR VFTIYLNNQT AEEEADVIAW AQ---GNGIP FHKDYVVNPP
Cflexuosa1       SPRITKINQR VFTIYLNNQT AEEEADVIAW AQ---GNGIP FHKDYVVNPP
Cflexuosa2       ASNNTKINQR VFTIYLNNQT AEPEADVIGW VG---GNGIA FHKDYVVNPP
Cflexuosa3       STNTTKSNQR VFAIYLNNQT AEPEADVIAW TGNQ-GNGIA FHKDYVVNPP
Ptrichocar       S-NITKINQR VFDIFLNNQT VEEAADVIAW AGGNGNNGVP VIKDYVVLVP
Osativa01g       QYPITMINQR VFNIYINNQT AFQGADVIAW TN-NNGIGSP VYQDFVVTT-
Osativa03g       QSGISKINQR TFDIYINNQT AFSGADVIAW S---TGLGIP VYKDFVVFP-
Zmaiz            L--LTKVNQR AFDIFVNNKT AQADADVIGW TS---GKDVP VYKDYATFMP
Clustal Co           :  *** .* :::**:* .   **: .*      . . . . :*:..

                 ....|....| ....|....| ....|....| ....|....| ....|....|
                         410        420        430        440        450
Boleracea        DGKGQQDLWL ALHPNTKNNP EYYDAILNGV EIFKMNNSDG NLAGPNPIPG
Brapa            DGKGQQDLWL ALHPNTRGKP EYYDAILNGV EIFKMNGSDG NLAGPNPIPG
Ahalleri1        VGNGQQDMWL ALHPNPINKP EYYDSILNGV EIFKMNTSDG NLAGPNPIPG
Ahalleri2        EGNGQQDMWL ALHPNPINKP EYYDSILNGV EIFKMNTSDG NLAGPNPIPG
Alyrata          EGNGQQDMWL ALHPNPINKP EYYDSILNGV EIFKMNTSDG NLAGPNPIPG
L-ER             EGNGQQDLWL ALHPNPVNKP EYYDSLLNGV EIFKMNTSDG NLAGTNPIPG
Cflexuosa4       EGKGQQDLWL ALHPNTRNKP EYYDSILSGV EIFKVNTSDG NLAGSNPIPG
Cflexuosa1       EGKGQQDLWL ALHPNTRNKP EYYDSILSGV EIFKVNTSDG NLAGSNPIPG
Cflexuosa2       DGKGQQDLWL ALTPNPRNKP QLYDSILNGV EIFKMNTSEG NLAGPNPIPG
Cflexuosa3       DGKGQQDLWL ALTPNQRTKP QYYDSILNGV EIFKVNTSDG NLAGPNPIPG
Ptrichocar       TGPPQQDMWL ALHPDLKAKP QYYDSILNGV EIFKLSSPNG NLAGPNPIPA
Osativa01g       VGSGAMDLWV ALYPDVQAKP QYYDAILNGL EVFKLPLSNG SLAGLNPVPT
Osativa03g       MGSGPMDLWV DLHPNVKNKP QYYNAILNGM EVFKLQLTNG SLAGLNPVPS
Zmaiz            AGTADKILWI ALHPSVSMKP EFYDAVLNGL EIFKMSDSSG NLAGPNPDPS
Clustal Co        *     :*:  * *.   :* : *:::*.*: *:**:  ..* .*** ** *
```

```
                 ....|....| ....|....| ....|....| ....|....| ....|....|
                         460        470        480        490        500
Boleracea        P-QVTADPSK VLRPR-TSQS KNHTAVVAGA ASGAVVLGLI VGLCAMIAYR
Brapa            P-QVTADPSR VLRPR-TGSS KSHTAIVAGV ISGAVVLGLI VGLCVMVAYR
Ahalleri1        P-QVTADPSK VLSPT-SGKS KSNTAIVAGA ASGAVVLALI IGFCVFGAYR
Ahalleri2        P-QVTADPSK VLSPT-SGKS KSNTAIVAGA ASGAVVLALI IGFCVFGAYR
Alyrata          P-QVTADPSK VLSPT-SGKS KSNTAIVAGA ASGAVVLALI IGFCVFGAYR
L-ER             P-QVTADPSK VLRPT-TRKS KSNTAIIAGA ASGAVVLALI IGFCVFGAYR
Cflexuosa4       P-KVTADPFK VLRPR-TSQS RNHTTIIVGA AIGAVVLALI IGLCVMVAYC
Cflexuosa1       P-KVTADPFK VLRPR-TSQS RNHTTIIVGA AIGAVVLALI IGLCVMVAYC
Cflexuosa2       P-KVTADPSK VVPAR-TGKS GNHTAIVAGA ASGAVVLALI IGLCVLVTYR
Cflexuosa3       P-KVTADPSK VLRPR-TSQS RNHTAIVAGA ASGAIVLALI IGLCVLVAYR
Ptrichocar       PEQDIIDPSR ARPASGSGHS KSQTAIIAGG VSGGVVLAVV IGFCVLAASR
Osativa01g       V-----EPS- -LDGG-AVKK SSVGPIVGGV IGGLVVLALG YCC-FMICKR
Osativa03g       I-----VPT- -ASGGNSGKK SSVGPIIGGV IGGLVVLALG CCCFFVICKR
Zmaiz            RMLEEAEMGV TQGQFKAKQS NLQAMVIGGA AGGAAAFGIV AAICVVAYHS
Clustal Co                       :  .      :: *    *  .:.:       .

                 ....|....| ....|....| ....|....| ....|....| ....|....|
                         510        520        530        540        550
Boleracea        RRNRGENQPA SDATSGWLPL SLYGNSHSGG SGKTNTTGSY ASSLPSNLCR
Brapa            RRKAGEYQPA SDATSGWLPL SLYGNSHSGG SGKTNTTGSY ASSLPSNLCR
Ahalleri1        RRKRGDYQPA SDATSGWLPL SLYGNSHSAG SAKTNTTGSY ASSLPSNLCR
Ahalleri2        RRKRGDYQPA SDATSGWLPL SLYGNSHSAG SAKTNTTGSY ASSLPSNLCR
Alyrata          RRKRGDYQPA SDATSGWLPL SLYGNSHSAG SAKTNTTGSY ASSLPSNLCR
L-ER             RRKRGDYQPA SDATSGWLPL SLYGNSHSAG SAKTNTTGSY ASSLPSNLCR
Cflexuosa4       RRNRGDYQPA SDATSGWLPL SLYGNSHSAG STKTNTTGSY ASSLPSNLCR
Cflexuosa1       RRNRGDYQPA SDATSGWLPL SLYGNSHSAG STKTNTTGSY ASSLPSNLCR
Cflexuosa2       RRNRVNYQPA SDATSGWLPL SLYGNTHSAG SGKTNTTGSY ASSLPANLCR
Cflexuosa3       RRNRVNYQPA SDATSGWLPL SLYGNSHSAG SAKTNTTGSY ASSLPSNLCR
Ptrichocar       RHRQGKEASS SDGPSGWLPL SLYGNSHSAG SAKTNTTGSY ASSLPSNLCR
Osativa01g       RSRVGKDTGM SDGHSGWLPL SLYGNSHSSG SAKSHTTGSY ASSLPSNLCR
Osativa03g       RQRAGKDSGM SDGHSGWLPL SLYGNSHTSS SAKSHTTGSH ASSLPSNLCR
Zmaiz            KKRRALGNSV SHS-SGWLPV YG-GNSHTNA SKSSGGKSAA LNPNITAMCR
Clustal Co       : .        *.. *****:    **:*: . * .:  ..:   ..  : :**

                 ....|....| ....|....| ....|....| ....|....| ....|....|
                         560        570        580        590        600
Boleracea        HFSFAEIKAA TKNFDESRVL GVGGFGKVYR GEIDGGTTKV AIKRGNPMSE
Brapa            HFSFAEIKAA TKNFDESRVL GVGGFGKVYR GEIDGGTTKV AIKRGNPMSE
Ahalleri1        HFSFAEIKAA TKNFDESRVL GVGGFGKVYR GDIDGGTTKV AIKRGNPMSE
Ahalleri2        HFSFAEIKAA TKNFDESRVL GVGGFGKVYR GDIDGGTTKV AIKRGNPMSE
Alyrata          HFSFAEIKAA TKNFDESRVL GVGGFGKVYR GEIDGGTTKV AIKRGNPMSE
L-ER             HFSFAEIKAA TKNFDESRVL GVGGFGKVYR GEIDGGTTKV AIKRGNPMSE
Cflexuosa4       HFSFAEIKAA TKNFDESRVL GVGGFGKVYR GEIDGGTTKV AIKRGNPMSE
Cflexuosa1       HFSFAEIKAA TKNFDESRVL GVGGFGKVYR GEIDGGTTKV AIKRGNPMSE
Cflexuosa2       HFSFAEIKVA TKNFDESRVL GVGGFGKVYR GEIDGGTTKV AIKRGNPMSE
Cflexuosa3       HFSFAEIKAA TKNFDESRVL GVGGFGKVYR GEIDGGTTKV AIKRGNPMSE
Ptrichocar       HFSFAEIKSA TNNFDEVLLL GVGGFGKVYK GEIDGGTTKV AIKRGNPLSE
Osativa01g       HFSFAEIKAA TNNFDESLLL GVGGFGKVYR GEIDGGVTKV AIKRGNPLSE
Osativa03g       HFSFVEIKAA TNNFDESLLL GVGGFGKVYR GEIDGGATKV AIKRGNPLSE
Zmaiz            HFSFQEIKAA TKNFDESLVI GVGGFGKVYR GIVDG-DTKV AIKRSNPSSE
Clustal Co       **** *** * *:****  :: *********: * :**  *** ****.** **
```

```
                 ....|....| ....|....| ....|....| ....|....| ....|....|
                         610        620        630        640        650
Boleracea        QGVHEFQTEI EMLSKLRHRH LVSLIGYCEE NCEMILVYDY MAHGTMREHL
Brapa            QGVHEFQTEI EMLSKLRHRH LVSLIGYCEE NCEMILVYDY MAHGTMREHL
Ahalleri1        QGVHEFQTEI EMLSKLRHRH LVSLIGYCEE NCEMILVYDY MAHGTMREHL
Ahalleri2        QGVHEFQTEI EMLSKLRHRH LVSLIGYCEE NCEMILVYDY MAHGTMREHL
Alyrata          QGVHEFQTEI EMLSKLRHRH LVSLIGYCEE NCEMILVYDY MAHGTMREHL
L-ER             QGVHEFQTEI EMLSKLRHRH LVSLIGYCEE NCEMILVYDY MAHGTMREHL
Cflexuosa4       QGVHEFQTEI EMLSKLRHRH LVSLIGYCEE NCEMILVYDY MAHGTMREHL
Cflexuosa1       QGVHEFQTEI EMLSKLRHRH LVSLIGYCEE NCEMILVYDY MAHGTMREHL
Cflexuosa2       QGVHEFQTEI EMLSKLRHRH LVSLIGYCEE NCEMILVYDY MAYGTMREHL
Cflexuosa3       QGVHEFQTEI EMLSKLRHRH LVSLIGYCEE NCEMILVYDY MAYGTMREHL
Ptrichocar       QGVHEFQTEI EMLSKLRHRH LVSLIGYCEE NTEMILVYDY MAHGTLREHL
Osativa01g       QGVHEFQTEI EMLSKLRHRH LVSLIGYCEE KNEMILVYDY MAHGTLREHL
Osativa03g       QGVHEFQTEI EMLSKLRHRH LVSLIGYCEE KNEMILVYDY MAHGTLREHL
Zmaiz            QGVLEFQTEI EMLSKLRHKH LVSLIGCCED DGEMVLVYDY MAHGTLREHL
Clustal Co       *** ****** ********:* ****** **: . **:***** **:**:****

                 ....|....| ....|....| ....|....| ....|....| ....|....|
                         660        670        680        690        700
Boleracea        YKTQNSPLPW KQRLEICIGA ARGLHYLHTG AKHTIIHRDV KTTNILLDEK
Brapa            YKTQNSPLPW KQRLEICIGA ARGLHYLHTG AKHTIIHRDV KTTNILLDEK
Ahalleri1        YKTQNPSLPW KQRLEICIGA ARGLHYLHTG AKHTIIHRDV KTTNILLDEK
Ahalleri2        YKTQNPSLPW KQRLEICIGA ARGLHYLHTG AKHTIIHRDV KTTNILLDEK
Alyrata          YKTQNPSLPW KQRLEICIGA ARGLHYLHTG AKHTIIHRDV KTTNILLDEK
L-ER             YKTQNPSLPW KQRLEICIGA ARGLHYLHTG AKHTIIHRDV KTTNILLDEK
Cflexuosa4       YKTQNSPLPW KQRLEICIGA ARGLHYLHTG AKHTIIHRDV KTTNILLDEK
Cflexuosa1       YKTQNSPLPW KQRLEICIGA ARGLHYLHTG AKHTIIHRDV KTTNILLDEK
Cflexuosa2       YKTQNSPLAW KQRLEICIGA ARGLHYLHTG AKHTIIHRDV KTTNILLDDK
Cflexuosa3       YKTQNSPLPW KQRLEICIGA ARGLHYLHTG AKHTIIHRDV KTTNILLDEK
Ptrichocar       YKTQKPPLPW KQRLEICIGA ARGLHYLHTG AKHTIIHRDV KTTNILLDEK
Osativa01g       YKTKNAPLTW RQRLEICIGA ARGLHYLHTG AKHTIIHRDV KTTNILLDEK
Osativa03g       YKTQNAPLSW RQRLDICIGA ARGLHYLHTG AKHTIIHRDV KTTNILLDEK
Zmaiz            YKSGKPALPW RQRLEITIGA ARGLHYLHTG AKYTIIHRDV KTTNILVDEN
Clustal Co       **: :..*.* :***:* *** ********** **:******* ******:*::

                 ....|....| ....|....| ....|....| ....|....| ....|....|
                         710        720    ▲▲  730        740        750
Boleracea        WVAKVSDFGL SKTGP-ALDH THVSTVVKGS FGYLDPEYFR RQQLTDKSDV
Brapa            WVAKVSDFGL SKTGP-TLDH THVSTVVKGS FGYLDPEYFR RQQLTDKSDV
Ahalleri1        WVAKVSDFGL SKTGP-TLDH THVSTVVKGS FGYLDPEYFR RQQLTEKSDV
Ahalleri2        WVAKVSDFGL SKTGP-TLDH THVSTVVKGS FGYLDPEYFR RQQLTEKSDV
Alyrata          WVAKVSDFGL SKTGP-TLDH THVSTVVKGS FGYLDPEYFR RQQLTEKSDV
L-ER             WVAKVSDFGL SKTGP-TLDH THVSTVVKGS FGYLDPEYFR RQQLTEKSDV
Cflexuosa4       WVAKVSDFGL SKTGP-TLDH THVSTVVKGS FGYLDPEYFR RQQLTDKSDV
Cflexuosa1       WVAKVSDFGL SKTGP-TLDH THVSTVVKGS FGYLDPEYFR RQQLTDKSDV
Cflexuosa2       WVAKVSDFGL SKTGP-TVDH THVSTVVKGS FGYLDPEYFR RQQLTEKSDV
Cflexuosa3       WVAKVSDFGL SKTGP-TLDH THVSTVVKGS FGYLDPEYFR RQQLTEKSDV
Ptrichocar       WVAKVSDFGL SKTGP-TLDH THVSTVVKGS FGYLDPEYFR RQQLTEKSDV
Osativa01g       WVAKVSDFGL SKTGP-SMDH THVSTVVKGS FGYLDPEYFR RQQLTEKSDV
Osativa03g       WVAKVSDFGL SKTGP-TMDH THVSTVVKGS FGYLDPEYFR RQQLTDKSDV
Zmaiz            WVAKVSDFGL SKTGPTAMNQ THVSTMVKGS FGYLDPEYFR RQQLTEKSDV
Clustal Co       ********** ***** :::: *****:**** ********** *****:****
```

```
                 ....|....| ....|....| ....|....| ....|....| ....|....|
                         760        770        780        790        800
Boleracea        YSFGVVLFEA LCARPALNPT LAKEQVSLAE WAPYCYKKGM LDQIVDPHLK
Brapa            YSFGVVLFEA LCARPALNPT LAKEQVSLAE WAPYCYKKGM LDQIVDPHLK
Ahalleri1        YSFGVVLFEA LCARPALNPT LAKEQVSLAE WAPYCYKKGM LDQIVDPYLK
Ahalleri2        YSFGVVLFEA LCARPALNPT LAKEQVSLAE WAPYCYKKGM LDQIVDPYLK
Alyrata          YSFGVVLFEA LCARPALNPT LAKEQVSLAE WAPYCYKKGM LDQIVDPYLK
L-ER             YSFGVVLFEA LCARPALNPT LAKEQVSLAE WAPYCYKKGM LDQIVDPYLK
Cflexuosa4       YSFGVVLFEA LCARPALNPT LAKEQVSLAE WAPYCYKKGM LDQIVDPYLK
Cflexuosa1       YSFGVVLFEA LCARPALNPT LAKEQVSLAE WAPYCYKKGM LDQIVDPYLK
Cflexuosa2       YSFGVVLFEA LCARPALNPT LAKEQVSLAE WAPYCYKKGM LDQIVDPYLK
Cflexuosa3       YSFGVVLFEA LCARPALNPT LAKEQVSLAE WAPYCYKKGM LDQIVDPYLK
Ptrichocar       YSFGVVLFEI LCARPALNPT LPKEQVSLAE WAAHCHKKGI LDQILDPYLK
Osativa01g       YSFGVVLFEV LCARPALNPT LAKEEVSLAE WALHCQKKGI LDQIVDPHLK
Osativa03g       YSFGVVLFEV LCARPALNPT LAKEEVSLAE WALHCQKKGI LDQIVDPHLK
Zmaiz            YSYGVVLFEV LCARPALNPS LPREQVSLAD HALSCQRKGT LEDIIDPVLK
Clustal Co       **:******  *********: *.:*:****:  *  * :**  *::*:** **

                 ....|....| ....|....| ....|....| ....|....| ....|....|
                         810        820        830        840        850
Boleracea        GKITPECFKK FAETAMKCVL DQGIERPSMG DVLWNLEFAL QLQESAEESG
Brapa            GKITPECFKK FAETAMKCVL DQGIERPSMG DVLWNLEFAL QLQESAEESG
Ahalleri1        GKITPECFKK FAETAMKCVL DQGIERPSMG DVLWNLEFAL QLQESAEESG
Ahalleri2        GKITPECFKK FAETAMKCVL DQGIERPSMG DVLWNLEFAL QLQESAEESG
Alyrata          GKITPECFKK FAETAMKCVL DQGIERPSMG DVLWNLEFAL QLQESAEESG
L-ER             GKITPECFKK FAETAMKCVL DQGIERPSMG DVLWNLEFAL QLQESAEENG
Cflexuosa4       GKITPECFKK FAETAMKCVL DQGIERPSMG DVLWNLEFAL QLQESAEENG
Cflexuosa1       GKITPECFKK FAETAMKCVL DQGIERPSMG DVLWNLEFAL QLQESAEENG
Cflexuosa2       GKITPECFKK FSETAMKCVL DQGIERPSMG DVLWNLEFAL QLQESAEENG
Cflexuosa3       GKITPECFKK FSETAMKCVL DQGIERPSMG DVLWNLEFAL QLQESAEENG
Ptrichocar       GKITPECFKK FAETAMKCVS DQSIDRPSMG DVLWNLEFAL QLQESAEDGG
Osativa01g       GKIAPQCFKK FAETAEKCVS DEGIDRPSMG DVLWNLEFAL QMQESAEDSG
Osativa03g       GKIAPQCFKK FAETAEKCVS DQGIDRPSMG DVLWNLEFAL QMQESAEESG
Zmaiz            GKIAPDCLKK YAETAEKCLC DHGVDRPSMG DVLWNLEFAL QMQDTFENGG
Clustal Co       ***:*:*:** ::*** **:  *..::***** ********** *:*:: *:.*

                 ....|....| ....|....| ....|....| ....|....| ....|....|
                         860        870        880        890 ▲    ▲ 900
Boleracea        KGICSEMDMD EIKYDDDNCK GKNNSEKGCD VYEGNVTDSR SSGIDMSIGG
Brapa            KEICSEMDMG EIKYDDDNCK GKSNNDKGSD VYEGNVSDSR SSGIDMSIGG
Ahalleri1        KGVGGDMDMD EIKYDDGNCK GKN--DKNSD VYEGNVTDSR SSGIDMSIGG
Ahalleri2        KGVGGDMDMD EIKYDDGNCK GKN--DKNSD VYEGNVTDSR SSGIDMSIGG
Alyrata          KGVCGDMDMD EIKYDDGNCK GKN--DKSSD VYEGNVTDSR SSGIDMSIGG
L-ER             KGVCGDMDMD EIKYDDGNCK GKN--DKSSD VYEGNVTDSR SSGIDMSIGG
Cflexuosa4       KGMSGDMDMD EIKYNDGNGK GKN--EMSSD VYEGNVTDSR SSGIDMSIGG
Cflexuosa1       KGMSGDMDMD EIKYNDGNGK GKN--EMSSD VYEGNVTDSR SSGIDMSIGG
Cflexuosa2       KGVGGDVDMD EIKYDDGNCK GKN--DMSSD VYEGNVTDSR SSGIDMSIGG
Cflexuosa3       KGVGGDMDMN EIKYDDGNCK GKN--DMSSD VYEGNVTDSR SSGIDMSIGG
Ptrichocar       KGIVG-ADDE EVPFN-VTYK GKA--PDASP GYDGIVTDSR SSGISMSIGG
Osativa01g       SIGCGMSDEG ----TPLVMP GKK--DPNDP SIESSTTTTT TT--SISMGD
Osativa03g       SLGCGMSDDS ----TPLVIV GKK--DPNDP SIESSTTTTT TT--SISMGE
Zmaiz            KPEGG----- ---------- ------RGSS SDSGTVSMAD SMAASAAALE
Clustal Co       .   .                            .. .: :  :   . :
```

```
                ....|....| ....|....| ....|.
                        910        920
Boleracea       RSLASEDSDG LTPSGVFSQI MNPKGR
Brapa           RSLVSEDSDG LTPSAVFSQI MNPKGR
Ahalleri1       RSLASEDSDG LTPSAVFSQI MNPKGR
Ahalleri2       RSLASEDSDG LTPSAVFSQI MNPKGR
Alyrata         RSLASEDSDG LTPSAVFSQI MNPKGR
L-ER            RSLASEDSDG LTPSAVFSQI MNPKGR
Cflexuosa4      RSLASEDSEG LTPSAVFSQI MNPKGR
Cflexuosa1      RSLASEDSEG LTPSAVFSQI MNPKGR
Cflexuosa2      RSLASEDSEG LTPSAVFSQI MNPKGR
Cflexuosa3      RSLASEDSEG LTPSAVFSQI MNPKGR
Ptrichocar      RSLASEDSDG LTPSAVFSQI MNPKGR
Osativa01g      QSVASIDSDG LTPSAVFSQI MNPKGR
Osativa03g      QSVASIDSDG LTPSAVFSQI MNPKGR
Zmaiz           LISEDMDEED IANSVVFSQL VHPTGR
Clustal Co          . *.:. :: * ****: ::*.**
```

Legend:

Putative Signal Peptide cleavage site

Conserved Cysteine in extracellular domain

Putative Transmembrane domain

Putative Kinase domain

Putative Membrane transfer stop signal

▲▲ **Identifies unambiguously assigned phosphorilation site**

▲ **Denotes a phosphorylation site on one of two neighbouring S residues**

6.2 Appendix Figure 2. IRES 5'and 3'UTR identified by UTRScan

5' UTR analyzed sequence:

CATTT TTAGA TCTGT G AAGTTT ATAGTTT CGATTT TCTTTC GTTT GATAGA TCTGA GAAGA AGATC TTC CCGGA GAAGTGC TCTTG ATCGATGA

mRNA secondary structrure prediction by GeneBee.

```
****  MEANING OF THE SIGNS  ****
   * - compensatory  exchange
   : - conservative  exchange
```

Free Energy of Structure = -4.1 kkal/mol

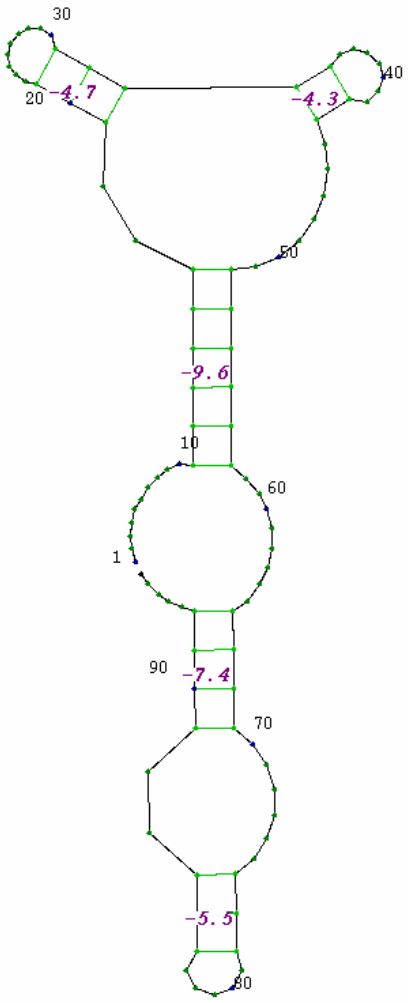

3’ UTR analyzed sequence:

TTCTA CAAAA ACATT AA ACATG AAT CGCGT CAATG TAC TATTT GGTTT GTTATC TATAA CGTT TTTGG TAATTG TTGCA TCTTTACTCT

mRNA secondary structrure prediction by GeneBee.

```
****  MEANING OF THE SIGNS  ****
   * - compensatory  exchange
   : - conservative  exchange
```

Free Energy of Structure = -4.9 kkal/mol

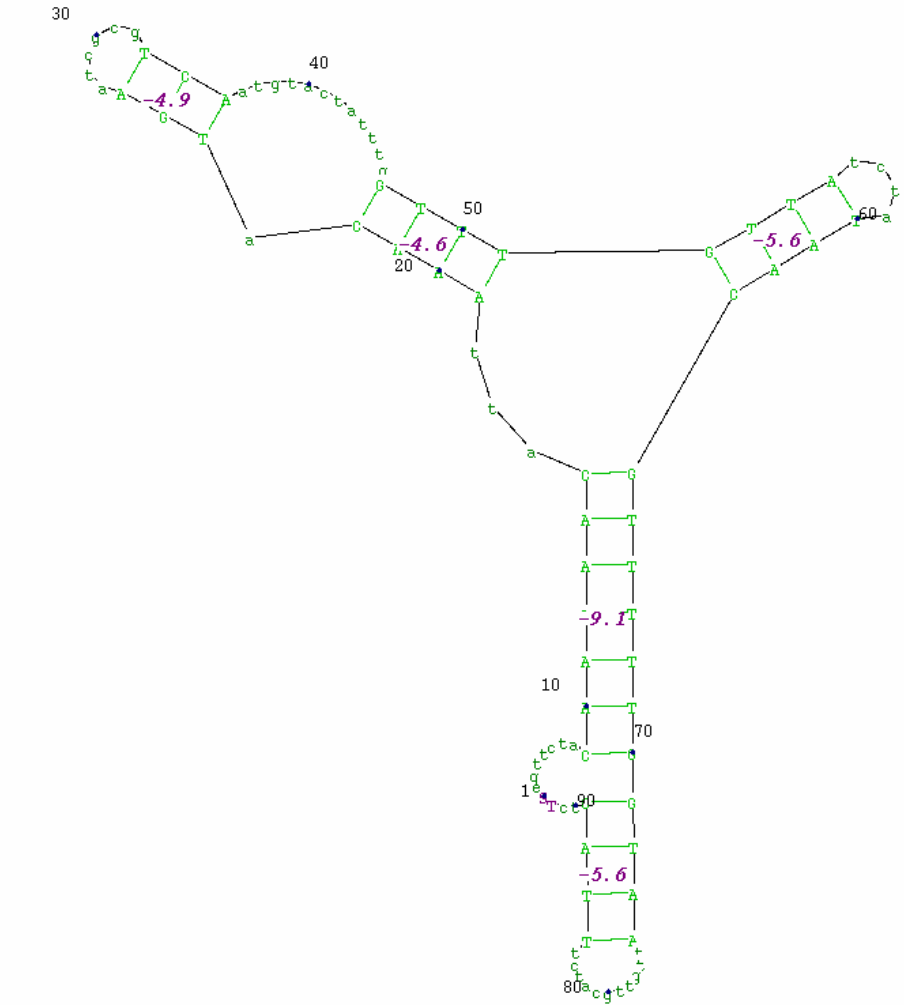

6.3 Appendix Figure 3. Amino acid alignment of *FER* and closest Arabidopsis homologues

```
                ....|....| ....|....| ....|....| ....|....| ....|....|
                         10         20         30         40         50
At3g04690       ---MSGKTR- --ILF-FLTC LSFLLVFPTR SNGQDLALSC G-TSEASADQ
At5g28680       ---MNEKLR- --ILFSFLCF FYVLLVSPSQ SNGQDISLSC G-ASEPAVDQ
At3g51550       MKITEGRFRL SLLLLLLLIS AATLISAADY SPTEKILLNC GGGASNLTDT
Consensus           . : *    :*: :*      *:  .   *  :.: *.* *  :.  .*


                ....|....| ....|....| ....|....| ....|....| ....|....|
                         60         70         80         90        100
At3g04690       DKKKWEPDTK --FLKTG--N SIHATATYQD PSLLSTVPYM TARIFTAPAT
At5g28680       DKKKWEPDTK --FLKTP--N TVHAPATYQD PSLLSTVPYM TSRIFTAPAT
At3g51550       DNRIWISDVK SKFLSSSSED SKTSPALTQD PSVP-EVPYM TARVFRSPFT
Consensus       *:: * .*.*   **.:   : :  :.*  ** **:   **** *:*:* :* *


                ....|....| ....|....| ....|....| ....|....| ....|....|
                        110        120        130        140        150
At3g04690       YEIPIKGDKR HLLRLYFYPS TYTGLNISNS YFTVEANDVT LLSNFSAAIT
At5g28680       YEIPVKGDKR HMLRLHFYPS TYTGLNILDS YFSVAANDLT LLSNFSAAIT
At3g51550       YTFPVASG-R KFVRLYFYPN SYDGLNATNS LFSVSFGPYT LLKNFSASQT
Consensus       * :*: .. * :::**:***. :* ***  :*  *:*  .  * **.****: *


                ....|....| ....|....| ....|....| ....|....| ....|....|
                        160        170        180        190        200
At3g04690       CQALTQAYLV KEYSLAPTDK DVLSIKFTPS DKYRDAFAFI NGIEVIQMPE
At5g28680       CQALTQAYLV REYSLAPSEK DVLSIIFTPS DKHPKAFAFI NGIEVIPMPE
At3g51550       AEALTYAFII KEFVVN-VEG GTLNMTFTPE SAPSNAYAFV NGIEVTSMPD
Consensus       .:*** *::: :*: :   :  ..*.: ***. .   .*:**: *****  **:


                ....|....| ....|....| ....|....| ....|....| ....|....|
                        210        220        230        240        250
At3g04690       LFD----TAA LVGFTDQTMD AKTANLQSMF RLNVGGQDIP GSQDSGGLTR
At5g28680       LFD----TAS LVGFSDQTSD TKTANLQTMF RLNVGGQDIP GSQDSGGLTR
At3g51550       MYSSTDGTLT MVGSSGSVTI DNSTALENVY RLNVGGNDIS PSADTG-LYR
Consensus       ::.    * : :** :...    ::: *:.:: ******:**.  * *:* * *


                ....|....| ....|....| ....|....| ....|....| ....|....|
                        260        270        280        290        300
At3g04690       TWYNDAPYIF SAGLGVTLQA SNNFRINYQN -MPVSIAPAD IYKTARSQGP
At5g28680       TWYNDAPYIF SAGLGVTLQA SNNFRIDYQK -MPVSTAPAD VYKTARSQGP
At3g51550       SWYDDQPYIF GAGLGIPETA DPNMTIKYPT GTPTYVAPVD VYSTARSMGP
Consensus       :**:* **** .****:.  * . *: *.* .   *.  **.* :*.**** **


                ....|....| ....|....| ....|....| ....|....| ....|....|
                        310        320        330        340        350
At3g04690       NGDINLKSNL TWMFQIDKNF TYILRLHFCE FQ--LSKINQ KVFNIYINNR
At5g28680       NGDINMKSNL TWMFQVDTNF TYIMRLHFCE FQ--LAKINQ KVFNIFINNR
At3g51550       TAQINLNYNL TWIFSIDSGF TYLVRLHFCE VSSNITKINQ RVFTIYLNNQ
Consensus       ..:**:: ** **:*.:*..* **::****** ..  ::**** :**.*::**:
```

```
                ....|....| ....|....| ....|....| ....|....| ....|....|
                       360        370        380        390        400
At3g04690       TAQADTTPAD IIGWTGEKGI PMYKDYAIYV DANNGG--EE ITLQMTPSTF
At5g28680       TAQGDTNPAD ILGWTGGKGI PTYKDYAIYV DANTGGGGEE ISLQMTPSTF
At3g51550       TAEP---EAD VIAWTSSNGV PFHKDYVVNP PEGNGQ--QD LWLALHPNPV
Consensus       **:     ** ::.**. :*: * :***.:     ..*   :: : * : *...

                ....|....| ....|....| ....|....| ....|....| ....|....|
                       410        420        430        440        450
At3g04690       GQPEYYDSSL NGLEIFKMDT MK-NLAGPNP EPSP---MQA EEEVKKEFKN
At5g28680       GQPEYYDSQL NGLEIFKIDT MK-NLAGPNP KPSP---MQA NEDVKKDFQG
At3g51550       NKPEYYDSLL NGVEIFKMNT SDGNLAGTNP IPGPQVTADP SKVLRPTTRK
Consensus       .:****** * **:****::*  . ****.**  *.*    :. .: ::   :

                ....|....| ....|....| ....|....| ....|....| ....|....|
                       460        470        480        490        500
At3g04690       EKR-HAFIIG SAGG--VLAV LIGALCFTAY KKKQG--YQG GDSHTSSWLP
At5g28680       DKRITAFVIG SAGG--VAAV LFCALCFTMY QRKRK--FSG SDSHTSSWLP
At3g51550       SKSNTAIIAG AASGAVVLAL IIGFCVFGAY RRRKRGDYQP ASDATSGWLP
Consensus       .*   *:: * :*.*  * *: ::    *  * ::::   :.  ... **.***

                ....|....| ....|....| ....|....| ....|....| ....|....|
                       510        520        530        540        550
At3g04690       --IYGNSTTS GTKSTISGKS NNGSHLSNLA AGLCRRFSLP EIKHGTQNFD
At5g28680       --IYGNSHTS ATKSTISGKS NNGSHLSNLA AGLCRRFSLS EIKHGTHNFD
At3g51550       LSLYGNSHSA GSAKTN---- TTGSYASSLP SNLCRHFSFA EIKAATKNFD
Consensus         :**** :: .: .*      ..**: *.*. :.***:**:. *** .*:***

                ....|....| ....|....| ....|....| ....|....| ....|....|
                       560        570        580        590        600
At3g04690       DSNVIGVGGF GKVYKGVIDG -TTKVAVKKS NPNSEQGLNE FETEIELLSR
At5g28680       ESNVIGVGGF GKVYKGVIDG -GTKVAIKKS NPNSEQGLNE FETEIELLSR
At3g51550       ESRVLGVGGF GKVYRGEIDG GTTKVAIKRG NPMSEQGVHE FQTEIEMLSK
Consensus       :*.*:***** ****:* ***   ****:*:. ** ****::* *:****:**:

                ....|....| ....|....| ....|....| ....|....| ....|....|
                       610        620        630        640        650
At3g04690       LRHKHLVSLI GYCDEGGEMC LVYDYMAFGT LREHLYNTKK PQLTWKRRLE
At5g28680       LRHKHLVSLI GYCDEGGEMC LIYDYMSLGT LREHLYNTKR PQLTWKRRLE
At3g51550       LRHRHLVSLI GYCEENCEMI LVYDYMAHGT MREHLYKTQN PSLPWKQRLE
Consensus       ***:****** ***:*. **  *:****: ** :*****:*:. *.*.**:***

                ....|....| ....|....| ....|....| ....|....| ....|....|
                       660        670        680        690        700
At3g04690       IAIGAARGLH YLHTGAKYTI IHRDVKTTNI LVDENWVAKV SDFGLSKTGP
At5g28680       IAIGAARGLH YLHTGAKYTI IHRDVKTTNI LLDENWVAKV SDFGLSKTGP
At3g51550       ICIGAARGLH YLHTGAKHTI IHRDVKTTNI LLDEKWVAKV SDFGLSKTGP
Consensus       *.******** *******:** ********** *:**:***** **********
```

```
                ....|....| ....|....| ....|....| ....|....| ....|....|
                       710        720        730        740        750
At3g04690       NMNGGHVTTV VKGSFGYLDP EYFRRQQLTE KSDVYSFGVV LFEILCARPA
At5g28680       NMNGGHVTTV VKGSFGYLDP EYFRRQQLTE KSDVYSFGVV LFEVLCARPA
At3g51550       TLDHTHVSTV VKGSFGYLDP EYFRRQQLTE KSDVYSFGVV LFEALCARPA
Consensus       .::  **:** ********** ********** ********** *** ******


                ....|....| ....|....| ....|....| ....|....| ....|....|
                       760        770        780        790        800
At3g04690       LNPSLPKEQV SLGDWAMNCK RKGNLEDIID PNLKGKINAE CLKKFADTAE
At5g28680       LNPSLSKEQV SLGDWAMNCK RKGTLEDIID PNLKGKINPE CLKKFADTAE
At3g51550       LNPTLAKEQV SLAEWAPYCY KKGMLDQIVD PYLKGKITPE CFKKFAETAM
Consensus       ***:*.**** **.:**  *  :** *::*:* * *****..* *:****:**


                ....|....| ....|....| ....|....| ....|....| ....|....|
                       810        820        830        840        850
At3g04690       KCLNDSGLER PTMGDVLWNL EFALQLQETA DGT------- ------RHRT
At5g28680       KCLSDSGLDR PTMGDVLWNL EFALQLQETA DGS------- ------RHRT
At3g51550       KCVLDQGIER PSMGDVLWNL EFALQLQESA EENGKGVCGD MDMDEIKYDD
Consensus       **: *.*::* *:******** ********:* : .             ::


                ....|....| ....|....| ....|....| ....|....| ....|....|
                       860        870        880        890        900
At3g04690       PNNGGS---S EDLGRGGMAV NV---AGRDD VS-DLSSEDN -----TEIFS
At5g28680       PSNGGG---S VDLGGGGGGV TVNISAGESD LGDDLSSEEN -----SGIFS
At3g51550       GNCKGKNDKS SDVYEGNVTD SRSSGIDMSI GGRSLASEDS DGLTPSAVFS
Consensus        .  *    *  *:  *.    .     . .   . .*:**:.      : :**


                ....|...

At3g04690       QIVNPKGR
At5g28680       QIVNPKGR
At3g51550       QIMNPKGR
Consensus       **:*****
```

Plant material

JE number	Description
JE-1	*LAT52::GFP*
JE-6-5	M2 screen
JE-4-8	M2 screen
JE-4-12	M2 screen
JE-13-5	M2 screen
JE-22-4	M2 screen
JE-24-6	M2 screen
JE-21-14	M2 screen
JE-93	*fer*/+ Complementation At3g1550 Plant 1 Homozygous *Ds*
JE-94	*fer*/+ Complementation At3g1550 Plant 2 Wild-type
JE-95	*fer*/+ Complementation At3g1550 Plant 3 Heterozygous *Ds*
JE-96	*fer*/+ Complementation At3g1550 Plant 4 Heterozygous *Ds*
JE-97	*fer*/+ Complementation At3g1550 Plant 5 Heterozygous *Ds*
JE-98	*fer*/+ Complementation At3g1550 Plant 6 Homozygous *Ds*
JE-99	*fer*/+ Complementation At3g1550 Plant 7 Heterozygous *Ds*
JE-100	*fer*/+ Complementation At3g1550 Plant 8 Wild-type
JE-101	*fer*/+ Complementation At3g1550 Plant 9 Wild-type
JE-102	*fer*/+ Complementation At3g1550 Plant 10 Heterozygous *Ds*
JE-103	*fer*/+ Complementation At3g1550 Plant 11 Homozygous *Ds*
JE-104	*fer*/+ Complementation At3g1550 Plant 12 Homozygous *Ds*
JE-105	*fer*/+ Complementation At3g1550 Plant 13 Heterozygous *Ds*
JE-106	*fer*/+ Complementation At3g1550 Plant 14 Wild-type
JE-107	*fer*/+ Complementation At3g1550 Plant 15 Heterozygous *Ds*
JE-108	*fer*/+ Complementation At3g1550 Plant 16 Heterozygous *Ds*
JE-109	*fer*/+ Complementation At3g1550 Plant 17 Homozygous *Ds*
JE-110	*fer*/+ Complementation At3g1550 Plant 18 Wild-type
JE-111	*fer*/+ Complementation At3g1550 Plant 19 Heterozygous *Ds*
JE-112	*fer*/+ Complementation At3g1550 Plant 20 Homozygous *Ds*
JE-113	*fer*/+ Complementation At3g1550 Plant 21 Homozygous *Ds*
JE-114	*fer*/+ Complementation At3g1550 Plant 22 Wild-type

JE-115	*fer*/+ Complementation At3g1550 Plant 23 Heterozygous *Ds*
JE-116	*fer*/+ Complementation At3g1550 Plant 24 Wild-type
JE-117	*fer*/+ Complementation At3g1550 Plant 25 Heterozygous *Ds*
JE-118	*fer*/+ Complementation At3g1550 Plant 26 Heterozygous *Ds*
JE-119	*fer*/+ Complementation At3g1550 Plant 27 Heterozygous *Ds*
JE-120	*fer*/+ Complementation At3g1550 Plant 28 Heterozygous *Ds*
JE-121	*fer*/+ Complementation At3g1550 Plant 29 Heterozygous *Ds*
JE-122	*fer*/+ Complementation At3g1550 Plant 30 Homozygous *Ds*
JE-123	*fer*/+ Complementation At3g1550 Plant 31 Wild-type
JE-124	*fer*/+ Complementation At3g1550 Plant 32 Wild-type
JE-125	*fer*/+ Complementation At3g1550 Plant 33 wild-type
JE-126	*fer*/+ Complementation At3g1550 Plant 34 Heterozygous *Ds*
JE-127	*fer*/+ Complementation At3g1550 Plant 35 Homozygous *Ds*
JE-128	*fer*/+ Complementation At3g1550 Plant 36 Heterozygous *Ds*
JE-129	*fer*/+ Complementation At3g1550 Plant 37 Heterozygous *Ds*
JE-130	*fer*/+ Complementation At3g1550 Plant 38 Heterozygous *Ds*
JE-131	*fer*/+ Complementation At3g1550 Plant 39 Wild-type
JE-167	*pFER::GUS*
JE-211	*Brassica oleracea* used for DNA extraction
JE-216	*pFER::FER-GFP* (13.1) L-*er*
JE-217	*pFER::FER-GFP* (3.1) L-*er*
JE-218	*pFER::FER-GFP* (13.1) transformant 42 *fer*/+. Homozygous *Ds*
JE-219	*pFER::FER-GFP* (3.1) transformant 50 *fer*/+. Homozygous *Ds*
JE-220	*pFER::FER-GFP* (3.1) transformant 53 *fer*/+. Homozygous *Ds*
JE-223	*pFER::FER-GFP* (13.1) transformant 36 *fer*/+. Heterozygous *Ds*
JE-224	*pFER::FER-GFP* (13.1) transformant 40 *fer*/+. Heterozygous *Ds*
JE-225	*pFER::FER-GFP* (13.1) transformant 41 *fer*/+. Heterozygous *Ds*
JE-226	*pFER::FER-GFP* (13.1) transformant 42 *fer*/+. Homozygous *Ds*
JE-227	*pFER::FER-GFP* (13.1) transformant 43 *fer*/+. Heterozygous *Ds*
JE-228	*pFER::FER-GFP* (13.1) transformant 44 *fer*/+. Heterozygous *Ds*
JE-229	*pFER::FER-GFP* (13.1) transformant 45 *fer*/+. Heterozygous *Ds*
JE-230	*pFER::FER-GFP* (13.1) transformant 46 *fer*/+. Heterozygous *Ds*
JE-231	*pFER::FER-GFP* (3.1) transformant 47 *fer*/+. Heterozygous *Ds*

JE-234	*pFER::FER-GFP* (3.1) transformant 50 *fer*/+. Homozygous *Ds*
JE-235	*pFER::FER-GFP* (3.1) transformant 51 *fer*/+. Heterozygous *Ds*
JE-236	*pFER::FER-GFP* (3.1) transformant 53 *fer*/+. Homozygous *Ds*
JE-237	*pFER::FER-GFP* (13.1) transformant 40 *fer*/+. Heterozygous *Ds*
JE-238	*pAtD123::EGFP-AtROP6C*
JE-250	T-DNA GABI-KAT106A06.04
Arabidopsis halleri	Pollen collected from Botanical Garden University of Zurich
Capsella bursa pastoris – rubella	Pollen collected from Botanical Garden University of Zurich
Boechera holboellii	Pollen collected from Botanical Garden University of Zurich
Lobularia maritime	Pollen collected from Botanical Garden University of Zurich
Cardamine trifolia	Pollen collected from Botanical Garden University of Zurich
Cardamine bulbifera	Pollen collected from Botanical Garden University of Zurich

6.4 Plasmids

pFER::FER-GFP (13.1) L-*er*	Cloned into pMDC 111[a]
pFER::FER-GFP (3.1) L-*er*	Cloned into pMDC 111 [a]
pFER::GUS	Cloned into pCAMBIA-1391z
35S::GFP-FER	Cloned into pMDC 43 [a]
35S::FER-GFP	Cloned into pMDC 84 [a]
35S::GFP	ppk100. A gift of Drs. Robert Blanvillain and Patrick Gallois, University of Manchester, UK)
in situ probe 900 bp	Cloned into pBluescript KS

[a] (Curtis and Grossniklaus 2003)

7. References

Adachi, J. and M. Hasegawa (1996). "MOLPHY Version 2.3: programs for molecular phylogenetics based on maximum likelihood method." Comput. Sci. Monogr **28**: 1-150.

Bairoch, A., P. Bucher, et al. (1997). "The PROSITE database, its status in 1997." Nucleic Acids Res **25**(1): 217-21.

Baroux, C., V. Gagliardini, et al. (2006). "Dynamic regulatory interactions of Polycomb group genes: MEDEA autoregulation is required for imprinted gene expression in Arabidopsis." Genes & Development **20**(9): 1081-1086.

Bendtsen, J. D., H. Nielsen, et al. (2004). "Improved prediction of signal peptides: SignalP 3.0." J Mol Biol **340**(4): 783-95.

Billeter, J. C., E. J. Rideout, et al. (2006). "Control of male sexual behavior in Drosophila by the sex determination pathway." Current Biology **16**(17): R766-R776.

Boyes, D. C. and J. B. Nasrallah (1993). "Physical Linkage of the Slg and Srk Genes at the Self-Incompatibility Locus of Brassica-Oleracea." Molecular & General Genetics **236**(2-3): 369-373.

Brodskii, L. I., V. V. Ivanov, et al. (1995). "[GeneBee-NET: An Internet based server for biopolymer structure analysis]." Biokhimiia **60**(8): 1221-30.

Catoire, L., M. Pierron, et al. (1998). "Investigation of the action patterns of pectinmethylesterase isoforms through kinetic analyses and NMR spectroscopy - Implications in cell wall expansion." Journal of Biological Chemistry **273**(50): 33150-33156.

Chao, L. (1988). "Evolution of sex in RNA viruses." J Theor Biol **133**(1): 99-112.

Charlesworth, D. (2006). "Evolution of plant breeding systems." Current Biology **16**(17): R726-R735.

Chen, C. Y. and A. B. Shyu (1995). "AU-rich elements: characterization and importance in mRNA degradation." Trends Biochem Sci **20**(11): 465-70.

Cheung, A. Y., H. Wang, et al. (1995). "A floral transmitting tissue-specific glycoprotein attracts pollen tubes and stimulates their growth." Cell **82**(3): 383-93.

Chinchilla, D., Z. Bauer, et al. (2006). "The Arabidopsis receptor kinase FLS2 binds flg22 and determines the specificity of flagellin perception." Plant Cell **18**(2): 465-476.

Christensen, C. A., S. W. Gorsich, et al. (2002). "Mitochondrial GFA2 is required for synergid cell death in Arabidopsis." Plant Cell **14**(9): 2215-32.

Clough, S. J. and A. F. Bent (1998). "Floral dip: a simplified method for Agrobacterium-mediated transformation of Arabidopsis thaliana." Plant J **16**(6): 735-43.

Curtis, M. D. and U. Grossniklaus (2003). "A gateway cloning vector set for high-throughput functional analysis of genes in planta." Plant Physiol **133**(2): 462-9.

Dacks, J. and A. J. Roger (1999). "The first sexual lineage and the relevance of facultative sex." J Mol Evol **48**(6): 779-83.

Danon, A., V. I. Rotari, et al. (2004). "Ultraviolet-C overexposure induces programmed cell death in Arabidopsis, which is mediated by caspase-like activities and which can be suppressed by caspase inhibitors, p35 and Defender against Apoptotic Death." Journal of Biological Chemistry **279**(1): 779-787.

Desfeux, C., S. J. Clough, et al. (2000). "Female reproductive tissues are the primary target of Agrobacterium-mediated transformation by the Arabidopsis floral-dip method." Plant Physiol **123**(3): 895-904.
Dickinson, H. G., J. Doughty, et al. (1998). "Pollen-stigma interactions in Brassica." Symp Soc Exp Biol **51**: 51-7.
Dinkova, T. D., H. Zepeda, et al. (2005). "Cap-independent translation of maize Hsp101." Plant Journal **41**(5): 722-731.
Esau, K. (1977). Anatomy of seed plants. New York, John Wiley and Sons.
Faure, J. E., N. Rotman, et al. (2002). "Fertilization in Arabidopsis thaliana wild type: developmental stages and time course." Plant J **30**(4): 481-8.
Ferguson, C., T. T. Teeri, et al. (1998). "Location of cellulose and callose in pollen tubes and grains of Nicotiana tabacum." Planta **206**(3): 452-460.
Fisher, R. A. (1930). The Genetical Theory of Natural Selection. Oxford, Oxford University Press.
Friedman, W. E. (2006). "Embryological evidence for developmental lability during early angiosperm evolution." Nature **441**(7091): 337-340.
Fu, Y. X. and W. H. Li (1993). "Statistical tests of neutrality of mutations." Genetics **133**(3): 693-709.
Galindo, B. E., V. D. Vacquier, et al. (2003). "Positive selection in the egg receptor for abalone sperm lysin." Proc Natl Acad Sci U S A **100**(8): 4639-43.
Garcia-Calvo, M., E. P. Peterson, et al. (1998). "Inhibition of human caspases by peptide-based and macromolecular inhibitors." Journal of Biological Chemistry **273**(49): 32608-32613.
Geitmann, A., B. N. Snowman, et al. (2000). "Alterations in the actin cytoskeleton of pollen tubes are induced by the self-incompatibility reaction in Papaver rhoeas." Plant Cell **12**(7): 1239-51.
Greenberg, J. T. and F. M. Ausubel (1993). "Arabidopsis mutants compromised for the control of cellular damage during pathogenesis and aging." Plant J **4**(2): 327-41.
Gunning, B. and J. Pate (1969). ""“Transfer cells” Plant cells with wall ingrowths, specialized in relation to short distance transport of solutes—Their occurrence, structure, and development." Protoplasma **68**: 107–33.
Hall, B. G. (2001). Phylogenetic Tress Made Easy: A How-To Manual for Molecular Biologists. Sunderland, MA, Sinauer Associates, Inc.
Hall, T. A. (1999). "BioEdit: a user-friendly biological sequence alignment editor and analysis program for Windows 95/98/NT." Nucl. Acids. Symp. Ser. **41**: 95-98.
Hepler, P. K., Wayne, R.O (1985). "Calcium and plant development." Annu. Rev. Plant Physiol **36**: 379–439.
Higashiyama, T., R. Inatsugi, et al. (2006). "Species preferentiality of the pollen tube attractant derived from the synergid cell of Torenia fournieri." Plant Physiol **142**(2): 481-91.
Higashiyama, T., H. Kuroiwa, et al. (1998). "Guidance in vitro of the pollen tube to the naked embryo sac of Torenia fournieri." Plant Cell **10**(12): 2019-2031.
Higashiyama, T., H. Kuroiwa, et al. (2000). "Explosive discharge of pollen tube contents in Torenia fournieri." Plant Physiol **122**(1): 11-4.
Higashiyama, T., H. Kuroiwa, et al. (2003). "Pollen-tube guidance: beacons from the female gametophyte." Current Opinion in Plant Biology **6**(1): 36-41.
Higgins, D. G., J. D. Thompson, et al. (1996). "Using CLUSTAL for multiple sequence alignments." Methods Enzymol **266**: 383-402.

Hiscock, S. J. and H. G. Dickinson (1993). "Unilateral Incompatibility within the Brassicaceae - Further Evidence for the Involvement of the Self-Incompatibility (S)-Locus." Theoretical and Applied Genetics **86**(6): 744-753.

Holcik, M., N. Sonenberg, et al. (2000). "Internal ribosome initiation of translation and the control of cell death." Trends in Genetics **16**(10): 469-473.

Howden, R., S. K. Park, et al. (1998). "Selection of T-DNA-tagged male and female gametophytic mutants by segregation distortion in Arabidopsis." Genetics **149**(2): 621-31.

Huang, B. Q. and S. D. Russell (1994). "Fertilization in Nicotiana-Tabacum - Cytoskeletal Modifications in the Embryo Sac during Synergid Degeneration - a Hypothesis for Short-Distance Transport of Sperm Cells Prior to Gamete Fusion." Planta **194**(2): 200-214.

Huck, N. (2003). The Female Control of Male Behaviour in Sexual Plant Reproduction: Characterization of the Female Gametophytic Mutant *feronia* in *Arabidopsis thaliana*. Zurich, University of Zurich. **Dr.sc.nat:** 116.

Huck, N., J. M. Moore, et al. (2003). "The Arabidopsis mutant feronia disrupts the female gametophytic control of pollen tube reception." Development **130**(10): 2149-59.

Hülskamp, M., S. D. Kopczak, et al. (1995). "Identification of genes required for pollen-stigma recognition in Arabidopsis thaliana." Plant J **8**(5): 703-14.

Hülskamp, M., K. Schneitz, et al. (1995). "Genetic-Evidence for a Long-Range Activity That Directs Pollen-Tube Guidance in Arabidopsis." Plant Cell **7**(1): 57-64.

Ikeda, K., B. Igic, et al. (2004). "Primary structural features of the S haplotype-specific F-box protein, SFB, in Prunus." Sexual Plant Reproduction **16**(5): 235-243.

Ishimizu, T., T. Endo, et al. (1998). "Identification of regions in which positive selection may operate in S-RNase of Rosaceae: Implication for S-allele-specific recognition sites in S-RNase." Febs Letters **440**(3): 337-342.

Janson, J. and M. Willemse (1995). "Pollen tube penetration and fertilization in *Lilium longiflorum* (Liliaceae)." Am. j. bot. **82**: 186-196.

Jensen, W. A. (1965). "The ultrastructure and histochemistry of the synergids in cotton." Amer. J. Bot. **52**: 238-256.

Jiang, L. X., S. L. Yang, et al. (2005). "VANGUARD1 encodes a pectin methylesterase that enhances pollen tube growth in the Arabidopsis style and transmitting tract." Plant Cell **17**(2): 584-596.

Kachroo, A., M. E. Nasrallah, et al. (2002). "Self-incompatibility in the Brassicaceae: Receptor-ligand signaling and cell-to-cell communication." Plant Cell **14**: S227-S238.

Kachroo, A., C. R. Schopfer, et al. (2001). "Allele-specific receptor-ligand interactions in Brassica self-incompatibility." Science **293**(5536): 1824-1826.

Kandasamy, M. K., J. B. Nasrallah, et al. (1994). "Pollen Pistil Interactions and Developmental Regulation of Pollen-Tube Growth in Arabidopsis." Development **120**(12): 3405-3418.

Kaul, V., J. L. Rouse, et al. (1986). "Early Events in the Embryo Sac after Intraspecific and Interspecific Pollinations in Rhododendron-Kawakamii and R-Retusum." Canadian Journal of Botany-Revue Canadienne De Botanique **64**(2): 282-291.

Kim, S., J. C. Mollet, et al. (2003). "Chemocyanin, a small basic protein from the lily stigma, induces pollen tube chemotropism." Proceedings of the National Academy of Sciences of the United States of America **100**(26): 16125-16130.
Kimura, M. (1968). "Evolutionary Rate at Molecular Level." Nature **217**(5129): 624-&.
Kinoshita, T., A. Cano-Delgado, et al. (2005). "Binding of brassinosteroids to the extracellular domain of plant receptor kinase BRI1." Nature **433**(7022): 167-71.
Kombrink, E., M. Schroder, et al. (1988). "Several Pathogenesis-Related Proteins in Potato Are 1,3-Beta-Glucanases and Chitinases." Proceedings of the National Academy of Sciences of the United States of America **85**(3): 782-786.
Koscinska-Pajak, M. and J. Bednara (2006). "Unusual microtubular cytoskeleton of apomictic embryo sac of Chondrilla juncea L." Protoplasma **227**(2-4): 87-93.
Kusaba, M., K. Dwyer, et al. (2001). "Self-incompatibility in the genus Arabidopsis: Characterization of the S locus in the outcrossing A-lyrata and its autogamous relative A-thaliana." Plant Cell **13**(3): 627-643.
Le, S. Y. and J. V. Maizel, Jr. (1997). "A common RNA structural motif involved in the internal initiation of translation of cellular mRNAs." Nucleic Acids Res **25**(2): 362-69.
Lee, Y. H., T. Ota, et al. (1995). "Positive selection is a general phenomenon in the evolution of abalone sperm lysin." Mol Biol Evol **12**(2): 231-8.
Lee, Y. J., D. H. Kim, et al. (2001). "Identification of a signal that distinguishes between the chloroplast outer envelope membrane and the endomembrane system in vivo." Plant Cell **13**(10): 2175-90.
Lewis, C. A., C. F. Talbot, et al. (1982). "A protein from abalone sperm dissolves the egg vitelline layer by a nonenzymatic mechanism." Dev Biol **92**(1): 227-39.
Liu, H. and E. Kubli (2003). "Sex-peptide is the molecular basis of the sperm effect in Drosophila melanogaster." Proc Natl Acad Sci U S A **100**(17): 9929-33.
Lyon, J. D. and V. D. Vacquier (1999). "Interspecies chimeric sperm lysins identify regions mediating species-specific recognition of the abalone egg vitelline envelope." Dev Biol **214**(1): 151-9.
Mansfield, S. G., Briarty, L.G., Erni. S. (1991). "Early embryogenesis in *Arabidopsis thaliana*. I. The mature embryo sac.
." Can. J. Bot. **69**: 447-460.
Marton, M. L., S. Cordts, et al. (2005). "Micropylar pollen tube guidance by egg apparatus 1 of maize." Science **307**(5709): 573-6.
Mathews, S. and M. J. Donoghue (1999). "The root of angiosperm phylogeny inferred from duplicate phytochrome genes." Science **286**(5441): 947-950.
Mayfield, J. A., A. Fiebig, et al. (2001). "Gene families from the Arabidopsis thaliana pollen coat proteome." Science **292**(5526): 2482-2485.
Maynard Smith, J. (1978). The Evolution of Sex. Cambridge Cambridge Univ. Press.
McDonald, J. H. and M. Kreitman (1991). "Adaptive protein evolution at the Adh locus in Drosophila." Nature **351**(6328): 652-4.
Moore, J. M., J. P. Calzada, et al. (1997). "Genetic characterization of hadad, a mutant disrupting female gametogenesis in Arabidopsis thaliana." Cold Spring Harb Symp Quant Biol **62**: 35-47.
Mori, T., H. Kuroiwa, et al. (2006). "GENERATIVE CELL SPECIFIC 1 is essential for angiosperm fertilization." Nature Cell Biology **8**(1): 64-71.

Nakayama, S., K. Kaiser, et al. (1997). "Ectopic expression of sex-peptide in a variety of tissues in Drosophila females using the P[GAL4] enhancer-trap system." Mol Gen Genet **254**(4): 449-55.

Nasrallah, J. B., T. H. Kao, et al. (1985). "A Cdna Clone Encoding an S-Locus-Specific Glycoprotein from Brassica-Oleracea." Nature **318**(6043): 263-267.

Nawaschin, S. G. (1898). "Resultate einer Revision der Befruchtungsvorgange bei *Lilium martagon* un *Fritllaria tenella*." Bull. Acad. Sci. St. Petersburg **9**: 377-382.

Nei, M. and T. Gojobori (1986). "Simple methods for estimating the numbers of synonymous and nonsynonymous nucleotide substitutions." Mol Biol Evol **3**(5): 418-26.

Nelson, C. J., A. D. Hegeman, et al. (2006). "A quantitative analysis of Arabidopsis plasma membrane using trypsin-catalyzed O-18 labeling." Molecular & Cellular Proteomics **5**(8): 1382-1395.

Nowack, M. K., P. E. Grini, et al. (2006). "A positive signal from the fertilization of the egg cell sets off endosperm proliferation in angiosperm embryogenesis." Nat Genet **38**(1): 63-7.

Nuhse, T. S., A. Stensballe, et al. (2004). "Phosphoproteomics of the arabidopsis plasma membrane and a new phosphorylation site database." Plant Cell **16**(9): 2394-2405.

Olsen, K. M., A. Womack, et al. (2002). "Contrasting evolutionary forces in the Arabidopsis thaliana floral developmental pathway." Genetics **160**(4): 1641-1650.

Page, R. D. (1996). "TreeView: an application to display phylogenetic trees on personal computers." Comput Appl Biosci **12**(4): 357-8.

Palanivelu, R., L. Brass, et al. (2003). "Pollen tube growth and guidance is regulated by POP2, an Arabidopsis gene that controls GABA levels." Cell **114**(1): 47-59.

Park, S. Y. and E. M. Lord (2003). "Expression studies of SCA in lily and confirmation of its role in pollen tube adhesion." Plant Mol Biol **51**(2): 183-9.

Pawson, T. (2002). "Regulation and targets of receptor tyrosine kinases." European Journal of Cancer **38**: S3-S10.

Pawson, T. and J. D. Scott (1997). "Signaling through scaffold, anchoring, and adaptor proteins." Science **278**(5346): 2075-2080.

Pesole, G. and S. Liuni (1999). "Internet resources for the functional analysis of 5' and 3' untranslated regions of eukaryotic mRNAs." Trends Genet **15**(9): 378.

Primakoff, P. and D. G. Myles (2002). "Penetration, adhesion, and fusion in mammalian sperm-egg interaction." Science **296**(5576): 2183-2185.

Qiao, H., F. Wang, et al. (2004). "The F-box protein AhSLF-S2 controls the pollen function of S-RNase-based self-incompatibility." Plant Cell **16**(9): 2307-22.

Qiao, H., H. Wang, et al. (2004). "The F-box protein AhSLF-S2 physically interacts with S-RNases that may be inhibited by the ubiquitin/26S proteasome pathway of protein degradation during compatible pollination in Antirrhinum." Plant Cell **16**(3): 582-95.

Rhee, S. Y., W. Beavis, et al. (2003). "The Arabidopsis Information Resource (TAIR): a model organism database providing a centralized, curated gateway to Arabidopsis biology, research materials and community." Nucleic Acids Res **31**(1): 224-8.

Rhee, S. Y., W. Beavis, et al. (2003). "The Arabidopsis Information Resource (TAIR): a model organism database providing a centralized, curated gateway

to Arabidopsis biology, research materials and community." Nucleic Acids Research **31**(1): 224-228.
Rotman, N., F. Rozier, et al. (2003). "Female control of male gamete delivery during fertilization in Arabidopsis thaliana." Curr Biol **13**(5): 432-6.
Rozas, J. and R. Rozas (1995). "DnaSP, DNA sequence polymorphism: an interactive program for estimating population genetics parameters from DNA sequence data." Comput Appl Biosci **11**(6): 621-5.
Sainudiin, R., W. S. Wong, et al. (2005). "Detecting site-specific physicochemical selective pressures: applications to the Class I HLA of the human major histocompatibility complex and the SRK of the plant sporophytic self-incompatibility system." J Mol Evol **60**(3): 315-26.
Sambrook, J., Fritsch, E. F. Maniatis, T (1989). Molecular Cloning. A laboratory manual. New York, Cold Spring Harbor Press.
Sato, K., T. Nishio, et al. (2002). "Coevolution of the S-locus genes SRK, SLG and SP11/SCR in Brassica oleracea and B. rapa." Genetics **162**(2): 931-40.
Schein, M., Z. H. Yang, et al. (2004). "Rapid evolution of a pollen-specific oleosin-like gene family from Arabidopsis thaliana and closely related species." Molecular Biology and Evolution **21**(4): 659-669.
Schiestl, F. P. (2005). "On the success of a swindle: pollination by deception in orchids." Naturwissenschaften **92**(6): 255-264.
Schopfer, C. R., M. E. Nasrallah, et al. (1999). "The male determinant of self-incompatibility in Brassica." Science **286**(5445): 1697-1700.
Schwacke, R., A. Schneider, et al. (2003). "ARAMEMNON, a novel database for Arabidopsis integral membrane proteins." Plant Physiol **131**(1): 16-26.
Shimizu, K. K. (2002). "Ecology meets molecular genetics in Arabidopsis." Population Ecology **44**(3): 221-233.
Shimizu, K. K., J. M. Cork, et al. (2004). "Darwinian selection on a selfing locus." Science **306**(5704): 2081-4.
Shimizu, K. K. and K. Okada (2000). "Attractive and repulsive interactions between female and male gametophytes in Arabidopsis pollen tube guidance." Development **127**(20): 4511-8.
Shiu, S. H. and A. B. Bleecker (2001). "Receptor-like kinases from Arabidopsis form a monophyletic gene family related to animal receptor kinases." Proc Natl Acad Sci U S A **98**(19): 10763-8.
Shiu, S. H. and A. B. Bleecker (2003). "Expansion of the receptor-like kinase/Pelle gene family and receptor-like proteins in Arabidopsis." Plant Physiol **132**(2): 530-43.
Shiu, S. H., W. M. Karlowski, et al. (2004). "Comparative analysis of the receptor-like kinase family in Arabidopsis and rice." Plant Cell **16**(5): 1220-1234.
Sijacic, P., X. Wang, et al. (2004). "Identification of the pollen determinant of S-RNase-mediated self-incompatibility." Nature **429**(6989): 302-5.
Sonnhammer, E. L., G. von Heijne, et al. (1998). "A hidden Markov model for predicting transmembrane helices in protein sequences." Proc Int Conf Intell Syst Mol Biol **6**: 175-82.
Stein, J. C., B. Howlett, et al. (1991). "Molecular-Cloning of a Putative Receptor Protein-Kinase Gene Encoded at the Self-Incompatibility Locus of Brassica-Oleracea." Proceedings of the National Academy of Sciences of the United States of America **88**(19): 8816-8820.
Stephens, J. C., J. A. Schneider, et al. (2001). "Haplotype variation and linkage disequilibrium in 313 human genes." Science **293**(5529): 489-493.

Strain, E. and S. V. Muse (2005). "Positively selected sites in the Arabidopsis receptor-like kinase gene family." Journal of Molecular Evolution **61**(3): 325-332.

Stryer, L. (1995). Biochemistry. New York, W.H. Freeman and Company.

Sundaresan, V., P. Springer, et al. (1995). "Patterns of gene action in plant development revealed by enhancer trap and gene trap transposable elements." Genes Dev **9**(14): 1797-810.

Swanson, W. J. and V. D. Vacquier (1995). "Extraordinary divergence and positive Darwinian selection in a fusagenic protein coating the acrosomal process of abalone spermatozoa." Proc Natl Acad Sci U S A **92**(11): 4957-61.

Swanson, W. J. and V. D. Vacquier (1995). "Liposome fusion induced by a M(r) 18,000 protein localized to the acrosomal region of acrosome-reacted abalone spermatozoa." Biochemistry **34**(43): 14202-8.

Swanson, W. J. and V. D. Vacquier (1997). "The abalone egg vitelline envelope receptor for sperm lysin is a giant multivalent molecule." Proc Natl Acad Sci U S A **94**(13): 6724-9.

Swanson, W. J. and V. D. Vacquier (2002). "The rapid evolution of reproductive proteins." Nat Rev Genet **3**(2): 137-44.

Szczesna-Skorupa, E., D. A. Mead, et al. (1987). "Mutations in the NH2-terminal domain of the signal peptide of preproparathyroid hormone inhibit translocation without affecting interaction with signal recognition particle." J Biol Chem **262**(18): 8896-900.

Tajima, F. (1989). "Statistical-Method for Testing the Neutral Mutation Hypothesis by DNA Polymorphism." Genetics **123**(3): 585-595.

Tajima, F. (1989). "Statistical method for testing the neutral mutation hypothesis by DNA polymorphism." Genetics **123**(3): 585-95.

Takebayashi, N., P. B. Brewer, et al. (2003). "Patterns of variation within self-incompatibility loci." Molecular Biology and Evolution **20**(11): 1778-1794.

Thomas, S. G. and V. E. Franklin-Tong (2004). "Self-incompatibility triggers programmed cell death in Papaver pollen." Nature **429**(6989): 305-9.

van der Hoorn, R. A. L., B. B. H. Wulff, et al. (2005). "Structure-function analysis of Cf-9, a receptor-like protein with extracytoplasmic leucine-rich repeats." Plant Cell **17**(3): 1000-1015.

van Doorn, W. G. and E. J. Woltering (2005). "Many ways to exit? Cell death categories in plants." Trends Plant Sci **10**(3): 117-22.

Van Valen, L. (1973). "A new evolutionary law." Evolutionary Theory **1**: 1-30.

Varagona, M. J., R. J. Schmidt, et al. (1992). "Nuclear localization signal(s) required for nuclear targeting of the maize regulatory protein Opaque-2." Plant Cell **4**(10): 1213-27.

Vielle-Calzada, J. P., R. Baskar, et al. (2000). "Delayed activation of the paternal genome during seed development." Nature **404**(6773): 91-4.

Vielle-Calzada, J. P., J. Thomas, et al. (1999). "Maintenance of genomic imprinting at the Arabidopsis medea locus requires zygotic DDM1 activity." Genes Dev **13**(22): 2971-82.

Wang, H. F., L. A. Feng, et al. (2007). "Relationship between mRNA stability and intron presence." Biochemical and Biophysical Research Communications **354**(1): 203-208.

Williams, E. G., V. Kaul, et al. (1986). "Overgrowth of Pollen Tubes in Embryo Sacs of Rhododendron Following Interspecific Pollinations." Australian Journal of Botany **34**(4): 413-423.

Wolf, B. B., M. Schuler, et al. (1999). "Caspase-3 is the primary activator of apoptotic DNA fragmentation via DNA fragmentation factor-45/inhibitor of caspase-activated DNase inactivation." Journal of Biological Chemistry **274**(43): 30651-30656.

Yang, Z. (1997). "PAML: a program package for phylogenetic analysis by maximum likelihood." Comput Appl Biosci **13**(5): 555-6.

Yang, Z. and J. P. Bielawski (2000). "Statistical methods for detecting molecular adaptation." Trends in Ecology and Evolution **15**(12): 496-503.

Yang, Z. and R. Nielsen (1998). "Synonymous and nonsynonymous rate variation in nuclear genes of mammals." J Mol Evol **46**(4): 409-18.

Yang, Z. and R. Nielsen (2002). "Codon-substitution models for detecting molecular adaptation at individual sites along specific lineages." Mol Biol Evol **19**(6): 908-17.

Ye, X. L., E. C. Yeung, et al. (2002). "Sperm movement during double fertilization of a flowering plant, Phaius tankervilliae." Planta **215**(1): 60-66.

Zimmermann, P., M. Hirsch-Hoffmann, et al. (2004). "GENEVESTIGATOR. Arabidopsis microarray database and analysis toolbox." Plant Physiol **136**(1): 2621-32.

Zinkl, G. M., B. I. Zwiebel, et al. (1999). "Pollen-stigma adhesion in Arabidopsis: a species-specific interaction mediated by lipophilic molecules in the pollen exine." Development **126**(23): 5431-40.

Zipfel, C., G. Kunze, et al. (2006). "Perception of the bacterial PAMP EF-Tu by the receptor EFR restricts Agrobacterium-mediated transformation." Cell **125**(4): 749-60.